



THE UNIVERSITY OF  
**WAIKATO**  
*Te Whare Wānanga o Waikato*

Research Commons

<http://researchcommons.waikato.ac.nz/>

## Research Commons at the University of Waikato

### Copyright Statement:

The digital copy of this thesis is protected by the Copyright Act 1994 (New Zealand).

The thesis may be consulted by you, provided you comply with the provisions of the Act and the following conditions of use:

- Any use you make of these documents or images must be for research or private study purposes only, and you may not make them available to any other person.
- Authors control the copyright of their thesis. You will recognise the author's right to be identified as the author of the thesis, and due acknowledgement will be made to the author where appropriate.
- You will obtain the author's permission before publishing any material from the thesis.

# Pyrolysis of Sawdust

A thesis submitted in fulfilment  
of the requirements for the degree  
of

**Masters of Engineering**  
**in Materials and Processing Engineering**

at  
**The University of Waikato**

by  
**Kavwa Sichone**

---

The University of Waikato

2013



THE UNIVERSITY OF  
**WAIKATO**  
*Te Whare Wānanga o Waikato*

# Abstract

Lakeland Steel Limited developed a pilot plant for biomass pyrolysis based on sawdust. The pilot plant was based on an auger screw design which was indirectly heated using a double pipe heat exchange configuration to prevent oxidation (combustion) of the feedstock. This thesis covers the preliminary assessment of sawdust pyrolysis for R.H Tregoweth sawmills on behalf of Lakeland Steel Limited.

Proximate and ultimate analyses were deployed on the sawdust to determine its composition. Proximate analysis results gave a moisture content of 60%. The dry solids had an organic matter content of 99.22% with ash making the balance. Ultimate analysis was used to determine content levels of elemental carbon, hydrogen, nitrogen sulphur and oxygen. The results on a dry basis were 47.2%, 6.5%, 0.3%, 0.3%, and 44.9 % respectively.

Drying models were also used to analyse the sawdust drying characteristics. Drying curves were obtained experimentally and four models: Newton; Page; Henderson and Pabis; and Simpson and Tschernitz, were fitted to the data and their accuracy of fit was determined using residual squared sum of errors. Page's model was used to describe the sawdust behaviour in the dryer design as it had the highest accuracy.

The sawdust reaction kinetics were determined using data from thermogravimetric analysis (TGA) and analysed using distributed action energy model. The kinetics were observed at three heating rates of 10, 20 and 30 °C/min with a maximum temperature of 900°C under an argon atmosphere. Sawdust was modelled as a mixture of water, hemicellulose, cellulose and lignin. Good agreement between Gaussian distribution functions for each component and experimental data were observed.

Pilot plant trials were performed using a three factor-three level design of experiment. The factors under investigation were; feedstock moisture content with levels at 15, 30 and 60; reaction temperature with levels at 400, 450 and 500°C;

and reactor auger speed with levels at 15, 20 and 25 rpm. Experiments at 60% moisture could not be performed to completion as the auger blocked repeatedly. The other two moisture contents showed that moisture content enhanced heat exchange properties of the feedstock and this generally increased the amount of volatile organic matter released. It was observed that for 15% moisture sawdust increase of temperature did not consistently exhibit an increase in degree of devolatilisation of organic matter. However, the 30% moisture sawdust showed an increase in devolatilisation with increase in temperature. The effects of increasing reactor auger speed had the most consistent trend with which an increase in speed showed a decrease in degree of devolatilisation thus increasing char yield.

The empirical data collected from lab scale and pilot plant experiments were used to create mass and energy balances. These were the basis of the large scale mobile pyrolysis plant which was designed to process 3.45 tonnes per hour. Due to size restrictions the large scale dryer was not fitted in the container. It was then determined that the feedstock would either be dried using an onsite kiln or the reactor would process green sawdust.

A preliminary economic feasibility assessment was performed for the base case scenario which processed pre-dried sawdust of 15% moisture content at 400°C and a retention time of 45 minutes. A sensitivity analysis based on predicted optimistic and pessimistic conditions showed that automation of the plant had the potential to increase the economic viability of the large scale process.

# Acknowledgements

Firstly, I would like to thank God, without Him, none of this would be possible.

I would like to thank my supervisor Dr. Mark Lay for his guidance and encouragement, Cory Leatherland from Lakeland Steel Limited for providing the project, MSI for agreeing to fund the project, John MacDonald-Wharry for helping with the Raman, Lisa Li for the GC, Yuanji Zhang for the TGA, furnace and ovens, Indar Singh for finding bits of equipment for me, Janis Swan and Mary Dalbeth for their peptalks, Stewart Findley for his encyclopaedic knowledge on health and safety, Cheryl Ward for helping with the literature and patent searching, and all the other students and staff who helped out in various ways.

I would like to thank my Dad, Mom, brother and sisters for their support over the years, and friends for entertaining me.

# Table of Contents

<b>Abstract</b> .....	i
<b>Acknowledgements</b> .....	iv
<b>List of Figures</b> .....	ix
<b>List of Tables</b> .....	xiii
<b>Chapter 1. Introduction</b> .....	1
1.1 Background .....	2
1.2 Project Brief .....	2
1.3 Research Objectives .....	3
<b>Chapter 2. Literature Review</b> .....	4
2.1 Introduction .....	5
2.1.1 Products.....	6
2.1.2 Modes of Pyrolysis.....	20
2.1.3 Related Technologies .....	21
2.1.4 Effects of Processing Parameters on Pyrolysis .....	23
2.1.5 Feedstock Considerations .....	24
2.1.6 Reaction Catalysts .....	27
2.2 Modelling of Pyrolysis Reactions .....	28
2.2.1 Reaction Kinetics .....	30
2.2.2 Lab-Scale Thermal Analysis Techniques .....	35
2.2.3 Conclusions .....	38

2.3	Pyrolysis Process Design.....	39
2.3.1	Dryer Technologies.....	39
2.3.2	Pyrolysis Reactor Technologies.....	48
2.3.3	Heat Exchanging Technology.....	60
2.3.4	Syngas Recovery System.....	68
2.3.5	Hazard Management.....	76
2.4	Process Economics.....	77
2.4.1	Current Market Scan.....	79
2.4.2	Pyrolysis Technology Patent Citation Report.....	82
2.5	Summary.....	85
<b>Chapter 3.</b>	<b>Methodology.....</b>	<b>87</b>
3.1	Introduction.....	88
3.2	Reagents.....	88
3.3	Equipment.....	88
3.4	Feedstock Characterisation Experiments.....	89
3.4.1	Proximate Analysis.....	89
3.4.2	Ultimate Elemental Analysis.....	90
3.4.3	Sawdust Drying Curves.....	90
3.4.4	Thermogravimetric Analysis.....	90
3.5	Pilot Plant Trials.....	91
3.5.1	Design of Experiments.....	91
3.5.2	Variables for Pilot Plant Trials.....	91

3.5.3	Experimental Setup and Procedure .....	93
3.6	Product Characterisation .....	93
3.6.1	Syngas Gas Chromatography Analysis .....	93
3.6.2	Raman Spectroscopy .....	93
<b>Chapter 4.</b>	<b>Results and Discussion</b> .....	<b>95</b>
4.1	Introduction .....	96
4.2	Feedstock Characterisation.....	96
4.2.1	Introduction .....	96
4.2.2	Composition Analysis .....	96
4.2.3	Drying Characteristics.....	97
4.2.4	Reaction Kinetics Model Development .....	107
4.2.5	Modelling Overview .....	120
4.3	Pilot Plant Trials .....	121
4.3.1	Experimental Data.....	121
4.3.2	Pilot Plant Pyrolysis Process Description .....	121
4.3.3	Feedstock Performance .....	122
4.3.4	Effects of Processing Parameters on Product Yields .....	126
4.4	Product Characterisation .....	129
4.4.1	Char Characterisation.....	129
4.4.2	Syngas Characterisation .....	138
4.4.3	Bio-Oil Characterisation .....	138
<b>Chapter 5.</b>	<b>Large Scale Plant Design Concept</b> .....	<b>140</b>



5.1	Introduction .....	141
5.1.1	Process Description .....	141
5.1.2	General Assumptions for Large Scale Plant Design .....	144
5.2	Large Scale Plant Design .....	144
5.2.1	Feed Preparation.....	144
5.2.2	Reaction stage .....	149
5.2.3	Reactor Design .....	154
5.2.4	Separation Phase .....	155
5.2.5	Product Handling .....	158
<b>Chapter 6.</b>	<b>Process Economics Modelling</b> .....	<b>160</b>
6.1	Introduction .....	161
6.1.1	Assumptions for Base Case Economic model .....	161
6.1.2	Base Case Economic model .....	161
<b>Chapter 7.</b>	<b>Conclusion and Recommendations</b> .....	<b>167</b>
7.1	General Findings .....	168
7.2	Recommendations for Future Work .....	169
<b>References</b>	.....	<b>171</b>

# List of Figures

Figure 1. Biomass pyrolysis schematic diagram.....	5
Figure 2. Char produced from Pinus Radiatta sawdust using Lakeland Steel Ltd.'s pilot plant.....	6
Figure 3. Bio-oil made from pyrolysis of wood.....	11
Figure 4. Syngas flare from Lakeland Steel's pilot plant processing green sawdust. ....	18
Figure5. A two-step global reaction map for biomass pyrolysis. ....	29
Figure 6. Schematic diagram showing the stages involved in relation to temperatures (Basu 2010).....	29
Figure 7. Constant heating rate model. T2 is the indirect heating temperature and T1 is the temperature inside the kiln. ....	37
Figure 8. Dynamic heating rate model. T2 is the indirect heating temperature and T1 is the temperature inside the kiln. ....	38
Figure 9. Large Scale plant concept for organic waste sludge pyrolysis (Sichone 2012).....	39
Figure 10. Screw conveyor dryer (Made-in-China.com 2011).....	42
Figure 11. Drum dryer (Fabrication 2011).....	43
Figure 12. Tunnel/ continuous tray dryer (AG 2011). ....	43
Figure 13. Continuous through-circulation (non-agitated) dryer (co.Ltd 2011)...	44
Figure 14. Continuous through circulation (agitation/ rotary) dryer (Pharmainfo.net 2007).....	44
Figure 15. Direct rotary dryer (Made-in-China.com 2008). ....	45
Figure 16. Multiple-Effect Evaporator (Exports 2011).....	46
Figure 17. Lakeland Steel Limited's pilot plant. ....	59
Figure 18. Double pipe heat exchanger in counter-current flow. ....	61
Figure 19. Typical shell and tube heat exchanger (ACUSIM).....	62
Figure 20. Air cooled (fin-fan).....	63
Figure 21. Plate and frame heat exchanger. ....	64
Figure 22. Spiral tube heat exchanger cross section <sup>4</sup> .....	65
Figure 23. Plate-fin heat exchanger. ....	65

Figure 24. Heat cross exchange schematic. ....	68
Figure 25. Separation efficiency with respect to particle grain size for a variety of equipment (Anis and Zainal 2011). ....	71
Figure 26. Directional schematic of cash-flow streams that can be associated with economics of pyrolysis (Sichone 2012). ....	78
Figure 27. Biomass pyrolysis patent yearly application count (a) to the left English patents only (b) to the right all patent search results no language limiters. ....	83
Figure 28. Biomass gasification patent yearly application count (a) to the left English patents only (b) to the right all patent search results no language limiters. ....	84
Figure 29. Biomass torrefaction patent yearly application count (a) to the left English patents only (b) to the right all patent search results no language limiters. ....	84
Figure 30. Biomass conversion patent yearly application count (a) to the left English patents only (b) to the right all patent search results no language limiters. ....	84
Figure 31. Drying rate vs time. ....	100
Figure 32. Mass vs. time for sawdust drying at 80, 90 and 100°C. ....	101
Figure 33. Mass fraction vs. time for sawdust drying at 80, 90 and 100°C. ....	102
Figure 34. Mass loss flux vs. time for sawdust drying at 80, 90 and 100°C. ....	103
Figure 35. Newton model. ....	104
Figure 36. Page model. ....	105
Figure 37. Henderson and Pabis model. ....	105
Figure 38. Simpson and Tschernitz model. ....	106
Figure 39. Normalised mass loss curves mass % vs temperature. ....	109
Figure 40. Mass loss rate vs temperature curves. ....	111
Figure 41. Derivative thermogravimetric (DTG) analysis curve for sawdust at 10°K/min. ....	112
Figure 42. First attempt at pseudo component mapping for sawdust at 10°K/min. ....	113
Figure 43. Gaussian distribution fitting for sawdust mass loss rate curve for sample heated at 10°K/ min. ....	113

Figure 44. Gaussian distribution fitting for sawdust mass loss rate curve for sample heated at 20°K/ min.....	114
Figure 45. Gaussian distribution fitting for sawdust mass loss rate curve for sample heated at 30°K/ min.....	115
Figure 46. Reaction rate vs. temperature. ....	116
Figure 47. Rate constant k vs. Temperature (°K). ....	117
Figure 48. Activation energy vs temperature for sawdust at 10°K/min.....	118
Figure 49. Loose sawdust being fed through bulk density 280 kg/m <sup>3</sup> . ....	122
Figure 50. Dry compacted sawdust prior to decomposition, bulk density 1,202 kg/m <sup>3</sup> . ....	123
Figure 51. Product yields with respect to change in temperature. ....	127
Figure 52. Product yields with respect to change in moisture. ....	128
Figure 53. Product yield with respect to change in auger speed.....	129
Figure 54. Plot of G band position as a function of heat treatment temperature for chars. Broad horizontal guide lines represent approximate G band positions measured for glassy carbon and graphite samples. Linear trend line and correlation based on mean data points (from chars derived from all three precursors) between HTT ≈ 420 ° C and HTT ≈ 700 ° C (John McDonald-Wharry 2012). ....	136
Figure 55. G band position for different pine char samples (sample number along the x axis refers to the sample ordered vertically on the right end). ....	137
Figure 56. Schematic for large scale pyrolysis process. ....	142
Figure 57. Arrangement of equipment in shipping container showing no space for dryer.....	143
Figure 58. Generic Anatomy of Chemical Processes.....	144
Figure 59. Mass and energy balance for sawdust drying. ....	148
Figure 60. Schematic of heat transfer to feedstock. ....	151
Figure 61. Indirect-fired small Rotary kiln reactor (Courtesy of Harper International, Lancaster, NY.). ....	153
Figure 62. Reactor mass and energy balance. ....	154
Figure 63. Large scale pyrolysis reactor. ....	155
Figure 64. Gas cyclone design commonly used in industry. ....	155
Figure 65. Mass and energy balance for flash tank.....	156

Figure 66. Mass and energy balance for condensing drum.....	157
Figure 67. Main plant equipment cost distribution for mobile large scale design.....	162

# List of Tables

Table 1. Test category A: basic biochar utility properties - required for all biochars (IBI 2011). .....	7
Table 2. Test category B: biochar toxicant report required for all feedstocks (IBI 2011).....	8
Table 3. Test category C: biochar advanced analysis and soil enhancement properties - optional for all biochars ((IBI) 2011).....	9
Table 4. Distribution of functional groups in bio-oil from switch grass(Imam and Capareda 2012).....	12
Table 5. Various compounds identified in bio-oil characterisation. ....	14
Table 6. Physico-chemical properties of different pyrolysis oils (Sipilä, Kuoppala et al. 1998).....	16
Table 7. Reported Syngas Composition (Apt, Newcomer et al. 2008).....	19
Table 8. Comparison of Pyrolysis modes (Zhang 2010 ).....	22
Table 9. Typical product yields (dry wood basis) of pyrolysis compared with those of gasification (Zhang 2010 ).....	23
Table 10. Expressions for the most common reaction mechanisms in solid state reactions.....	31
Table 11. Kinetic Capabilities of Hi-Res <sup>TM</sup> TGA methods (Sauerbrunn and Gill). .....	38
Table 12. Warm-Air Direct- Heat Co-current Rotary Dryers: Typical Performance Data*(Moyers. and Baldwin 1999). ....	47
Table 13. Pyrolysis reactors and heating methods <sup>a</sup> (Bridgwater 1999). ....	51
Table 14. Research on pyrolysis reactors (Crocker 2010). ....	52
Table 15 Commercial carbonizers (Dutta 2007).....	55
Table 16. Reactor types and heat transfer (Bridgwater 1999). ....	58
Table 17. Common materials used in heat exchangers (Intelligence 2012). ....	67
Table 18. Tar classification system defined by the Energy Research Centre of the Netherlands (ECN). ....	69
Table 19. Comparison of particle limit specifications (Anis and Zainal 2011)....	70
Table 20. Physical/mechanical scrubbers. ....	71

Table 21. Catalytic cracking equipment (Anis and Zainal 2011). .....	75
Table 22. Current commercial pyrolysis ventures. ....	80
Table 23. Patent search hits for a combination of keywords. ....	82
Table 24. Three factor-three level range assignment. ....	92
Table 25. Three factor-three level combination setup. ....	92
Table 26. Proximate analysis composition for pine sawdust. ....	97
Table 27. Comparative ultimate analysis of pinus radiatta sawdust and other organic feedstock.....	97
Table 28. Drying models.....	104
Table 29. Quality of fit assessment for drying curves. ....	104
Table 30. Mass loss rate prediction using Gaussian prediction. ....	120
Table 31. Global kinetic parameters. ....	120
Table 32. Processing parameter level assignment.....	121
Table 33. Raw data collected from pilot plant. ....	125
Table 34. Pilot plant trial product distribution. ....	126
Table 35. Proximate analysis of biochars. ....	130
Table 36. Ultimate elemental analysis for biochar.....	131
Table 37. Summarised spectra analysis results. ....	136
Table 38. Syngas characterisation for pilot plant trial samples. ....	139
Table 39. Bio oil ultimate analysis.....	139
Table 40. : Prospective dryer ratings.....	147
Table 41. Rotary dryer specifications. ....	149
Table 42. Reactor design morphology overview. ....	150
Table 43. Reactor options ranking. ....	153
Table 44. Reactor specifications. ....	154
Table 45. Flash tank specification sheet. ....	156
Table 46. Condensing drum specifications sheet. ....	157
Table 47. Total capital investment breakdown. ....	162
Table 48. Operating cost breakdown for mobile pyrolysis plant base case. ....	163
Table 49. Sensitivity analysis for capital costs. ....	165
Table 50. Sensitivity analysis for operating costs. ....	166

# **Chapter 1.**

## **Introduction**



## **1.1 Background**

An awareness of the effects of emissions on global warming has increased the focus on waste minimisation. Industries are also now looking to ways in which they can lower their dependence on fossil fuel derived energy. Biofuels have been recognised as an alternative to fossil derived energy. These fuels have been perceived to be more environmentally friendly and are of interest as they have the potential to be used as a tool against climate change. From a financial point of view, this shift in paradigm (eco-friendly/ going green) can only be justified if the biofuels offers benefits of equal or extra value to their fossil-derived counterparts in terms of cost and performance.

As the world aims for a more environmentally approach to attaining its energy demands, a number of processes and technologies have been considered. Concepts such as waste minimisation, waste to energy, waste recycling are the basis of the efforts being made to drive the biofuel initiative. Pyrolysis has been identified as a potential means of meeting these demands.

With this in mind, Lakeland Steel Limited (Rotorua, New Zealand) has a prototype slow-pyrolysis unit that was developed for sawdust. However this pilot plant has also shown promising trials on other feedstock such as sewage sludge, dissolved air flotation sludge from chicken processing facilities, and paunch grass. The company is currently interested in optimising the plants performance. Optimisation of this technology will enable them to reduce their net energy consumption which will reduce their carbon footprint and improve returns.

## **1.2 Project Brief**

Lakeland Steel limited has been approached by R.H Tregoweth sawmill which currently processes 252,000 tonnes of timber per year. About 45% of the wood ends up as sawmill waste such as bark, sawdust, woodchip and chip fines. Lakeland Steel had been given the task of designing a pyrolysis unit that can process 3.45 tonnes per hour of sawdust which accounts for 11.5% of the wood handled by a client. The sawdust has been identified as a low price commodity which only has a value of \$4 per tonne. The main aim of the project is to increase

the revenue from the sawdust stream from \$4 per tonne using pyrolysis technology. Lakeland Steel Ltd. already has a pyrolysis pilot plant patented within New Zealand. This will be used to assess the performance of the Pinus Radiata sawdust as a feedstock for the process.

### **1.3 Research Objectives**

Based on the areas identified in the project brief, the objectives of this thesis include:

1. Perform pilot plant trials to obtain processing data that will be used to build empirical process models for Lakeland Steel's patented pilot pyrolysis plant.
2. Design a mobile large scale plant for sawdust pyrolysis using the empirical data from the pilot plant trials.
3. Performing an economic feasibility assessment of the large scale plant.

# **Chapter 2.**

## **Literature Review**

## 2.1 Introduction

Pyrolysis can be described as the thermal decomposition of organic materials in the absence of oxygen at temperatures ranging from 400 to 900°C (Lédé 1994, Rezaiyan and Cheremisinoff 2005, Basu 2010). The thermal modification involves two transforming and concurrent reactions: pyrolysis and carbonisation. In pyrolysis, gases are liberated. In carbonisation, carbon atoms are changed into the solid graphite structures that give char its long-term durability (Taylor 2010). The products of the thermal decomposition are gaseous syngas, solid char and liquid bio-oils.

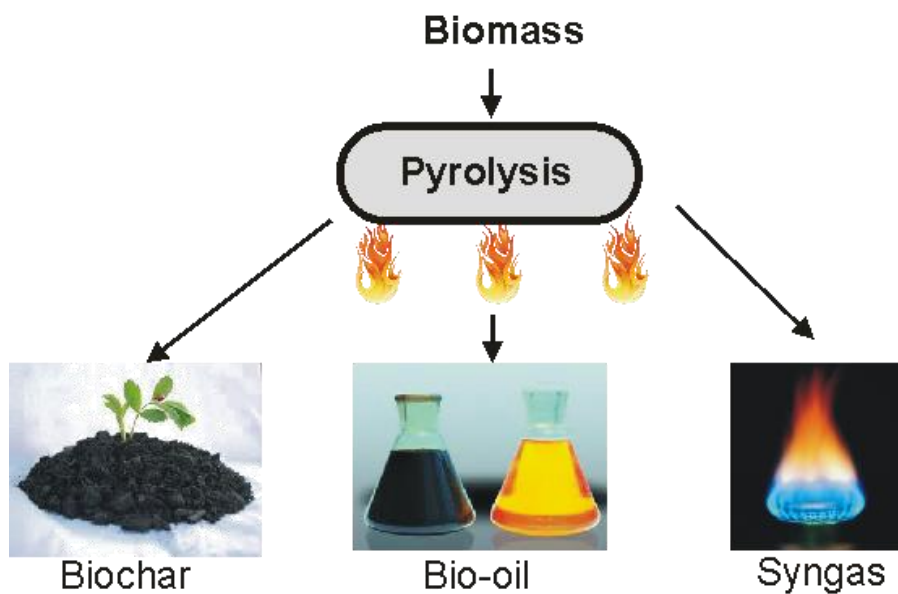


**Figure 1.** Biomass pyrolysis schematic diagram.

The main process parameters used to control the pyrolytic process are the temperature, pressure, reaction time, and internal heat transfer rates. By manipulating these parameters different modes of pyrolysis can be setup (Slesser. and Lewis. 1979, Rezaiyan and Cheremisinoff 2005, Basu 2010, Crocker 2010, Taylor 2010, Zhang 2010 ). The most common modes are fast which is typically used for liquid products, slow and conventional which are used predominantly for carbonisation/ char production. These modes are further explained in section 2.1.2

## 2.1.1 Products

This section provides literature on the products of biomass pyrolysis. It gives a description of the product, its potential applications, its marketability and concerns associated with it.

### 2.1.1.1 Char



**Figure 2.** Char produced from Pinus Radiatta sawdust using Lakeland Steel Ltd.'s pilot plant.

Char is the solid product from the pyrolysis process. Biochar is a carbon-rich material that is virtually non-biodegradable and thus stable in soils (Taylor 2010). It is a type of charcoal, however, biochar is the term used for charcoal produced solely for land application to increase agricultural performance (Taylor 2010). Char comes in different forms such as granules, powder, flakes, and briquettes depending on the method of production and the end use. The desired properties of the char will also vary depending on the end use. This thesis focuses on the use of char for bioremediation. Therefore, going by the International Biochar Initiative (IBI's), proposed classification systems for biochar are shown in Table 1 to Table 3. The tests are used to categorize biochar for; basic biochar utility properties; toxicant concentrations; and advanced utility properties associated with soil performance enhancement. These requirements have raised mixed reactions as some in the field as accepting researchers suggest the standards will provide a reliable basis of pricing biochar. Others view them as being detrimental to the development of the biochar market because it only allows big firms to produce biochar due to smaller businesses not being able to afford the cost of testing chars.

As a result the easiest marketing approach for char remains to be in the form of charcoal.

**Table 1.** Test category A: basic biochar utility properties - required for all biochars (IBI 2011).

Requirement	Criteria <sup>1</sup>	Unit	Test Method
<b>Moisture</b>	Declaration	% of total mass, dry basis	ASTM D1762-84 (specify measurement date with respect to time from production)
<b>Organic Carbon</b>	Class 1: ≥60% Class 2: ≥30% and <60% Class 3: ≥10% and <30%	% of total mass, dry basis	C, H, N analysis by dry combustion (Dumas method), before (total C) and after (organic C) HCl addition
<b>H:C<sub>org</sub></b>	0.7  (Maximum)	Molar Ratio	
<b>Total Ash</b>	Declaration	% of total mass, dry basis	ASTM D1762-84
<b>Total Nitrogen</b>	Declaration	% of total mass, dry basis	Dry combustion (Dumas method) and gas chromatography, following same procedure as for C, H, N analysis above, without HCl addition.
<b>pH</b>	Declaration	pH	pH analysis procedures as outlined in section 04.11 of US Composting Council and US Department of Agriculture (2001), following dilution and sample equilibration methods from Rajkovich et al. (2011)
<b>Electrical Conductivity</b>	Declaration	dS/m	EC analysis procedures as outlined in section 04.10 of US Composting Council and US Department of Agriculture (2001), following dilution and sample equilibration methods from Rajkovich et al.
<b>Liming (if pH is above 7)</b>	Declaration	% CaCO <sub>3</sub>	Rayment & Higginson (1992)
<b>Particle size distribution</b>	Declaration	% <420µm; % 420-2,380 µm; % 2,380-4,760 µm; % >4,760 µm;	Progressive dry sieving with 4760µm, 2380µm and 420µm sieves, as outlined in ASTM D2862- 10 Method for activated carbon.

<sup>1</sup> All values will be reported to one decimal place significant digit (0.1), unless otherwise indicated within the criteria for any reporting requirement. (e.g., if the analysis is 0.73, it can be reported as 0.7)

The second test is aimed at regulating the allowable amount of toxins.

**Table 2.** Test category B: biochar toxicant report required for all feedstocks (IBI 2011).

<b>Requirement</b>	<b>Range of Maximum Allowed thresholds</b>		<b>Test method</b>
<b>Earthworm Avoidance Test</b>	Pass/Fail		ISO 17512-1:2008 methodology and OECD methodology (1984a) as described by Van Zwieten et al. (2010)
<b>Germination Inhibition Assay</b>	Pass/Fail		OECD methodology (1984b) 3 test species, as described by Van Zwieten et al. (2010)
<b>Polycyclic Aromatic Hydrocarbons (PAH)</b>	6 – 20	mg /kg TM	Method following US Environmental Protection Agency (1996)
<b>Dioxin/Furan (PCCD/F)</b>	9	ng/kg ITEQ	Method following US Environmental Protection Agency (2007)
<b>Polychlorinated Biphenyls</b>	0.2 – 0.5	mg/kg ITEQ	Method following US Environmental Protection Agency (1996)
<b>Arsenic</b>	12 –100	mg/kg dry wt	US Composting Council and US Department of dry wt Agriculture (2001)
<b>Cadmium</b>	1.4 – 39	mg/kg dry wt	US Composting Council and US Department of dry wt Agriculture (2001)
<b>Chromium</b>	64 – 100	mg/kg dry wt	US Composting Council and US Department of dry wt Agriculture (2001)
<b>Cobalt</b>	100 – 150	mg/kg dry wt	US Composting Council and US Department of dry wt Agriculture (2001)
<b>Copper</b>	63 – 1500	mg/kg dry wt	US Composting Council and US Department of dry wt Agriculture (2001)
<b>Lead</b>	70 – 500	mg/kg dry wt	US Composting Council and US Department of dry wt Agriculture (2001)
<b>Molybednum</b>	5 –75	mg/kg dry wt	US Composting Council and US Department of dry wt Agriculture (2001)
<b>Mercury</b>	1 – 17	mg/kg dry wt	US Composting Council and US Department of dry wt Agriculture (2001)
<b>Nickel</b>	47 – 600	mg/kg dry wt	US Composting Council and US Department of dry wt Agriculture (2001)
<b>Selenium</b>	1 – 100	mg/kg dry wt	US Composting Council and US Department of dry wt Agriculture (2001)
<b>Zinc</b>	200 – 2800	mg/kg dry wt	US Composting Council and US Department of dry wt Agriculture (2001)
<b>Boron</b>	Declaration	mg/kg dry wt	US Composting Council and US Department of dry wt Agriculture (2001)
<b>Chlorine</b>	Declaration	mg/kg dry wt	US Composting Council and US Department of dry wt Agriculture (2001)
<b>Sodium</b>	Declaration	mg/kg dry wt	US Composting Council and US Department of dry wt Agriculture (2001)

The third test is specifically for the high end biochar which would be expected to cost more than that of the preceding classes.

**Table 3.** Test category C: biochar advanced analysis and soil enhancement properties - optional for all biochars ((IBI) 2011).

Requirement	Criteria	Unit	Test Method
<b>Mineral N (ammonium and nitrate)</b>	Declaration	mg/kg	2M KCl extraction, followed by spectrophotometry (Rayment and Higginson 1992)
<b>Total Phosphorus &amp; Potassium (P&amp;K)*</b>	Declaration	% of total mass, dry basis	Modified dry ashing followed by ICP (Enders and Lehmann 2012)
<b>Available P</b>	Declaration	mg/kg	2% formic acid followed by spectrophotometry (modified from Rajan et al 1992, Nutrient Cycl in Agroecosystems 32:291-302 and AOAC 2005, as used by Wang et al 2011)
<b>Volatile Matter</b>	Declaration	% of total mass, dry basis	ASTM D1762-84
<b>Total Surface Area</b>	Declaration	m <sup>2</sup> /g	ASTM D 6556-10 Standard Test Method for Carbon Black – Total and External Surface Area by Nitrogen Adsorption
<b>External Surface Area</b>	Declaration	m <sup>2</sup> /g	

\* Total K is sufficiently equivalent to available K for the purpose of this characterization

#### **2.1.1.1.1 Applications**

Applications of biochar include:

- Fuel source – this is the oldest known use of char. It was used for cooking due to its low smoke production attributes.
- Filter medium – char has a large surface area/ volume ratio, this is because of its mesoporous structure. This structure allows it to be used as a filter medium for water and air purification.
- Catalyst support – the mesoporous structure also allows char to have a favourable surface for reactions and nucleation especially when housing catalysts.
- Bio remediation – biochar has been credited for improving cation exchange capacity of soils. This means it can be used improving nutrient transfer mechanisms in soil.
- Reducing agent – char is a very powerful reducing agent due to its carbon content. Carbon rich char products such as coke are used in the smelting industry to reduce ores into higher purity metals, as is the case in iron and aluminium smelting processes.



### **2.1.1.1.2 Marketability**

Despite the wide range of potential applications, there still appears to be no established market for biochar. This is because the benefits have not been proven over the long term. For example one of the claims being made is that biochar will enhance the soil's ability to retain nutrients. This claim has been made in response to analysis of terra preta soils of the amazon which contain high amounts of carbon compared to surrounding areas. The high carbon content has been credited to the agricultural practices of the ancient South Americans that involved burning organic matter and burying the residue (Taylor 2010, Barrow 2012). Terra preta typically has three- or more times the total soil organic carbon than soils it lies on (a 14% organic matter content is common) and it usually contains far more P, Ca and humus than surrounding soils (Barrow 2012).

### **2.1.1.1.3 Concerns**

Field trials using char have been done in recent years at char application levels of 2.5 kg per 100 m<sup>2</sup>. Achieving high concentrations of char in the soil on a large scale seems less favourable compared to conventional fertiliser application operations. The reason behind this is the low density of the biochar 0.3 – 0.43 kg/m<sup>3</sup> (Lehmann and Joseph 2012) which means larger volumes need to be applied to the soil. It has been proposed that the char is too light to apply on top of the soil so a layer of heavier medium (topsoil) needs to be used to prevent it from blowing off in the wind. Another concern is the hydrophobic nature of the char which hinders it from intimately mixing with top soils leaving it to wash off in wet conditions.

Different soils will have different requirements. Biochar has been credited for improving the aeration properties of high density, waterlogged soils whilst improving the aggregation potential of sandy soil (Taylor 2010, Verheijen, Jeffery et al. 2010, Lehmann, Rillig et al. 2011, Barrow 2012, Lehmann and Joseph 2012). However, the interaction of the biochar with various sorts of soil needs to be determined individually. The differences in physical structure between biochar and soils lead to altered soil tensile strength, hydrodynamics, and gas transport in

a soil biochar mixture; all of which can be expected to have major impacts on soil biota (Lehmann, Rillig et al. 2011).

### 2.1.1.2 Bio-Oil



**Figure 3.** Bio-oil made from pyrolysis of wood.

Bio-oil is the liquid product from pyrolysis. It is generally acidic in nature (pH~2.5) (PYNE 2006, Oasmaa and Peacocke 2010) and is comprised of a number of organic compounds such as acetaldehyde, acetone, formic acid, acetic acid, methanol, formaldehyde and furfuryl alcohol. Bio-oil produced from woody biomass is normally a dark brown, viscous liquid with a strong characteristic, smoky smell. Bio-oil produced via pyrolysis has been known to age rapidly due to its high tendency to be oxidised. For more information regarding the properties of the bio-oil refer to Appendix “Bio-oil MSDS”. Bio-oil has been identified to contain a number of organic derivatives and precursors which are formed as by-products. These by-products serve as niche markets which offer alternative pathways for marketing bio oil. An extensive characterisation of bio-oil produced from switch grass is presented by Imam and Capreda,(Imam and Capareda 2012), where the following organic function groups are identified (Table 4).

Lu and Li et al concluded that bio-oil properties are generally affected by its water content (Lu, Li et al. 2009) . This statement has been supported by works from other sources, (Sipilä, Kuoppala et al. 1998, Mohan, Pittman et al. 2006, Imam

and Capareda 2012) who attribute bio-oil's relatively poor performance as a fuel in comparison to petroleum based oils to its water content.

**Table 4.** Distribution of functional groups in bio-oil from switch grass(Imam and Capareda 2012).

<b>Functional Group</b>	<b>Total%</b>
Alkanes	36.2
Phenolic compounds	20.5
Aromatics	8.8
Napthalene	1.7
Toluene	1.4
Benzene	2.2
Furans	4.2
Ketones	5.1
Fame/acids	8.7
Alcohols	7.4
Esters	2.4
Amides	1.5

Table 5 shows various compounds that have been identified using mass spectrometry on bio oil from a range of feedstocks.

**Table 5.** Various compounds identified in bio-oil characterisation.

Compound Name	Feedstock	Reference
<b>Acids and Esters</b>		
Methanoic (formic)	Straw, pine,	(Sipilä, Kuoppala et al. 1998)
Ethanoic (acetic)	Hardwood	
Propanoic(propionic)		
2-Methylpropanoic (isobutyric)		
Hydroxyethanoic (glycolic)		
Butanoic(butyric)		
Hydroxypropanoic (lactic)		
Allyl acetic		
Pentanoic acid (valeric acid)		
Hexanoic (caproic)		
Benzoic acid, 4-isopropenylcyclohexenylmethyl ester	switchgrass	(Imam and Capareda 2012)
9-Hexadecenoic acid, methyl ester, (z)-		
Pentadecanoic acid, 14-methyl-, methyl ester		
Pentadecanoic acid		
Oxalic acid, 2-isopropylphenyl pentyl ester		
Oxalic acid, isobutyl 2-isopropylphenyl ester		
Oxalic acid, 6-ethyloct-3-yl ethyl ester		
Dodecanoic acid, methyl ester		
Acetic acid, trichloro-, nonyl ester		
<b>Alkanes</b>		
Dodecane	switchgrass	(Imam and Capareda 2012)
Undecane, 2,6-dimethyl-		
Octane, 3,6-dimethyl-		
Tridecane		
Dodecane, 2,5-dimethyl-		
Hexadecane, 1-bromo-		
Tridecane, 4-methyl-		
Decane, 3,8-dimethyl-		
Dodecane, 2,6,10-trimethyl-		
Cyclotetradecane		
Cyclododecane		
Dodecane, 4,6-dimethyl-		
Tridecane, 2-methyl-		
Decane, 1-bromo-2-methyl-		
Hexane, 2-phenyl-3-propyl-		
Hexadecane		
Octadecane		
Heptadecane		
<b>Alcohol</b>		
Methanol	Straw, pine, Hardwood	(Sipilä, Kuoppala et al. 1998)
Thymol	switchgrass	
Benzenepropanol, 2-methoxy-		
1-Dodecanol, 3,7,11-trimethyl-		
1h-Benzimidazole, 5,6-dimethyl-		

**Table 5.** Various compounds identified in bio-oil characterisation

3,7,11,15-Tetramethyl-2-hexadecen-1-ol		
Benzeneethanol, -methyl-		
3-buten-2-ol, 4-phenyl-		
Isodecyl methacrylate		
Methyl n-isopropyl-3-phenylpropanimidate		
Cyclohexanone, 4-(benzoyloxy)-		
2-Tridecanone		
2-Pentadecanone, 6,10,14-trimethyl-		
Cyclopentanone, 2-ethyl-		
<b>Phenols</b>		
Phenol, 2-ethyl-	switchgrass	(Imam and Capareda 2012)
Phenol, 4-ethyl-		
Phenol, 3,5-dimethyl-		
2-methoxy-5-methylphenol		
Phenol, 2-1-methylethyl-acetate		
Phenol, 2,4,5-trimethyl-		
Phenol, 4-propyl-		
Phenol, 4-ethyl-2-methoxy-		
Phenol, 5-methyl-2-acetate		
Phenol, 2,6-dimethoxy-		
Phenol, 2-methoxy-4-methyl-		
<b>Aromatics</b>		
1h-Indene, 2,3-dihydro-4,7-dimethyl-	switchgrass	(Imam and Capareda 2012)
1h-Indene, 2,3-dihydro-1,1,5,6-tetramethyl-		
1-Tetradecene		
3-Octadecene, (e)-		
1-Heptadecene		
9-Eicosene, (e)-		
2-Hexadecene, 3,7,11,15-tetramethyl		
1-Decene, 3,3,4-trimethyl-		
2,4-Diphenyl-4-methyl-1-pentene		
5,8-Dimethylenebicyclo[2.2.2]oct-2-ene		
1,4-Dihydronaphthalene		
5-Octadecene, €		
<b>Napthalene, Toluene, Benzene, Amides</b>		
Acetamide, 2-(1-naphthyl)-n-(3,4-methylendioxybenzyl)-	switchgrass	(Imam and Capareda 2012)
Napthalene, 2-methyl-		
Napthalene, 1,2,3,4-tetrahydro-5,6,7,8-tetramethyl-		
Napthalene, 1,5-dimethyl-		
Toluene, 4-(1,1-dimethyl-2-propynyloxy)-		
1,1-Bicyclohexyl		
Fluorene, 2,4a-dihydro-		
Benzene, 1-ethyl-3-methyl-		
Benzene, 1,1-[3-(3-cyclopentylpropyl)-1,5-pentanediy]bis-		
Benzene, nonyl-		
Benzene, 1,2,3-trimethyl-		

**Table 6.** Physico-chemical properties of different pyrolysis oils (Sipilä, Kuoppala et al. 1998).

<b>Analysis</b>	<b>Straw oil</b>	<b>Pine oil</b>	<b>Ensyn oil (hardwood)</b>
pH	3.7	2.6	2.8
Water (wt%)	19.9	11.1	23.3
Solids, (wt%)	0.35	0.18	0.30
Density (kg/dm <sup>3</sup> )	1.186	1.266	1.233
Viscosity, cSt, at 50°C	11	46	50
LHV (MJ/kg)	16.9	19.2	16.6
LHV (MJ/kg) <sub>a</sub>	21.1	21.6	21.6
C (wt%) <sub>a</sub>	55.3	56.4	58.4
H (wt%) <sub>a</sub>	6.6	6.3	6.0
N (wt%) <sub>a</sub>	0.4	0.1	0.1
O (wt%) <sub>a</sub>	37.7	37.2	35.5
Ash (wt%)	0.14	0.07	0.09
CCR (wt%)	18	18	23
Flash point (°C)	56	76	>106
Pour point (°C)	−36	−18	−9
Sulfur (wt%)	0.05	0.006	0.02
Chlorine (wt%)	0.033	0.008	<0.001
Water-insolubles (wt%)	23	28	40
LHV (MJ/kg)	27.1	27.7	25.9
C (wt%)	68.6	69.3	65.8
H (wt%)	6.6	6.4	6.2
N (wt%)	0.7	0.2	0.2
O (wt%)	24.1	24.1	27.8
Water-solubles/ether-insol. (wt%)	28	41	25
C (wt%)	47.2	45.7	44.7
H (wt%)	6.5	6.3	6.4
N (wt%)	0.6	0.2	0.1
O (wt%)	45.7	47.8	48.8

### **2.1.1.2.1 Applications**

Applications of bio-oil include:

- Organic molecule derivatives – bio-oil can be used as a precursor for the production of chemicals adhesives and resins.
- Fuel – it can be combusted and used for heat or power generation (LHV of 14-18 MJ/kg (Lu, Li et al. 2009)).

- Biodiesel feedstock – bio oil can also be used as a feedstock for the production of biodiesel. This is more carbon neutral than diesel obtained from fossil derived oil because it is derived from sustainable carbon source.

#### **2.1.1.2.2 Marketability**

Pyrolysis oil from woody biomass is an ideal clean fuel because it is CO<sub>2</sub> neutral and usually produces approximately half the NO<sub>x</sub> (nitrogen oxide) emissions in comparison with fossil fuels (Bradley 2006).

There is currently no market for bio-oil prior to upgrading. Upgrading improves compatibility with conventional engines as raw pyrolysis oil which is highly oxygenated normally hardens with time (Slesser. and Lewis. 1979, A.V.Bridgewater. 2004, Rezaiyan and Cheremisinoff 2005, Strezov, Evans et al. 2008, Smith., M.Garcia-Perez. et al. 2009, Crocker 2010, French and Czernik 2010, Oasmaa and Peacocke 2010, Anis and Zainal 2011, Bulushev and Ross 2011, Vamvuka 2011). The main property that affects its marketability is its high corrosion potential because it has a low pH ~ 2-4(D.Zhang. and S.Lilly. 2005, Bradley 2006, Mohan, Pittman et al. 2006, Lu, Li et al. 2009, Vamvuka 2011) which makes it hard to be handled or transported cheaply (Oziemen. and Karaosmanoglu. 2004, Dominguez., Menendez et al. 2006, Anis and Zainal 2011, Vamvuka 2011, White, Catallo et al. 2011). Another property that affects its marketability is its inconsistent flash point 40 to 100°C because it cannot be handled by conventional engines or equipment. The high moisture content of 14-20% reduces the lower heating value (LHV) of the oil to about 14 MJ/kg.

#### **2.1.1.2.3 Concerns**

Bio oil has been associated with acute dermal toxicity due to its corrosive nature (PYNE 2006). Inhalation of fumes may also pose human risk as it could contain toxic compounds polyaromatic hydrocarbons, depending on the production methods and feedstock used. It has a high rate of biodegradation under aerobic conditions. This biodegradation via oxidation causes the bio-oil to form a waxy substance.



### 2.1.1.3 Syngas



**Figure 4.** Syngas flare from Lakeland Steel's pilot plant processing green sawdust.

Syngas, also known as synthesis gas is mainly composed of hydrogen, carbon monoxide, methane, carbon dioxide and small hydrocarbons. It is primarily the incondensable gas product of pyrolysis left over once the oil is condensed out. Table 7 shows reported properties of syngas from various sources.

**Table 7.** Reported Syngas Composition (Apt, Newcomer et al. 2008).

	Composition % volume									
	CO	H <sub>2</sub>	CO <sub>2</sub>	CH <sub>4</sub>	Ar	N <sub>2</sub>	S (ppmv)	H <sub>2</sub> O	HHV (Btu)	LHV (Btu)
Coal, E- Gas gasifier, Wabash (Lynch 1998)	45.3	34.4	15.8	1.9	0.6	1.9	68		277	
Petcoke, E- Gas gasifier, Wabash (Lynch 1998)	48.6	33.2	15.4	0.5	0.6	1.9	69		268	
Coal, Dow gasifier, Dow plasquimine (Hannemann, Koestlin, Zimmerman and Haupt 2005)	38.5	41.4	18.5	0.1	--	1.5	n/r		n/r	n/r
Coal/Petcoke, Shell gasifier, Elcogas Puetrollano (Hannemann, Koestlin et al. 2005)	29.2	10.7	1.9	0.01	0.6	5.31	n/r	4.2	n/r	n/r
Coal/Biomass, Shell gasifier, Nuon Power (Hannemann, Koestlin et al. 2005)	24.8	12.3	0.8	--	0.6	42.0	n/r	19.1	n/r	n/r
Coal, GE/Texaco gasifier, Polk (Todd and Battista undated)	46.6	37.2	13.3	0.1	2.5	2.5	n/r	0.3		253
Petcoke, GE/Texaco gasifier, El Dorado (Todd and Battista undated)	45.0	35.4	17.1	0.0	2.1	2.1	n/r	0.4		242
Lignite/Waste, BG/ Lurgi gasifier, Schwarze Pumpe (Todd and Battista undated)	26.2	61.9	2.8	6.9	1.8	1.8	n/r	--		317
Fuel oil, GE/Taxaco, (Todd and Battista undated)	35.4	44.5	17.9	0.5	1.4	1.4	n/r	0.44		241
Coal, ErgoExergy, Eskom (Walker, Blinderman and Brun 2001; Blinderman and Anderson 2003)	8.3	6.7	9.5	1.0	n/r	n/r	n/r	17.0		150

**Note:** Natural gas and LPG have typical calorific values of 48.8 and 46.3 MJ/kg respectively

**HHV** = High heating value;

**LHV** = Low heating value;

n/r = not reported

### **2.1.1.3.1 Applications**

Syngas can be used as a:

- Fuel 5.59 – 12.63 MJ/m<sup>3</sup> (Apt, Newcomer et al. 2008) for electricity generation, heating, gas cells.
- Biodiesel feedstock in the Fischer-Tropsch process.

### **2.1.1.3.2 Marketability**

Unlike gasification, pyrolysis is highly endothermic. The syngas is usually recycled and burned to cater for some of the process heating requirements to improve the process autogenesis. Autogenesis is the ability for a process to be self-sustainable. This means the amount of syngas being burned can be used to lower external fuel inputs that drive the process. This approach is generally favoured over selling the syngas because of the issues highlighted in the next subsection.

### **2.1.1.3.3 Concerns**

Syngas production has been associated with the production of eco-toxic compounds such as hydrogen sulphide, dioxins, polychlorinated biphenyls (PCB) and poly-aromatic hydrocarbons (PAHs). Some of these compounds are also toxic to human and can pose a health risk. These toxins can be extracted using scrubbers. Hydrogen sulphide is very acidic so it can cause corrosion issues when handling.

Syngas homogeneity is also an issue because its calorific value can vary depending on the properties of the feedstock and the processing parameters such as reaction temperature, reaction order and catalyst contact time (char has been identified as a syngas cracking catalyst therefore contact time needs to be monitored).

## **2.1.2 Modes of Pyrolysis**

A wide range of designs, temperatures, and pressures are used for pyrolysis systems. Typically, for a simple batch type reactor, a drum or kiln-shaped

structure for continuous type is heated externally by recycled syngas or another fuel. Regardless of whether they are batch or continuous, pyrolysis systems can be categorised as follows:

- **Slow/conventional pyrolysis:** Used to maximise the production of char . The steady heating rate settings (varying from ~5-20 °C/ min to isothermal temperatures at around 400°C in batch systems) favour the production of bio char and syngas. Modern systems designed for commercial bio char production, such as that operated by Pacific Pyrolysis Pty Ltd, the bio-oil produced is cracked to syngas to avoid marketing or disposal of bio-oil (A.V.Bridgewater. 2004, Rezaiyan and Cheremisinoff 2005, Dominguez., Menendez et al. 2006, Downie 2008, Balat, Balat et al. 2009, Papadikis, Gu et al. 2009, Smith., M.Garcia-Perez. et al. 2009, Basu 2010, Crocker 2010, Elliott 2010, Jones 2010, Downie 2010-2011, Berg., Sichone. et al. 2011, Bridle 2011, Mcbirdle 2011, Vamvuka 2011, Choi, Choi et al. 2012).
- **Fast pyrolysis:** Fast Pyrolysis is optimised to produce bio-oil, which requires fast heating rates. Fast pyrolysis is currently the most studied pyrolysis system in conjunction with woody biomass. This is because most ventures focus on using bio-oil as a biodiesel precursor (A.V.Bridgewater. 2004, Rezaiyan and Cheremisinoff 2005, Dominguez., Menendez et al. 2006, Downie 2008, Balat, Balat et al. 2009, Papadikis, Gu et al. 2009, Smith., M.Garcia-Perez. et al. 2009, Basu 2010, Crocker 2010, Elliott 2010, Jones 2010, Downie 2010-2011, Berg., Sichone. et al. 2011, Bridle 2011, Mcbirdle 2011, Vamvuka 2011, Choi, Choi et al. 2012).

### **2.1.3 Related Technologies**

This section covers alternative processes to pyrolysis that have similar end products. These include gasification, Fischer Tropsch, and torrefaction. These processes are quite similar to pyrolysis since they are based on thermochemical decomposition of carbonaceous matter (Slessor. and Lewis. 1979, Rezaiyan and Cheremisinoff 2005, Basu 2010). However, there are some differences in operating parameters such as the maximum temperature used and amount of air added. These differences are quite significant and alter the reaction mechanisms

and end products (Slesser. and Lewis. 1979, Rezaiyan and Cheremisinoff 2005, Basu 2010).

**Gasification** – This is the process by which organic matter is heated to 1200-1500 °C in the presence of oxygen, but using less oxygen than stoichiometric ratios to prevent complete feedstock combustion (Slesser. and Lewis. 1979, Rezaiyan and Cheremisinoff 2005, Basu 2010). Combustion is highly exothermic and provides energy for gasification of the feedstock. This process is often used on pyrolysis by-products to produce syngas for electricity and heat generation, but is also be used on raw feedstock.

**Fischer Tropsch** – This process is used to convert natural gas and syngas into liquid alkane fuels. The process normally uses pyrolysis or gasification or a combination of both to produce the syngas which is then converted into the liquid fuels via catalytic cracking and reformation of gases.

**Torrefaction** – this is a mild form of pyrolysis where the biomass is heated to temperatures ranging from 230- 300°C in the absence of oxygen (Basu 2010). It is usually used as an intermediate process in most cases with the exception of coffee bean roasting. As the biomass is heated, it is dried and some volatile matter is driven off. This leaves a brittle material with low oxygen and water content which can make a better feedstock for gasification or combustion (Basu 2010).

**Table 8.** Comparison of Pyrolysis modes (Zhang 2010 ).

Pyrolysis Process	Residence Time	Heating Rate	Final Temperature (°C)	Desired Products
<b>Carbonisation</b>	Days	Very low	400	Charcoal
Conventional	5- 30 min	Low	600	Char,bio-oil, gas
<b>Fast</b>	<2 s	Very high	~500	Bio oil
<b>Flash</b>	<1 s	High	<650	Bio-oil chemicals, gas
Ultra-rapid	<0.5 s	Very High	~1000	Chemical, gas
Vacuum	2 – 30 s	Medium	400	Bio-oil
Hydropyrolysis	< 10 s	High	< 500	Bio-oil
Methanol-pyrolysis	<10s	High	>700	Chemicals

**Table 9.** Typical product yields (dry wood basis) of pyrolysis compared with those of gasification (Zhang 2010 ).

Mode	Liquid	Char	Gas
Fast	75%	12%	13%
Conventional	50%	20%	30%
Slow	30%	35%	35%
Modern Slow (Downie 2008)	0%	25%	75%
Gasification	5%	10%	85%

### 2.1.4 Effects of Processing Parameters on Pyrolysis

The pyrolysis reaction kinetics rates are mainly dependent on the following parameters:

- Residence Time – longer residence time of feedstock, char and volatiles is generally used for char production because it allows secondary and tertiary reactions which crack the hot volatiles (vaporised oil and tars) into more syngas components and char (Slessor and Lewis, 1979, Rezaiyan and Cheremisinoff 2005, Basu 2010). The char acts as a cracking catalyst for the tar and char yield is increased by two mechanisms. Firstly tar vapour is adsorbed onto the char surface causing reformation of tars at the solid-gas interphase similar to that seen in crystal growth in solid-liquid interfaces (Brinkman and Carles 1998). Secondly, the tar attaches itself to the pores of the char eventually clogging the pores (Antal and Grønli 2003)
- Heating rate – A higher heating rate is used to produce oil and syngas. This is because it allows the feedstock to reach a higher degree of volatilisation in a shorter amount of time. However, literature also states that lower heating rates facilitate char formation (Antal and Grønli 2003, Rezaiyan and Cheremisinoff 2005, Basu 2010). A high gas yield due to the increase of volatile diffusion relative to case hardening which is a critical phase of carbonisation reactions. The case hardening reduces the rate of diffusion/ mass transfer of the volatiles and also affects heat transfer from the grain surface to the core.

- Reaction temperature - this determines the extent of volatilisation exhibited by the feedstock. High reaction temperatures promote gas production while lower reaction temperatures promote char and tar formation (Rezaiyan and Cheremisinoff 2005). Hydrogen fraction and calorific value of the syngas also increases with increase in reaction temperature.
- Operating pressure – this affects the equilibrium temperature for volatilisation. A lower pressure reduces the required reaction temperature. This concept is normally used in flash pyrolysis to reduce the amount of heat required to drive the process (FAO and Department unknown)

In pyrolytic reactions, volatile matter is liberated from its solid/liquid state and vaporised. The main competing process for pyrolysis of solids is carbonisation. This process involves realignment of carbon atoms into graphite like structure. The extent of other reactions such as methanation, steam reformation, solid melting and interactions between the products of the two main reactions are variables that will affect the selectivity of the product yields or product composition. This is covered in more detail in the section on Modelling of Pyrolysis Reactions.

### **2.1.5 Feedstock Considerations**

Prospective biomass feedstocks include but are not limited to

- Animal wastes such as carcasses, paunch grass and litter.
- Waste water effluent such as activated sludge or poultry dissolved air floatation (DAF) sludge.
- Agricultural wastes such as corn stover, sugarcane bagasse
- Energy crops
- Food wastes
- Forestry and timber wastes

Alternatives to biomass feedstock for pyrolysis include plastics and coals (basically all carbonaceous mater).

A feedstock's composition can affect the by-product quality and cost of operating a pyrolysis system. The feedstock composition will vary depending on origin, however it can be noted that most of the solid matter will be organic.

The properties of the feedstock that will be of relevance include:

- **Moisture content** – This is important as it can affect the quality of products. The water content has been known to inhibit volatilisation of organic matter during the decomposition process. The high moisture content can also interfere with carbon fixing reactions effectively reducing the carbon content in the char product and the extent of pyrolysis (Boyles 1984). Feedstock is generally required to have a moisture content less than 20% (Elliott 2010, Downie 2010-2011).
- **Product calorific value/ starting calorific value** – This property is used to assess which feedstock is more compatible to fuel production processing, the higher the ratio, the higher the probability of having an energy self-sufficient process.
- **Final carbon content** – The degree of carbon enrichment in the char is of major concern as it can be used to assess carbon sequestration. It also moderates what type of applications the product can be used for (Elliott 2010, Downie 2010-2011). For example high carbon char could be used for catalysts or analytical applications or even cathodes whilst low grade can be burned as a fuel.
- **Reproducibility of yields** – The ability for a feedstock to give products with consistent properties is desired because it reduces product rejects and cost of monitoring. Wood has been identified to have the highest reproducibility within the biomass feedstock (Slesser. and Lewis. 1979, Boyles 1984).
- **Trace element contaminants** –Some metallic contaminants reduce char performance, for example adsorption properties and health and safety rating, and evolution of toxic compounds. These contaminants are normally produced as char ash. Arsenic and mercury are two examples of contaminants (Purchas., Tammik. et al. 2009).



- **Fibre content** – The fibre content of the feedstock generally ensures a network structure. Fibrous feedstock has been reported to have good mechanical abilities and porosity after pyrolysis. Plant based biomass is generally preferred due to its ability to retain its fibrous structure (Slesser. and Lewis. 1979). A good example of this is activated carbon obtained from coconut shells or other nut species.
- **Transportation** – The transportation of the feedstock can add to the cost of the venture therefore, factors like resource location, density will have to be taken in consideration (Boyles 1984).

Of the specified parameters, the one with the highest impact on the economic feasibility of the process is the feedstock moisture content. In order for pyrolysis to take place the feedstock needs to have a maximum moisture content of 20% (Elliott 2010, Downie 2010-2011). Lower moisture content will also mean lower transportation costs for the same amount of product.

Bio-char and syngas products are considered most valuable for carbon sequestration and energy generation via electricity and process heat. Bio-oil is mainly considered as a bio-fuel precursor; however it needs to undergo further processing before it reaches stability that will render it a convenient liquid fuel.

Heavy metal contamination of feedstock can pose environmental concerns (Elliott 2010, Jones 2010, Downie 2010-2011). Therefore, sawdust from treated woods (e.g copper oxide- chromic acid- arsenic acid, (CCA)) are normally not used because they release toxic and/or carcinogenic compounds. IARC has classified untreated hardwood and hardwood/softwood mix wood dust as a Group I human carcinogen ((USA) 2013).

### **2.1.5.1 Sawdust**

Sawdust, being a ligno-cellulosic biomass has a heterogeneous composition comprising of three components which have different temperature ranges for the initiation of pyrolysis (Basu 2010):

- Hemicellulose: 150-350 °C

- Cellulose: 275-350 °C
- Lignin: 250-500 °C

These components exhibit different properties when they experience pyrolysis due to the difference in structure. Cellulose and hemicellulose have a higher tendency to form volatiles with cellulose being the main contributor to the condensable vapour fraction (Rezaiyan and Cheremisinoff 2005, Basu 2010, Várhegyi, Bobály et al. 2010, Aboyade, Hugo et al. 2011, White, Catallo et al. 2011).

### **2.1.6 Reaction Catalysts**

The use of catalysts to increase desired yields and reduce energy requirements is a crucial step in process optimisation. Pyrolysis being a highly endothermic process by nature has driven researchers to study means by which catalysis can be used to optimise the process conditions to improve the economic favourability of prospective commercial scale operations (Alden, Humerick et al. 2009). To perform an extensive review on catalysts used for biomass pyrolysis is beyond the scope of this thesis, however, this section provides a brief overview in regards to how catalysis is applicable to biomass pyrolysis.

The main benefits of catalysis for pyrolysis include:

- Increased yield of desired product
- Lower heating costs
- Product conditioning

Based on these benefits, catalysts can be placed into two categories; primary and secondary catalysts.

Primary catalysts refer to catalysts that are involved in the reaction. They are either mixed with the feedstock prior to the reaction or placed in the reactor where they can come in contact with the feedstock as it is processed (Anis and Zainal 2011). They can be used for one, two or all three of the listed benefits. Müller-Hagedorn et al. (2003) found that alkaline metal chlorides can lower the pyrolysis temperature of biomass. This can prove beneficial in reducing heating costs and thus lowering operating costs.

Secondary catalysts are normally used for product conditioning. This includes processes such as catalytic cracking of tars (Anis and Zainal 2011) and char conditioning by thermal activation or introduction of soil nutrients in the case of biochar (Antal and Grønli 2003). This topic is discussed in more detail in section 2.3.4.2 Catalytic Cracking”.

## **2.2 Modelling of Pyrolysis Reactions**

The pyrolysis process involves many reactions that occur in series and also parallel. These reactions can be grouped into different classes based on the reagents and the products.

- Primary reactions – These are naturally considered as decomposition reactions because they refer to the direct conversion of the organic matter into char, and volatile gas. Oil, tars and syngas are produced as the hot volatile gas. The oil and tar products are formed from the condensable fractions of the hot volatiles.
- Secondary reactions can be considered as synthesis reactions. They refer to reactions of the products to produce more char and syngas (Antal and Varhegyi 1995, Fake, Nigam et al. 1997, Demirbaş 2000, Rezaiyan and Cheremisinoff 2005, Kovács, Zsély et al. 2007, Strezov, Evans et al. 2008, Basu 2010, Bulushev and Ross 2011, Butler, Devlin et al. 2011, White, Catallo et al. 2011, Mehrabian, Scharler et al. 2012). The diagram below shows a proposed breakdown of a two-step global reaction map.

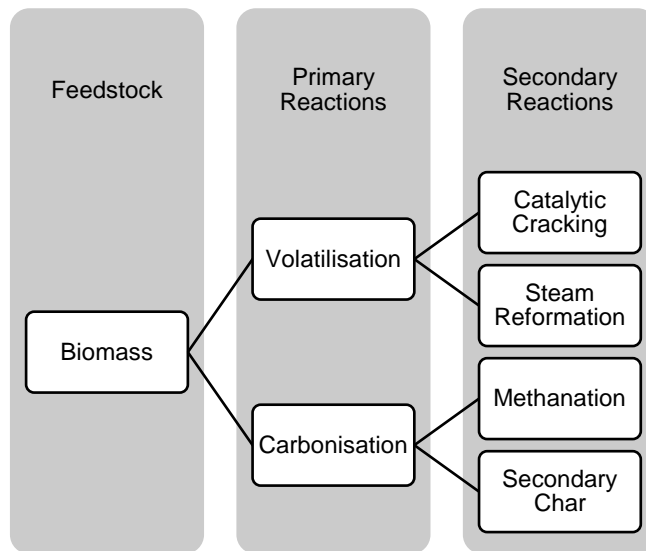


**Figure 5.** A two-step global reaction map for biomass pyrolysis.

Pyrolysis can be broken into four separate stages. These can be divided based on temperature ranges. These stages do not happen at one specific temperature so in reality they will happen simultaneously. Figure 6 shows the stages involved in relation to temperatures (Basu 2010).

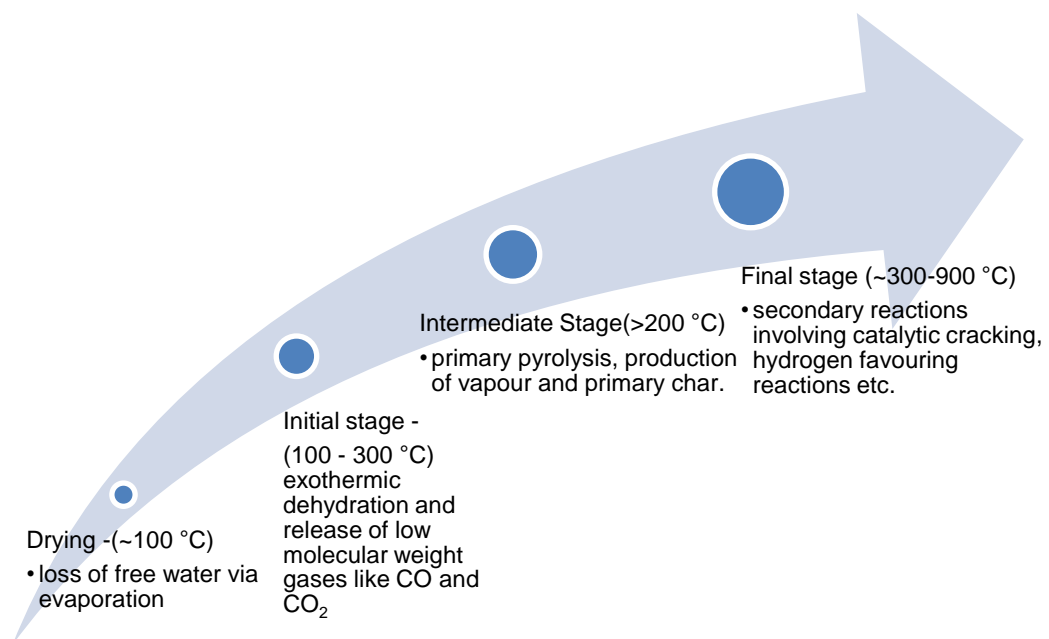


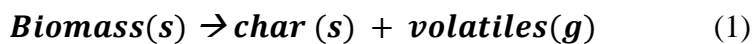
**Figure 6.** Schematic diagram showing the stages involved in relation to temperatures (Basu 2010).

### 2.2.1 Reaction Kinetics

Biomass pyrolysis reactions are considered to be heterogeneous solid state reactions. There are many models for solid state reactions most of which can be classified by the following mechanisms (Behrens 2013):

- Reaction order – uses the rate law based on homogeneous kinetics.
- Diffusion – the reaction rate is limited by the diffusion of the reactant or product.
- Nucleation – the favourability of nuclei formation and growth define the reaction rates simultaneously.
- Geometrical contraction – a reduction in active reactive surface area are definitive of the reaction rates.

A simple heterogeneous solid state reaction of biomass pyrolysis is represented by the following reaction:



Volatiles comprise of condensable vapours from large hydrocarbon and non-condensable gases like CO, CO<sub>2</sub> CH<sub>4</sub>, and H<sub>2</sub>.

Heterogeneous reactions usually involve a superposition of several elementary processes such as nucleation, adsorption, desorption, interfacial reaction, and surface/bulk diffusion, each of which may become rate-limiting depending on the experimental conditions (White, Catallo et al. 2011).

**Table 10.** Expressions for the most common reaction mechanisms in solid state reactions.

Reaction model	Differential Form $f(\alpha) = (1/k)(d\alpha/dt)$	Integral form $g(\alpha) = kt$
Reaction order		
Zero order	$(1 - \alpha)^n$	$\alpha$
First order	$(1 - \alpha)^n$	$-\ln(1 - \alpha)$
$n$ th order	$(1 - \alpha)^n$	$(n - 1)^{-1} (1 - \alpha)^{(1-n)}$
Nucleation		
Power law	$n(\alpha)^{(1-1/n)}$ ; $n = 2/3, 1, 2, 3, 4$	$\alpha^n$ ; $n = 3/2, 1, 1/2, 1/3, 1/4$
Exponential law	$\ln \alpha$	$\alpha$
Avrami - Erofeev (AE)	$n(1 - \alpha) [-\ln(1 - \alpha)]^{(1-1/n)}$ ; $n = 1, 2, 3, 4$	$[-\ln(1 - \alpha)]^{1/n}$ ; $n = 1, 2, 3, 4$
Prout - Tompkins (PT)	$\alpha (1 - \alpha)$	$\ln[\alpha (1 - \alpha)^{-1}] + C$
Diffusional		
1-D	$1/2 \alpha$	$\alpha^2$
2-D	$[-\ln(1 - \alpha)]^{-1}$	$(1 - \alpha) \cdot \ln(1 - \alpha) + \alpha$
3-D (Jander)	$3/2(1 - \alpha)^{2/3} [1 - (1 - \alpha)^{1/3}]^{-1}$	$[1 - (1 - \alpha)^{1/3}]^2$
3-D (Ginstling-Brounshtein)	$3/2[(1 - \alpha)^{-1/3} - 1]^{-1}$	$1 - 2/3 \alpha - (1 - \alpha)^{2/3}$
Contracting geometry		
Contracting area	$(1 - \alpha)^{(1-1/n)}$ ; $n = 2$	$1 - (1 - \alpha)^{(1/n)}$ ; $n = 2$
Contracting volume	$(1 - \alpha)^{(1-1/n)}$ ; $n = 3$	$1 - (1 - \alpha)^{(1/n)}$ ; $n = 3$

Ultimately, regardless of reaction mechanisms, all pyrolysis kinetic models can be divided into three principal categories: single-step global reaction models, multiple-step models, and semi-global models (White, Catallo et al. 2011).

### 2.2.1.1 Single-Step Global Reaction Kinetics

Single step reactions are based on equation (1) where the biomass is converted into char and volatiles.

The global kinetics of single step biomass pyrolysis reactions can be described as:

$$\frac{d\alpha}{dt} = k(T) \cdot f(\alpha) \quad (2)$$

Where  $\alpha$  is the amount of mass converted into gas at a given time,

$$\alpha_t = \frac{w_0 - w}{w_0 - w_f} = \frac{v}{v_f} \quad (3)$$

Where  $w$  is the mass of substrate present at any time  $t$ ,  $w_0$  is the initial substrate mass,  $w_f$  is the final mass of solids (i.e., residue and unreacted substrate) remaining after the reaction. The combination of  $A$ ,  $E_a$ , and  $f(\alpha_c)$  is often designated as the kinetic triplet, which is used to characterize biomass pyrolysis reactions (Dupont, Chen et al. 2009, Van de Velden, Baeyens et al. 2010, White, Catallo et al. 2011).

Most cited kinetic models proposed a rate law that obeys the Arrhenius rate expression:

$$k = A \exp\left(\frac{-E_a}{RT}\right) \quad (4)$$

where  $T$  is the absolute temperature in  $^{\circ}K$ ,  $R$  is the universal gas constant 8.314 J/mol,  $k$  is the temperature-dependent reaction rate constant,  $A$  is the frequency factor, or pre-exponential, and  $E_a$  is the activation energy of the reaction (J/mol).

Putting equation (4) into equation (2) gives the expression for single step isothermal reaction

$$\frac{d\alpha}{dt} = A \exp\left(\frac{-E_a}{RT}\right) \cdot f(\alpha) \quad (5)$$

Isothermal methods have been widely criticised for not being able to accurately simulate the conditions in reactors due to errors that cannot be accounted for during the pre-heating phase (Müller-Hagedorn, Bockhorn et al. 2003, Branca, Albano et al. 2005, White, Catallo et al. 2011). To account for the non-isothermal nature of pyrolysis, the following relationship is used:

$$\frac{d\alpha}{dT} = \frac{d\alpha}{dt} \frac{dt}{dT} \quad (6)$$

where,  $d\alpha/dT$  is the nonisothermal reaction rate,  $d\alpha/dt$  is the isothermal reaction rate, and  $dt/dT$  is the reciprocal of the heating rate ( $1/\beta$ ). Substituting eq (6) into eq (5) gives the differential form of the non-isothermal rate law,

$$\frac{d\alpha}{dT} = \left(\frac{A}{\beta}\right) \exp\left(\frac{-E_a}{RT}\right) \cdot f(\alpha) \quad (7)$$

The term  $\beta$  applies to linear heating rate  $\beta = \frac{dT}{dt}$  which is constant. Separating variables and integrating equations (5) and (7) give the integral forms of the isothermal rate law:

$$g(\alpha) = A \exp\left(\frac{-Ea}{RT}\right) t \quad (8)$$

and nonisothermal rate law:

$$g(\alpha) = \left(\frac{A}{\beta}\right) \int_{T_0}^T \exp\left(\frac{-Ea}{RT}\right) \cdot dT \quad (9)$$

Where  $g(\alpha)$  is the integral reaction model defined by:

$$g(\alpha) = \int_0^\alpha \frac{d\alpha}{f(\alpha)}. \quad (10)$$

### 2.2.1.2 Multiple-Step Models

These models involve rigorous kinetic treatment of pyrolysis data to account for the formation rates of all the individual product species, along with any potential heat and mass transfer limitations (White, Catallo et al. 2011). Some researchers have been able to define the kinetics of biomass pyrolysis using up to seven steps (Diebold 1994).

Although useful in some applications, multi-step reaction models are limited by their incorporation of several interdependent serial reactions, wherein subtle inaccuracies in the kinetic parameters obtained for the first rate equation can be greatly magnified in successive reactions (White, Catallo et al. 2011). These models are seldom used as they involve tedious modelling operations and are limited in cases of accounting for unidentified products especially from the tar mixtures.

### 2.2.1.3 Semi-Global Reaction Kinetics Models

This type of kinetics model attempts to compensate for the heterogeneous composition of biomass whilst keeping calculations as simple as possible. They assume the production of three products: char, tars and syngas (White, Catallo et al. 2011). The models have gained a common acceptance as they allow for a



lumped kinetic analysis which makes them relatively easier than the multiple step model analysis and more accurate than single step reaction kinetics. Examples include, model free analysis and distributed activation energy models.

#### **2.2.1.3.1 Iso-Conversional Analysis**

Iso-conversional kinetic analysis, also commonly called ‘Model free analysis’ (Sewry and Brown 2002) has gained popularity due to its ability to calculate the three kinetic parameters without deploying the assumptions used by reaction mechanism models (White, Catallo et al. 2011). It is proposed that the kinetic parameters can be derived from analysing repeated thermal analysis of the sample at a number of heating rates. The data can be converted to differential thermogravimetric (DTG) curves and with a specific conversion fraction  $g(\alpha)$  selected using equation (9) the parameters can be obtained simultaneously.

#### **2.2.1.3.2 Distribution of Activation Energy Model (DAEM)**

This approach is based on a model of parallel reactions with Gaussian activation energy distribution as shown in the work produced by Sonobe et al (2008). They chose Gaussian distribution because of the favourable experience with this type of modelling on similarly complex materials. According to this model, the sample is regarded as a sum of M pseudo-components, where M is between 2 and 4. Here a pseudo-component is the totality of those decomposing species that can be described by the same reaction kinetic parameters in the given model. On a molecular level, each constituent in the pseudo-component is assumed to undergo a first-order decay.

#### **2.2.1.3.3 Biomass Deactivation model**

An interesting deactivation theory was proposed by Balci et al. (1993) that is based on kinetic models typically applied toward catalyst deactivation. In the biomass deactivation model (DM) the biomass surface area reduces with time as the residual matter at the surface is normally rendered inert once it undergoes decomposition (White, Catallo et al. 2011). This model is worth noting because the pyrolysis of most biomass is associated with a high degree of volume

reduction. Volume reductions of up to 70% were observed in previous research (Sichone 2012).

## 2.2.2 Lab-Scale Thermal Analysis Techniques

Lab scale pyrolysis experiments can be analysed using thermal analysis methods such as:

- Differential thermal analysis (DTA)
- Thermo gravimetric analysis (TGA)
- Differential scanning calorimetry (DSC)
- Simultaneous DSC and TGA (SDT)

The data from these experimental methods are plotted and the shape of the graph will determine which reaction mechanism best suits the reaction kinetics of the process.

There are various techniques devised to model the reaction kinetics for the pyrolysis process. They use TG-MS analysis and usually provide a pseudo-reaction kinetics model. This section is explained well by the TA Decomposition techniques using TGA report (Sauerbrunn and Gill). These are:

- The constant heating rate TGA
- The constant reaction rate TGA
- The dynamic heating rate TGA

These techniques can be used to predict the decomposition rates of homogeneous organic matter. However, most biomass does not have a homogeneous structure. For example pine sawdust is mainly comprised of lignin, cellulose and hemicellulose. Decomposition kinetics can be obtained from TGA tests performed in inert atmosphere to prevent combustion or addition of oxygen. In this model, the reaction order is normally assumed to be 1. This means the model can be described using the Arrhenius equation for decomposition.

$$k = A \exp\left(\frac{-E}{RT}\right) \quad (4)$$

This is because the reaction order  $x_n$  is set to 1 for  $\frac{dx}{dt} = -kx_n$ .

The constants relating to the activation energy and frequency factor can be calculated using empirical data whilst the reaction rate constant will normally be calculated using the change in mass.

### 2.2.2.1 Constant Heating Rate TGA

This model is simple and assumes the reactor has a constant heating rate. This makes it easier to approximate the thermal properties of the sawdust as it is conveyed through the reactor. This means the temperature profile of the feedstock and the heating medium will be linear assuming no heat losses.

The approach assumes the basic Arrhenius equation.

$$\frac{d\alpha}{dt} = A \exp\left(\frac{E_a}{RT}\right) (1 - \alpha)^n \quad (11)$$

where:

$\alpha$  = fraction of decomposition

t = time (seconds)

A = pre-exponential factor (1/seconds)

$E_a$  = activation energy (J/mole)

R = gas constant (8.314 J/mole K)

n = reaction order (dimensionless)

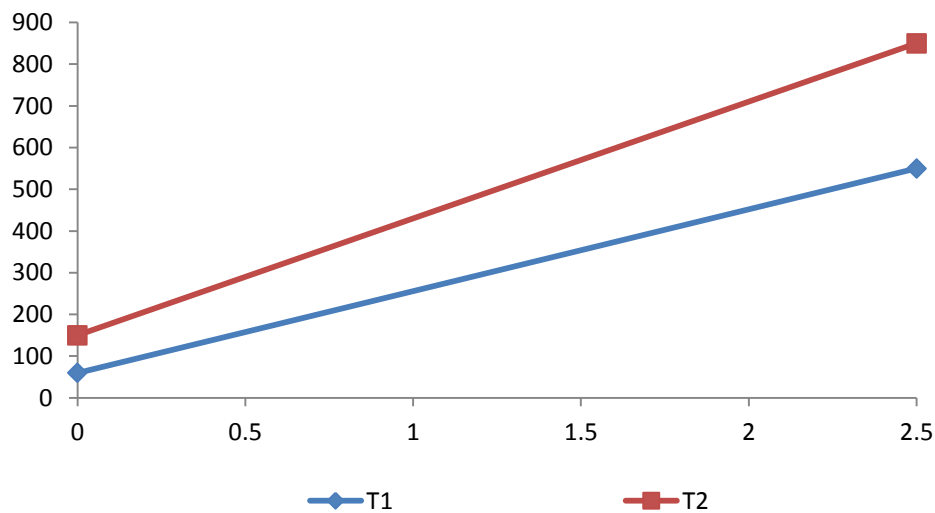


**Figure 7.** Constant heating rate model. T2 is the indirect heating temperature and T1 is the temperature inside the kiln.

### 2.2.2.2 The Constant Reaction Rate TGA

In this type of experiment, a desired reaction rate is defined and the feedstock is heated gradually. Once the desired reaction rate is achieved, the heating rate is adjusted by automatic control functions in an attempt to keep the mass loss rate constant.

### 2.2.2.3 Dynamic Heating Rate TGA

This model attempts to improve on the accuracy by accounting for the change of heat exchange driving force. This means the thermal properties of the feedstock changes as it is conveyed along the reactor. This approach is less pessimistic but more detailed and therefore requires more monitoring and calculations.

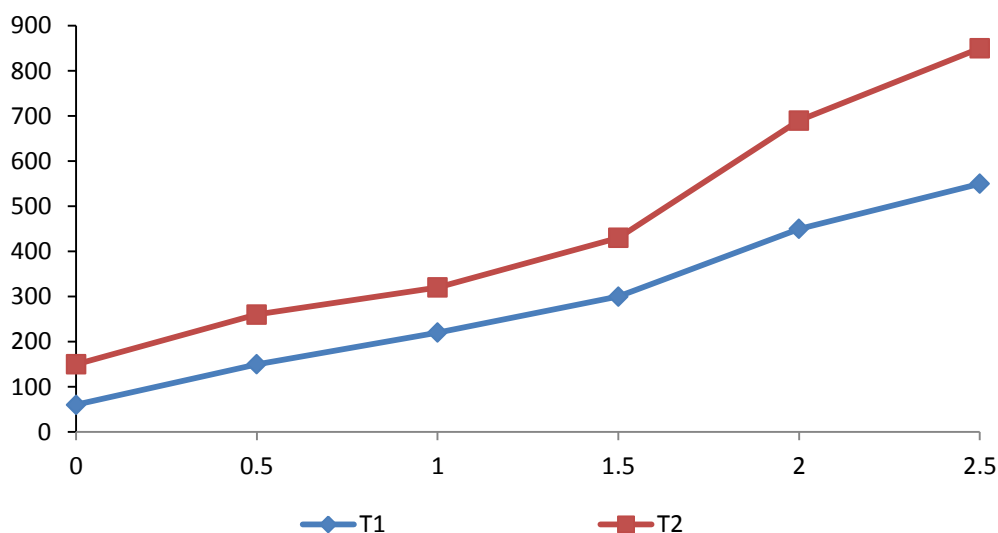


**Figure 8.** Dynamic heating rate model. T2 is the indirect heating temperature and T1 is the temperature inside the kiln.

Table 11 shows the recommended methods for high-resolution TGA analysis

**Table 11.** Kinetic Capabilities of Hi-Res™ TGA methods(Sauerbrunn and Gill).

TGA Method	Scans	Order	Components
Constant Heating Rate	more than 2	Fixed at 1	Single
Constant Reaction Rate	1	Fixed at 1	Multiple
Dynamic Heating Rate	more than 2	Independent	Multiple
Stepwise Isothermal	1	Determined	Multiple

### 2.2.3 Conclusions

Empirical models are generally suited to experimental conditions thus the derived constants will vary for each type of model. Empirical models can be built using the following steps.

1. Perform thermal analysis experiments.
2. Define the nature of the reaction mechanisms. This is the most important step as it sets basis of the reaction rate prediction
3. Define the modelling approach – picking from multiple step models vs. Isoconversional techniques this will typically control the flexibility and accuracy of the model.

## 2.3 Pyrolysis Process Design

This section reviews literature on various aspects involved in the design of a pyrolysis plant. It gives an insight on the equipment currently being used in industry for pyrolysis and related technologies.

A good understanding of pyrolysis theory in regards to governing mechanisms and practical limitations in regards to processing conditions is needed to design sustainable processing equipment. Figure 9 gives an example of a large scale pyrolysis plant process flow diagram that was developed for an organic waste pyrolysis project assessment (Sichone 2012).

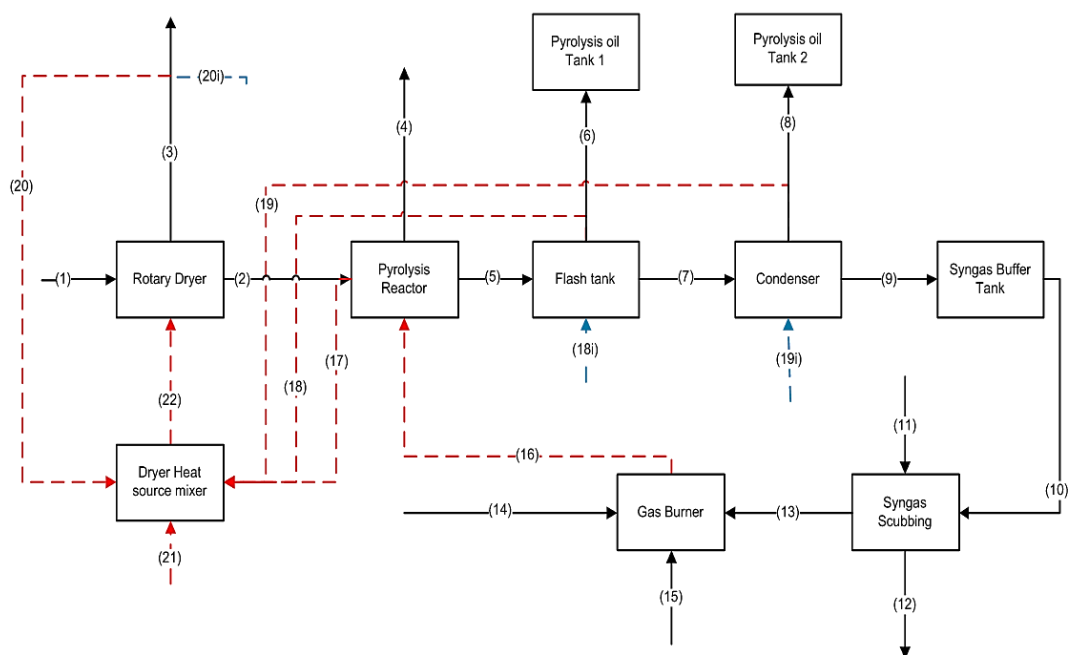


**Figure 9.** Large Scale plant concept for organic waste sludge pyrolysis (Sichone 2012).

### 2.3.1 Dryer Technologies

Water in the feedstock reduces the efficiency of pyrolysis as it requires energy to evaporate the water before pyrolysis can begin. Removing some of this water improves the efficiency of the pyrolysis process making it an attractive option. There is a wide variety of drying methods available, not all of them suited to

sawdust. Selection of the drying method relies heavily on the mechanical properties of the feed stock (Peters 1991, Moyers. and Baldwin 1999, Cheremisinoff 2000, Branan 2005, Exports 2011) such as particle size, consistency and stickiness. Without knowledge and experience of these properties, it will be more difficult to predict the suitability of some methods but some available options will be presented here.

Some important criteria in the selection of drying method include the properties of the material and dried product, the drying characteristics, flow of material and facilities available. More detailed sub-criteria are:

- Physical characteristics when wet
- Physical characteristics when dry
- Toxicity
- Particle size
- Thermal stability
- Available space
- Available heat/electricity
- Initial and final moisture content
- Quantity dried per hour

As already stated the physical characteristics of the feed and output are very important. The feed needs to be compatible with the type of dryer. For example, drying sludge with a spray dryer would cause pumping and clogging problems so the two are incompatible. One must also consider what final moisture content is best with regard to both safety considerations and requirements of downstream processes. Feeds dried to 100% solids can create dust clouds if particulates are small enough. These can be toxic or cause explosions (Peters 1991, Moyers. and Baldwin 1999, Cheremisinoff 2000, Branan 2005, Rezaiyan and Cheremisinoff 2005, Basu 2010). In addition, volatile components will become more prone to evaporation as water is removed, polluting the air.

With these considerations in mind, a dryer can be selected based on the following process outlined in Perry's (Moyers. and Baldwin 1999) initial selection, comparison, drying tests and finally selection based on results. From the initial selection stage, the following drying techniques for sawdust showed potential: pan drying, fluid beds, batch through-circulation, tray drying, direct rotary and vacuum shelf. Some combination of these methods is also possible to recycle heat and maximise efficiency. One such combination is multiple effect evaporation where the vapour of one process is used as the heating medium for another (Peters 1991, Moyers. and Baldwin 1999, Branan 2005).

High temperatures increase the drying rate but can also be more demanding as they might require more sophisticated means of heating. Another disadvantage is case hardening. High temperatures can cause a crust to form on the surface of the material. This crust has shrunken pores for the passage of water to the surface, causing a reduction in drying rate (Moyers. and Baldwin 1999).

Based on energy balances performed in previous studies (Sichone 2012) the dehydration phase will be responsible for most of the energy demands.

Drying is a very common operation in the processing industry. However, each case depends on the material being handled. Different drying technology options were considered and rated for suitability. After elimination, the top two options being considered were rotary dryers and multiple effect evaporators. This section gives a basic description of the dryers and compares them using criteria shown in the ratings table.

### **2.3.1.1 Prospective Dryer Types**

**Dryer type:** *Screw conveyor and indirect rotary*

**Operation mode:** *Indirect type, continuous operation includes paddle, horizontal agitated and steam tube dryers, rotary kilns*

**Performance description:** This type operates by conveying the feedstock through a screw/auger in a trough configuration as shown in Figure 10. The trough is normally heated using hot air or steam although sometime electrical heating can also be applied. The configuration generally requires recirculation of



dry product to minimise product sticking. There is usually only little dusting occurs compared to direct rotary systems due to plug flow and the lack of agitation/fluidisation of the feed.



**Figure 10.** Screw conveyor dryer (Made-in-China.com 2011).

**Dryer type:** *Drum*

**Operation mode:** *Indirect type, continuous operation*

**Performance description:** This type can only be used when the feed paste or sludge can be made to flow. This is because it works on the principle of a rotating a heated drum in the feed so that only a small segment is immersed. As the drum contacts the feed, the paste wets the contact surface and gets dried as the drum rotates on the spindle. The dry feed gets scraped off before the point on the drum gets immersed again. Possible configurations include single, double or twin drums under atmospheric or vacuum pressure. The product is flaky and usually dusty due to the scraping. Maintenance costs may be high due to the abrasions inflicted by the scraping.



**Figure 11.** Drum dryer (Fabrication 2011).

**Dryer type:** *Tunnel/ Continuous Tray*

**Operation mode:** *Direct type continuous operation. Includes tunnel turbo-tray*

**Performance description:** Suitable for small scale and large-scale production. Feed is normally placed on an apron conveyor that is supported to keep it horizontal. The air is then blown through the tunnel using either alongside or countering the feed flow.



**Figure 12.** Tunnel/ continuous tray dryer (AG 2011).

**Dryer type:** Continuous through- circulation (non-agitated).

**Operation mode:** Direct type, continuous operation (Includes perforated band, moving bed, centrifuge–dryer).

**Performance description:** This dryer is suitable for materials that will be pre-formed. This is because the airflow can be controlled quite easily due to the closed but simple geometry. It has the potential to handle large capacities. It works on a similar principle as the tunnel dryer except that there is no agitation, therefore airflow is kept laminar.



**Figure 13.** Continuous through-circulation (non-agitated) dryer (co.Ltd 2011).

**Dryer type:** Continuous through circulation (agitation/ rotary).

**Operation mode:** Direct heating, continuous operation (Includes high speed convective paddle, rotary louvre).

**Performance Description:** Suitable for materials that are pre-formed. This dryer is capable of handling large capacities. The rotary –louvre type requires dry-product recirculation.

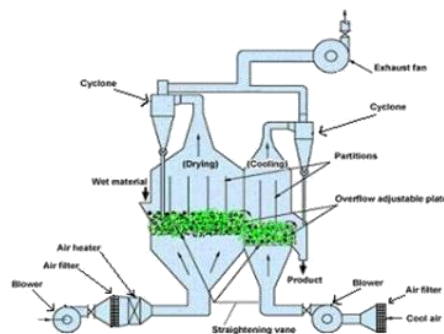


**Figure 14.** Continuous through circulation (agitation/ rotary) dryer (Pharmainfo.net 2007).

**Dryer type:** *Direct rotary type*

**Operation mode:** *Continuous operation*

**Performance Description:** Suitable only if product does not dry to walls and does not dust. Recirculation of product may prevent sticking. The rotary dryer is a long cylindrical vessel positioned on an incline/decline. Hot air is blown through it as the feedstock is conveyed and the cylinder normally has internal attachments such as flights to aid in agitating the feed.



**Figure 15.** Direct rotary dryer (Made-in-China.com 2008).

**Dryer type:** *Multiple effect evaporation*

**Operation mode:** *Continuous*

**Performance description:** This is suitable for large scale applications. Only requires enough energy for the first batch at the highest pressure to be dried. The multiple effect evaporation (MEE) design is based on calculating the amount of feedstock that can be readily dried by the available energy. Then the vapour produced from the drying can be used to dry another fraction of the feedstock. This can be repeated until the whole throughput has been dried [13]. However, it should be noted that each effect adds more capital cost because of extra components needed and utility costs via the cost of pressure manipulation. A schematic diagram of the dryer is shown in Figure 16 . Multiple effect evaporators are designed for liquids or thin pasty films so the technology will not directly be applicable with sawdust. However the concept of recycling heat will be coupled with the appropriate drying technique. Multiple dryers can be used similar to cascade dryers

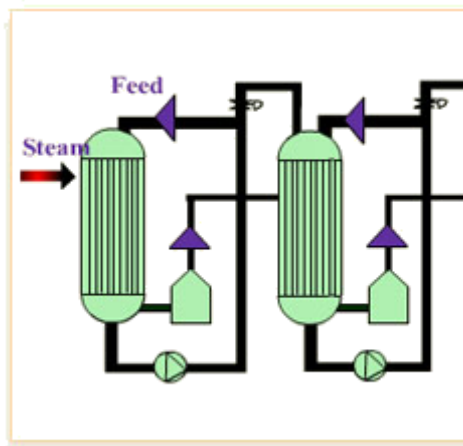


**Figure 16.** Multiple-Effect Evaporator (Exports 2011).

Drying is a highly endothermic process, therefore preference will be given to a dehydration process that can dehydrate the feedstock with minimal energy input and have a low capital cost. Sawdust will be well suited to direct rotary continuous drying and multiple effect evaporation.

Table 12 shows some typical performance data provided by Swenson Process Equipment Inc. (Moyers. and Baldwin 1999). This table is based on dryers designed for feedstock such as minerals, cement and fertilisers, therefore the reduction of moisture will vary from that required by sawdust dryers . However, it gives a good indication of how much energy will be needed to evaporate ‘x’ kg/h of water; the power consumption for motors used as drives and fans in dryers of the respective weight and size. The cost of the dryers is based on costing data collected in 1994; therefore performance indices calculations can be used to adjust for inflation. It is important to notice that the data states that the maximum solids temperature is 65°C. Woody biomass can be dried at higher temperatures depending on the required final moisture and the particle size.

**Table 12.** Warm-Air Direct- Heat Co-current Rotary Dryers: Typical Performance Data\*(Moyers. and Baldwin 1999).

Dryer Size m x m	1.219 x 7.62	1.372 x 9.144	1.524 x 9.144	1.839 x 10.668	2.134 x 12.192	2.438 x 13.716	3.048 x 16.767
Evaporation kg/h	136.1	181.4	226.8	317.5	408.2	544.3	861.8
Work, 10 <sup>8</sup> J/h	3.61	4.60	5.70	8.23	1.12	1.46	2.28
Steam kg/h at kg/m <sup>2</sup> gauge	317.5	408.2	521.6	725.7	997.9	131.5	2041
Discharge, kg/hr.	408	522	685	953	1270	1633	2586
Exhaust velocity m/min	70	70	70	70	70	70	70
Exhaust volume m <sup>3</sup> /min	63.7	80.7	100.5	144.4	196.8	257.7	399.3
Exhaust Fan, kW	3.7	3.7	5.6	7.5	11.2	18.6	22.4
Dryer drive, kW	2.2	5.6	5.6	7.5	14.9	18.6	37.3
Shipping weight, kg	7,700	10,900	14,500	19,100	35,800	39,900	59,900
Price FOB, Chicago	\$158,000	\$168,466	\$173,066	\$204,400	\$241,066	\$298,933	\$393,333

\*Courtesy of Swenson Process Equipment Inc.

NOTE:

*Material: heat-sensitive solid*

*Maximum solids temperature: 65°C*

*Feed conditions: 25 percent moisture, 27°C*

*Product conditions: 0.5 percent moisture, 65°C*

*Inlet-air temperature: 165°C*

*Exit-air temperature: 71°C*

*Assumed pressure drop in system: 200 mm.*

*System includes finned air heaters, transition piece, dryer, drive, product collector, duct, and fan.*

*Prices are for carbon steel construction and include entire dryer system (November, 1994).*

*For 304 stainless-steel fabrication, multiply the prices given by 1.5.*

Mass and energy balances performed in the earlier stages of the project suggest that the drying phase is the major contributor to pyrolysis plant energy costs. This normally requires additional gas to be added to the system, nullifying the autogenesis state of the process. To achieve a state of autogenesis, the energy

demands can be met using either multiple effect evaporation (MEE) or a heat-pump driven direct-heating rotary kiln. This is because these units allow for optimised heating with lower input requirements.

### **2.3.2 Pyrolysis Reactor Technologies**

The pyrolysis process is highly endothermic due to the lack of oxygen input into the process. This makes efficient heating of the process slightly more challenging as conventional methods which involve contact between the heating medium and the reagents is not appropriate. Various methods can be deployed to counter this and they will differ for batch and continuous operations. Heating jackets are probably the most affordable.

Factors that will determine the type of reactor used include:

- Feeding mechanisms/ feed transportation mechanisms
- Heating method

The choice of continuous versus batch will be decided by scale of operation and the design specification. This choice will usually affect the flexibility in design for the feeding/ heating methodology e.g. batch normally eliminates the feeding/ transportation issues especially when considering oxygen elimination however it can take up too much space at large scales.

#### **2.3.2.1 Reactor Classification**

There is very little information on the classification of pyrolysis reactors due to the limited number of proven ventures. However, Dutta's criteria for pyrolysis technology classification based on feeding mechanisms of biomass are as follows (Dutta 2007):

- Type A: No solid movement through the reactor during pyrolysis (batch reactors)
- Type B: Moving bed (shaft furnaces)
- Type C: Movement caused by mechanical forces (e.g., rotary kiln, rotating screw etc.)

- Type D: Movement caused by fluid flow (e.g., fluidized bed, spouted bed, entrained bed etc.)

#### **2.3.2.1.1 Type A - Batch**

Most batch pyrolysis operations will use an airtight vessel that can be placed in an oven or furnace. This makes it a lot easier to stop oxygen from entering the system.

Batch pyrolysis is commonly used for carbonisation where the desired product is charcoal, therefore the residence time can be very long (weeks). A common design is a rotary drum which is sealed and placed into the heating medium. The drum can be rotated to enhance heat exchange when it is not fully immersed in the heating medium. This type of reactor is normally used for carbonisation and some examples can be seen in Table 15.

Separation of products is normally done at high temperatures where the oil and tars are still in their vapour phase. The hot volatiles gas can be vented out prior to the char being cooled.

#### **2.3.2.1.2 Types B-D -Continuous**

Continuous pyrolysis operations are slightly more complex as a lot of effort is focused on restricting introduction of oxygen into the system whilst conveying the feedstock. The heating methods also need to be more sophisticated as the residence time of the feedstock in the reactor can be crucial to setting up the preferred mode of pyrolysis.

Dutta also classified pyrolysis reactors depending on the way heat is supplied to biomass as follows:

- Type 1: Part of the raw material burns inside the reactor to provide heat needed to carbonize the remainder.
- Type 2: Direct heat transfer from hot gases produced by combustion of one or more of the pyrolysis products or any other fuel outside the reactor.
- Type 3: Direct heat transfer from inert hot material (hot gases or sand introduced into the reactor).



- Type 4: Indirect heat transfer through the reactor walls (i.e. external heat source due to combustion of one of or more pyrolysis products or any other fuel)

#### **2.3.2.1.3 Type 1 and 2**

Type 1 typically defines the generic gasifier. The partial combustion of the feed provides sufficient heat for the pyrolysis of the remainder thus a limited amount of oxygen will be needed. As a result, a higher content of soot can be expected.

Type 2 on the other hand, proposes the combustion of the product gas within the reactor. This concept, sounds straight forward and easy, however, the combustion will require oxygen and this means oxygen/air will be fed directly into the reactor. It is impractical to totally assume that none (absolutely 0%) of the oxygen will come in contact with the feedstock as it is being heated. This also sets up a gasification reaction.

#### **2.3.2.1.4 Types 3 and 4**

Theoretically, these ensure that there is no addition of oxygen to feedstock as it decomposes under the heat. Traditionally, they work by the addition of heat indirectly to avoid combustion in the reactor. This can be achieved by:

- Heat exchange through the reactor walls via a heating jacket or double pipe configuration
- The use of hot shots. Hot shots are inert medium such as stainless steel that are pre-heated and mixed in with the feedstock as they are fed into the reactor.
- Dielectric heating of feedstock.

Types 3 and 4 accurately represent the definition of pyrolysis which states that carbonaceous matter decomposes under heat in the absence of oxygen.

#### **2.3.2.1.5 Commercial Reactors**

It is very hard to find many proven cases for biomass pyrolysis on a commercial scale. Most biomass pyrolysis reactors used on an industrial scale are

predominantly used for carbonisation to produce charcoal. This means they will most likely use slow pyrolysis. Bridgewater performed an excellent review of pyrolysis reactor technology (Bridgewater 1999) In this paper Bridgewater presented a summative table listing the types of reactors available as shown in Table 13. An extensive list was presented recently by Crocker (2010) in Table 14 and a table of commercial carbonizers is presented in Table 15 as reported by Dutta (2007).

**Table 13.** Pyrolysis reactors and heating methods<sup>a</sup> (Bridgewater 1999).

Reactor Type	Method of heating	Organisation
Ablative coil	Wall heating	BBC [4]Castle Capitalc now Enervision [5]
Ablative mill	Wall (disc) heating	Colorado School Mines [6]
Ablative plate	Wall heating	U. Aston [7], CNRS—Nancy [8]
Ablativevortex	Wall heating	Interchem [9], NREL [10]
Auger kiln	Wall heating	U. Tübingen [11], WTC [12]
Circulating fluid bed	In-bed gasification of char to heat sand	CRESAgric. U. Athens [13]
Cyclone or vortex	Wall heating	CNRS-Nancy, See also Ablati6e 6ortex
Entrained flow	Combustion products Hot sand	Egemin (14), GTRI (15) U. Western Ontario [16]
Fixed bed	Combustion products Partial gasification Overfired gas	Bio-Alternative [17], Chemvion [18] Alten [19], Italenergiec U. Cardiff [20]
Fluid bed	Heated recycle gas Hot inert gas Partial gasification Fire tubes	Dynamotive [21], INETI [22], IWC [23] RTI [24], Union Fenosa [8], U. Hamburg [25] U. Waterloo [26], Wellman, Worthing [27] CPERI [28], NREL, U. Aston [29] U. Leeds [30], U. Sassari [31], U. Stuttgart [32] Alten [19], Italenergiec MTC1c[33] AE1b, Pyrosolb [34], Wastechb U. Laval [35]
Horizontal bed	Fire tubes	U. Laval [35]
Multiple hearth	Hearth heating	Deutsche Babcockb, PKA b [36], Stenaub [37]
Rotary kiln	Wall heating	SiemensKWU b [38], Waste Gasb
Rotating cone	Wall and sand heating	U. TwenteBTGKARA [39]
Stirred bed	Partial gasification	Alten d [19]
Transported bed	Recirculated hot sand	Ensyn [40] (& at ENEL, VTT [41], Red Arrow [42])
Vacuum moving bed	Direct contact with hot surface	U. LavalPyrovac [43]

<sup>a</sup> Organisations underlined are believed to be active in 1998. Except where indicated, all processes gives liquids. A representative reference is provided.

<sup>b</sup> Used for solid waste processing, not liquids production.

<sup>c</sup> Used for gas production.

<sup>d</sup> Operational mode unclear.

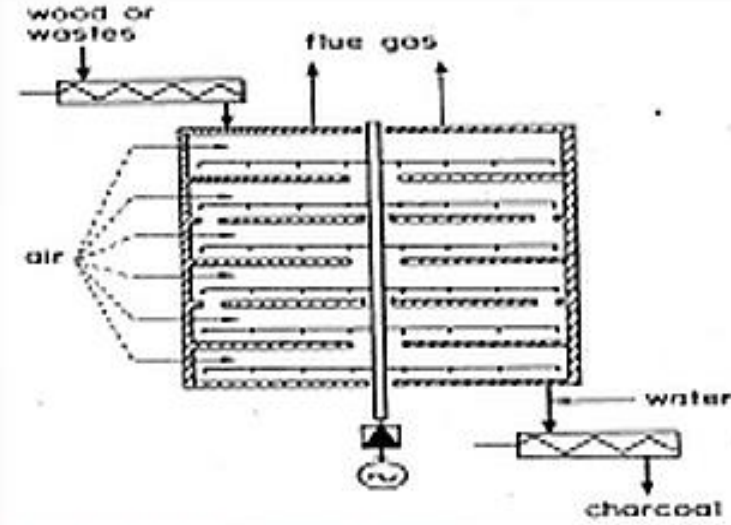
**Table 14.** Research on pyrolysis reactors (Crocker 2010).

Reactor Type	Industrial	Units built	Max size kg/hr.	Research	Max size kg/hr.
Fluid Bed	Agritherm, Canada	2	200	Adelaide U ., Australia	1
	Biomass Engineering Ltd, UK	1	200	Aston U., UK	5
	Dynamotive, Canada	4	8,000	Cirad, France	2
	RTI, Canada	5	20	Curtin U., Australia	2
				ECN, NL	1
				East China U. Science and Technology, Shanghai, China	nk
				Gent U., Belgium	
				Guangzhou Inst. Energy Conversion, China	0.3
				Harbin Institute of Technology	10
				Iowa State U., USA	nk
				Monash U., Australia	6
				NREL, USA	1
				PNNL, USA	10
				Shandong U., Technology	1
				Shanghai Jiao Tong U.,	nk
				Shenyang ., U China	1
				South East U., China	1
				Texas A &M U., USA	1
				TNO, Netherlands	42
				U.Basque Country, Spain	10
			U. Campinas, Brazil	nk	
			U.Maine, USA	100	
			U.Melbourne, Australia	0.1	
			U.Naples, Italy	0.1	
			U.Science and Technology of China	1	
			U.Seoul, Korea	650	

<b>Table 15 Continued.</b> Research on pyrolysis reactors (Crocker 2010).					
<b>Reactor Type</b>	<b>Industrial</b>	<b>Units built</b>	<b>Max size kg/hr.</b>	<b>Research</b>	<b>Max size kg/hr.</b>
Fluid Bed				U. Twente, Netherlands U. Western Ontario, Canada U. Zaragoza, Spain USDA, ARS, ERRC, USA Virginia Tech. U., USA Virginia Tech. U., USA VTT, Finland vTI, Germany Zhejiang U., China Zhengzhou U., China	nk 1 nk nk 1 0.1 1 6 3 2
Ceramic ball downflow Unspecified				U. Kentucky, USA U. Texas, USA Technical U. Compiegne, France	nk nk nk
Rotating cone Integral catalytic pyrolysis	BTG, Netherlands BioEcon, Netherlands + Kior USA	4 nk	2000	BTG, Netherlands Battelle Columbus, USA PNNL, USA Technical U. of Munich U. Massachusetts – Amhurst, USA Virginia Tech. U., USA TNO, Netherlands Technical U. Denmark	10 1 1 nk nk 3? 30 nk
Augur or screw	Abritech, Canada Lurgi LR, Germany Renewable Oil Intl, USA	4 1 4	2083 500 200	Auburn U. USA KIT (FZK), Germany Mississippi State U., USA Michigan State U. USA Texas A&M U., USA	1.0 500 2 0.5 30
Vacuum	Pyrovac, Canada	1	3500	None known	

<b>Table 15 Continued.</b> Research on pyrolysis reactors (Crocker 2010).					
<b>Reactor Type</b>	<b>Industrial</b>	<b>Units built</b>	<b>Max size kg/hr.</b>	<b>Research</b>	<b>Max size kg/hr.</b>
Vortex centrifuge reactor Ablative	PyTec, Germany	2	250	Aston U., UK Institute of Engineering Thermophysics, Ukraine Latvian State Institute, Latvia Technical U., Denmark	20 15 0.15 1.5
Microwave	Carbonscape New Zealand & UK Bioenergy 2020 + gmbh, Austria	nk 1	nk nk	National Inst. Advanced Industrial Sci. & Technolo., Japan Shandong U., China Technical U., Vienna, Austria U. Malaysia Sarawak U. Minnesota, USA U. Mississippi U. Nottingham, UK and China U. York, UK Washington State U.-Tricities, USA	<0.1 <0.1 nk <0.1 10 nk nk nk <1
Spouted fluid bed	Ikerlan, Spain	1	10	Anhui U. Of Science & Technology, China U. Basque Country, Spain	5 nk
Transported bed and Circulated fluidised bed	Ensyn, Canada Metso/UPM, Finland	8 1	4000 400	CPERI, Greece Guangzhou Inst. Energy Conversion, China U. Birmingham, UK U. Nottingham, UK VTT, Finland	1 nk nk nk 20
Radiative convective entrained flow				CNRS – Nancy U., France Dalian U., of Technology, China Institute for Wood Chemistry, Latvia Shandong U. of Technology, China Chinese Academy of Science, Dalian, China	nk nk nk 0.05 nk
Moving bed and fixed bed		3	600	U. Autònoma de Barcelona, Spain U. Science & Technology of China Shandong University of Technology, China	nk ~0.5 110

**Table 15** Commercial carbonizers (Dutta 2007).

Reactor Type	Description	Diagram
Hereshoff Carbonizer	<p>Consists of four to six circular hearths stacked one above the other inside a cylindrical refractory lined shell. The raw material is fed to the uppermost hearth and falls from one hearth to the lower under the action of a rotating shaft which is fitted with rabble arm at each hearth level. The normal operating temperature of the hearth is 900 – 1000° C, and air introduced for partial combustion passes upwards through the furnace. Charcoal produced leaves the furnace at the bottom and is cooled before storage. The capacity of this type of carbonizer is in the range of 4 – 10 tons of wood or other residues per hour.</p>	

<p>Pillard Rotary Carbonizer</p>	<p>The converter consists of an inclined rotary furnace. A part of the pyrolytic gas is recycled and burned to provide heat necessary for carbonization. The hot flue gas comes in direct contact with the raw material slowly moving down the inclined furnace.</p>	
<p>Keil-Pfaulder Converter</p>	<p>Normally used for batch carbonization of waste wood with a cycle time of 6–8 hours. The blower extracts volatile products from the bottom of the converter. The tar is separated from the gas by condensation after which the gas is burned to provide heat for carbonization. Oil is burned mostly during start-up</p>	

<p>Cornell Retort</p>	<p>Normally used for carbonising coarse residues. Operation of the oil burner is thermostatically controlled. Once carbonisation is well underway, the volatile gases are burned and recycled.</p>	<p>The diagram shows a vertical cylindrical retort. At the top, there is a 'discharge opening'. Below it, a hopper is labeled 'hopper charge'. The retort is connected to a burner at the bottom, which has its own 'discharge opening' and a 'damper'. A 'stack' is located to the right of the retort. A legend in the top right corner defines the symbols: a solid arrow for 'flue gas', a dashed arrow for 'wood gas', a double-lined arrow for 'exhaust and recycled gases', and a triangle for 'thermocouple'. The retort contains several thermocouples and a damper is located between the burner and the stack.</p>
<p>Thompson Converter</p>	<p>One of the oldest indirectly heated screw-fed converters. It consists of a number of metal tubes heated externally. The raw material is conveyed through the heated tubes by means of screws and gets carbonized in the process. The volatile gases are fed into the burner so that the whole operation becomes self-sustaining.</p>	<p>The diagram illustrates a horizontal screw-fed carbonizing system. It features an 'infeed screw' at the top right leading into a 'distribution bin'. Below the bin is a 'carbonizing tube' containing a screw. This tube leads into a 'carbonizing chamber', which also contains a screw. Below the chamber is a 'dutch oven' with a 'charcoal take-off screw'. A 'motor' is connected to the screws. On the left side, there is a 'wood gas return flue' and a 'gas' outlet. A 'stack' is shown at the top left. Arrows indicate the flow of material and gases through the system.</p>



From a design point of view, each type of reactor has its limitations in regards to applicable heating methods. Bridgewater further went on to classify the typical form of heat transfer exhibited by the main reactor types as shown in Table 16

**Table 16.** Reactor types and heat transfer (Bridgewater 1999).

Reactor type	Mode of heat transfer	Advantages/disadvantages/features
Ablative	95% conduction 4% convection 1% radiation	Accepts large size feedstocks Very high mechanical char abrasion from biomass Compact design Heat supply problematical Heat transfer gas not required Particulate transport gas not always required
Circulating fluid bed	80% conduction 19% convection 1% radiation	High heat transfer rates High char abrasion from biomass and char erosion leading to high char in product; char/Solid heat carrier separation required Solids recycle required Increased complexity of system Maximum particle sizes up to 6 mm Possible liquids cracking by hot solids Possible catalytic activity from hot char Greater reactor wear possible
Fluid bed	90% conduction 9% convection 1% radiation	High heat transfer rates Heat supply to fluidising gas or to bed directly Limited char abrasion Very good solids mixing Particle size <2 mm Simple reactor configuration
Entrained flow	4% conduction 95% convection 1% radiation	Low heat transfer rates Particle size <2 mm Limited gas/solid mixing

### 2.3.2.2 Lakeland Steel's patented pilot plant

Lakeland has developed a screw type reactor for sawdust pyrolysis Figure 17. The feedstock is force fed into an auger kiln which serves as the reactor using two augers from the hopper. The kiln is indirectly heated to ~600°C using a shell and tube arrangement and the products leave as hot volatiles and char. The char goes down a small funnel (cyclone like) whilst the hot volatiles are passed through a flash tank, which separates the heavy oils and tars. The vapour then flows through a condenser where the remaining water vapour and oil condenses allowing the syngas to go through. These auger reactors have the tendency of getting blocked when the feedstock flow properties are not appropriate. For example, if the

feedstock has a high moisture content it will normally cake and compress in the auger. Ways around this problem include increasing the force being applied by the auger or by pre-drying the feedstock. Another concern with the plant is the lack of syngas recycling. The current setup only allows for the syngas product to be flared off.



**Figure 17.** Lakeland Steel Limited's pilot plant.

### 2.3.3 Heat Exchanging Technology

Pyrolysis is a highly endothermic process. A vast amount of energy is used to heat up the feedstock to the reaction temperature and the decomposition and carbonisation processes also require energy inputs. 272 kJ/kg for drying and 148 kJ/kg for pyrolysis based on the initial feedstock mass prior to drying to 15% moisture (Sichone 2012). However, a significant amount of this heat can be recovered from the products via heat exchange. The recovery of this heat not only increases the energy efficiency of the process, it also reduces the potential for risks or hazards such as fires and explosions.

In most cases, the products (bio-oil, syngas, char) are being cooled. The biggest barrier to efficient cooling of these products is ensuring that there is no mass exchange between the heat exchange medium and the product. This is because introduction of air or water might allow for oxygen to enter the process, resulting in oxidation of the products, and in the case of char, potential fire.

Based on the process flow diagram in Figure 9 heat exchangers will be required for the following:

- Pre-drying of the feedstock
- Indirect heat application in the reactor
- Heavy volatile condensation
- Light volatile condensation
- Char cooling
- Char cooling loop recovery

These operations are not all identical as they have different limiting factors such as:

- Operating temperature ranges – This is one of the most crucial variables as it determines which heating methods or medium apply. For example steam can be used for heating process temperatures up to approximately 100 °C under atmospheric pressure. High pressure steam is more expensive due to the increased pressure. Failure to sustain dry steam at high pressure can cause corrosion problems.

- Physical properties of the mediums involved - generally, the heat exchanging medium phase change points (e.g boiling point, dew point) will have to be verified to ensure there is no phase change. Some machines such as pumps will become less efficient if a two-phase medium is used. For the pyrolysis plant, heating is used to evaporate the water from the feedstock, and melt, sublime or evaporate various components in the feedstock during pyrolysis. Cooling is needed to condense the heavy and light volatiles after the pyrolysis reaction, as well as to recover heat from the char.

### 2.3.3.1 Prospective Heat exchangers

This section briefly describes the prospective heat exchanger types that might be considered in a pyrolysis plant.

**Heat Exchanger Type:** Double pipe

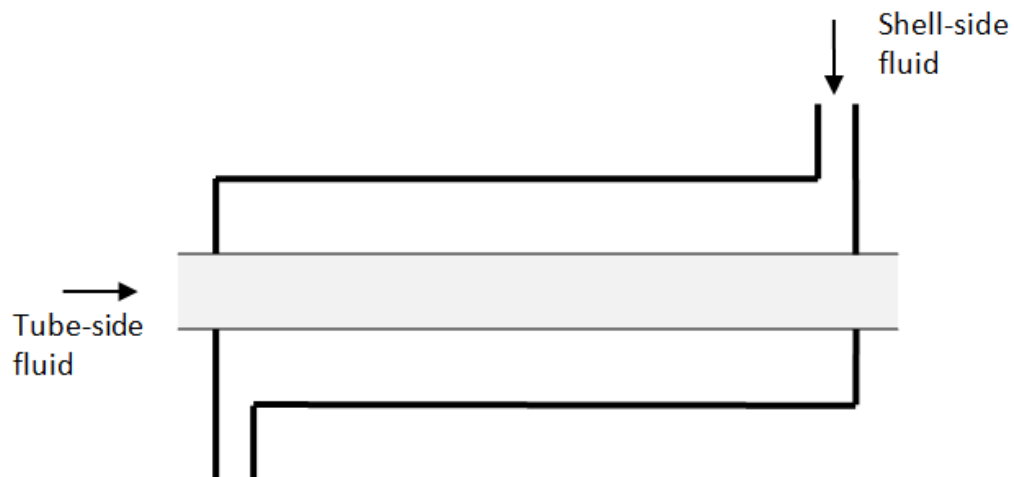


**Figure 18.** Double pipe heat exchanger in counter-current flow<sup>1</sup>.

<sup>1</sup> Viewed from [http://www.mapleprimes.com/view.aspx?sf=100529/317244/figure1\\_Double\\_Pipe\\_.png](http://www.mapleprimes.com/view.aspx?sf=100529/317244/figure1_Double_Pipe_.png)

### Performance Description:

This is the simplest form of shell and tube heat exchanger, it is easy to maintain and analyse. However, it requires large flow rates of heat exchange medium in cases of high heat transfer. This is because it does not possess the same amount of heat-transfer area per unit volume as a shell and tube heat exchanger of the same shell dimensions.

This can be used to heat reactor walls because it allows for simple indirect heat transfer. It can also be used for cooling jackets for the char and flash tank using either water or air depending on the required amount of heat transfer. Water can be used for higher heat fluxes.

The main limitation of using this heat exchanger is associated with not having sufficient contact time for short length pipes. This can be countered by having a helical path for the fluid in the shell.

### Heat Exchanger Type: Shell and tube

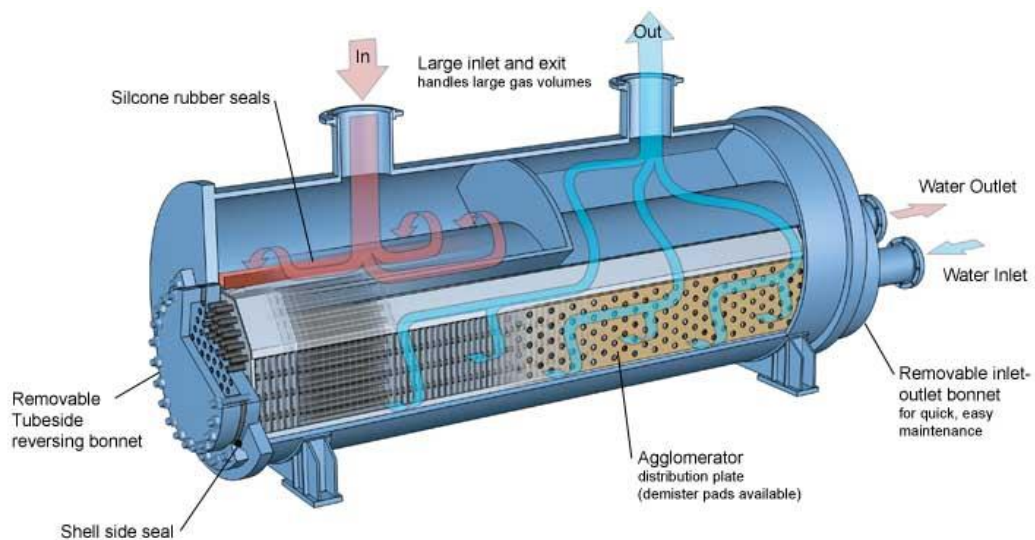


**Figure 19.** Typical shell and tube heat exchanger (ACUSIM).

### Performance Description:

The shell and tube design is commonly used because of its high heat-transfer area per unit volume. This is achieved by placing a large number of small diameter tubes inside a shell that doubles as a pressure vessel. The design of this heat

exchanger has been standardised by the Tubular Exchanger Manufacturers Association (TEMA).

The shell and tube heat exchanger would have a low score in regards to practicality for this process. The heat exchange is being used for phase change of volatile products. Condensable volatiles such as bio oil and tars have high fouling tendencies which will reduce heat exchange efficiencies and increase maintenance costs associated with cleaning.

Ideally, since the condensate will be fouling, it could be passed through the shell side, in accordance with design heuristics however this does not address the corrosion issues associated with the bio-oil.

**Heat Exchanger Type: Air cooled (fin-fan)**

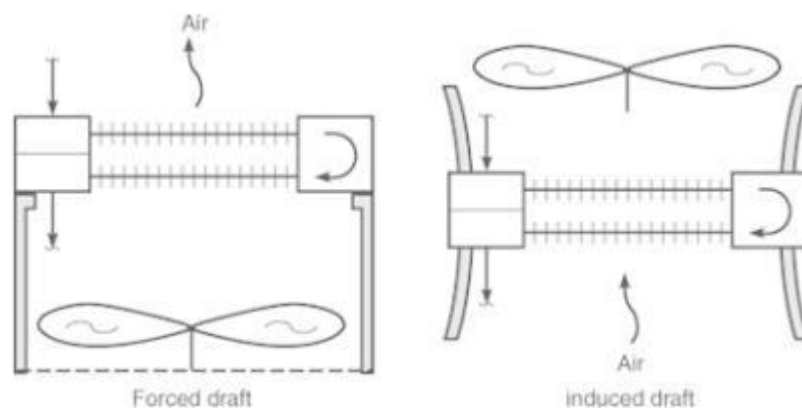


**Figure 20.** Air cooled (fin-fan)<sup>2</sup>.

**Performance Description:**

This type of heat exchanger is normally used in scenarios where water is scarce and costly. The conventional design is made of pipes or tubes with fins attached to increase the surface area available for heat transfer. This in turn lowers the outside

<sup>2</sup> Viewed from [http://images.books24x7.com/bookimages/id\\_26162/f0194-01\\_thm.jpg](http://images.books24x7.com/bookimages/id_26162/f0194-01_thm.jpg)

thermal resistance so that it approaches the thermal resistance inside the tube. The fluid passes through the tubes and the air blows across the tubes and fins.

This can be used for preheating of air intake in heat recovery operations from the char or the oil product line. The product would pass through the pipe or tube.

### Heat Exchanger Type: Compact

- a) Plate-and-frame

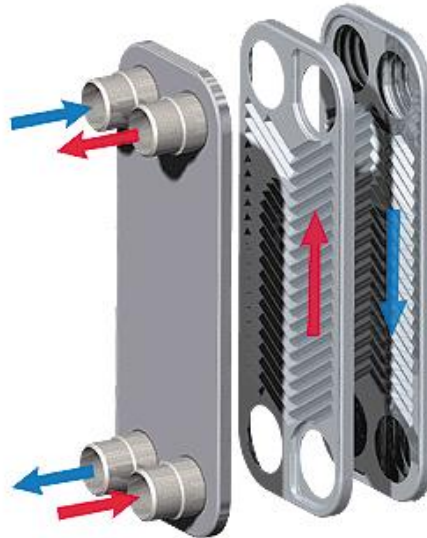


**Figure 21.** Plate and frame heat exchanger<sup>3</sup>.

- b) Spiral-plate



<sup>3</sup> Viewed from [http://2.bp.blogspot.com/\\_L-cNNS3j7UU/S52ZVudIeTI/AAAAAAAAOw/HSTL3RBoLfM/s400/movingheatexchanger.gif](http://2.bp.blogspot.com/_L-cNNS3j7UU/S52ZVudIeTI/AAAAAAAAOw/HSTL3RBoLfM/s400/movingheatexchanger.gif)

c) Spiral-tube

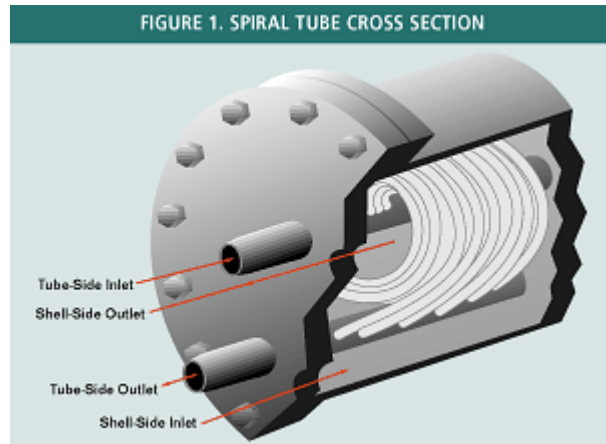


**Figure 22.** Spiral tube heat exchanger cross section<sup>4</sup>.

A spiral tube heat exchanger uses multiple parallel tubes connected to pipe-like manifolds to create a tube-side flow path.

d) Plate-fin

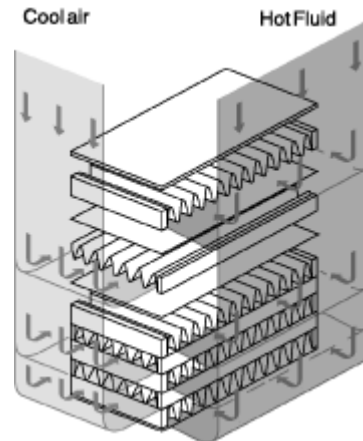


**Figure 23.** Plate-fin heat exchanger<sup>5</sup>.

---

<sup>4</sup> Viewed from [http://4.bp.blogspot.com/\\_l-cNNS3j7UU/S52Wijynjl/AAAAAAAAAOo/1radEZhTums/s200/Picture1.jpg](http://4.bp.blogspot.com/_l-cNNS3j7UU/S52Wijynjl/AAAAAAAAAOo/1radEZhTums/s200/Picture1.jpg)

<sup>5</sup> Viewed from <http://www.mxmach.com/wp-content/uploads/2011/06/plate-fin-2.gif>



### **Performance Description:**

As the name suggests, these heat exchangers are compact and occupy a small space. They are normally used when the fluids exchanging heat need to be kept clean. They have high heat transfer coefficients due to the corrugated plates on the heat exchanger surfaces. The compact heat exchanger is used in applications where a high heating flux is required without increasing thickness of the heat exchange medium. By having a coil as the path or corrugated surfaces, the residence time of the heat exchange medium is increased thus increasing the amount of heat exchange for a fixed volume.

### **2.3.3.2 Design considerations**

The heat exchangers described in the preceding section will have different levels of appropriateness based on compatibility with the fluids exchanging heat. The main fluids of concern will be the bio-oil (both light fraction and heavy fraction), hot volatiles stream, syngas and water or air. The bio-oil is a very dirty, acidic fluid. Other products from pyrolysis with the exception of the char can be treated similarly. The air is the cleanest heat exchange fluid being used while water is clean it still has the potential to foul and scale materials at elevated temperatures. But water has high heat transfer capability. Consideration will be needed to account for equipment corrosion, temperature crossover and fouling.

#### **2.3.3.2.1 Corrosion**

The bio-oil has been identified to be corrosive due to its acidic pH ranging from ~2-4. Basu (2010) offers the following solutions:

- Contact avoidance
- Corrosion-resistant barriers
- Process adjustments
- Corrosion resistant materials

The most practical solution in this case appears to be material selection. It should be noted that there will be a trade-off between heat exchange performance due to conductivity potential and corrosion resistance.

Materials used in heat exchangers will depend on the type of heat exchanger being deployed and the materials being processed. For example, in cases where biomass is being processed, it is advised that the material being used does not promote the formation of biofilms as these generally increase the potential for fouling to occur.

**Table 17.** Common materials used in heat exchangers (Intelligence 2012).

Material	Comment
High conductivity coppers	Best heat exchange, but poor corrosion resistance.
Brasses	Poor corrosion resistance
Wrought martensitic stainless steel	Good performance but heavier than copper
Aluminium bronzes	An economical and practical choice

Basu (2010) presented a list of materials in order of least-to-most corrosion resistance:

- Stainless steel
- Nickel-based alloys
- Titanium
- Tantalum
- Niobium
- Ceramics

Traditional ceramics cannot be considered due to their poor thermal properties which might lead to difficulties such as thermal shock. Thermal shock is the fracture mechanism experienced by traditional ceramics due to rapid uneven heating or cooling.

### **2.3.3.2.2 Temperature Crossover**

The biggest barrier to be faced in recovering heat in the process is upgrading low grade heat. It is not possible to use heat from a low temperature to heat a process at a higher temperature without the use of a heat pump. Industrial heat pumps can be used for temperatures of up to ~ 240°C

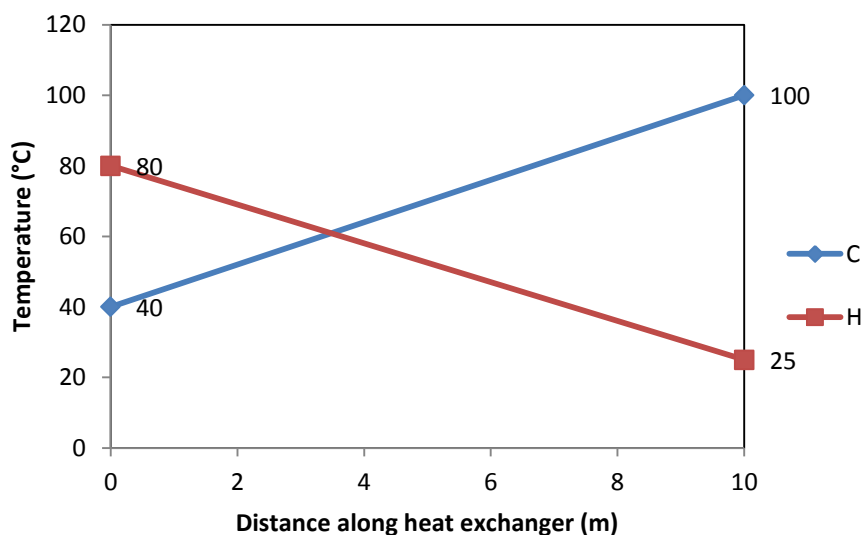


**Figure 24.** Heat cross exchange schematic.

The temperature vs position graph (Figure 24) shows an extreme case of temperature cross-over where the cold stream is heated past the initial temperature of the hot stream. This is not practically feasible without the aid of the heat pump. Further on, heat exchange is more efficient when the temperature difference between the target temperatures of the two streams is above the minimum approach temperature threshold. The value of the minimum approach temperature will depend on properties of the two substances exchanging heat but is typically around 10 to 20°C for liquids and can be higher for gases due to the lower heat capacities (Peters 1991, Moyers. and Baldwin 1999, Branan 2005). Having a high approach temperature will facilitate faster heat exchange due to a higher temperature driving force.

### 2.3.4 Syngas Recovery System

Similar to coal, biomass pyrolysis is associated with the liberation of many unwanted gases. These unwanted gases may include hydrogen sulphide (H<sub>2</sub>S), nitrous oxides (NO<sub>x</sub>s), polycarbonate aromatics poly aromatic carbons (PAH), etc. Classification of compounds developed by the Energy Research Centre of the Netherlands is presented in Table 18.

**Table 18.** Tar classification system defined by the Energy Research Centre of the Netherlands (ECN).

Class	Type	Examples
1	GC undetectable tars.	Biomass fragments, heaviest tars (pitch)
2	Heterocyclic compounds. These are components that generally exhibit high water solubility.	Phenol, cresol, quinoline, pyridine
3	Aromatic components. Light hydrocarbons, which are important from the point view of tar reaction pathways, but not in particular towards condensation and solubility.	Toluene, xylenes, ethylbenzene (excluding benzene)
4	Light poly aromatic hydrocarbons (2-3 rings PAHs). These components condense at relatively high concentrations and intermediate temperatures.	Naphthalene, indene, biphenyl, anthracene
5	Heavy poly aromatic hydrocarbons ( $\geq 4$ -rings PAHs). These components condense at relatively high temperature at low concentrations.	Fluoranthene, pyrene, crysene
6	GC detectable, not identified compounds.	Unknowns

These gases will need to be extracted before the syngas can be used in most applications with the exception of direct combustion (Rezaiyan and Cheremisinoff 2005, Sharma, Dolan et al. 2008, Könemann 2009, Anis and Zainal 2011). This involves macroscopic techniques such as dust removal, dehumidification and scrubbing. Scrubbing is the extraction of unwanted compounds from the raw gas in an attempt to obtain a gas of higher quality. Compared to raw gas, higher quality gas has a higher specific heating value; produces cleaner combustion emissions and fewer issues with handling in regards to human health, corrosion and fouling of equipment. It is for these reasons that the presence of tars and particulates in syngas are seen as the biggest barrier faced by bio-syngas in its acceptance as a reliable fuel (Rezaiyan and Cheremisinoff 2005, Sharma, Dolan et al. 2008, Könemann 2009, Anis and Zainal 2011).

Gas cleaning technologies can be split into three groups depending on the principles or separation.

- Physical/ mechanical separation
- Catalytic cracking
- Thermal cracking

### 2.3.4.1 Physical/Mechanical Techniques

Physical and mechanical techniques are generally used for the capture of particulates in gas streams and can also be deployed to remove tars and unwanted volatile compounds (Rezaiyan and Cheremisinoff 2005). They work on either physical properties such as solubility and mass transfer phenomena or mechanical elements such as centrifugal forces.

#### 2.3.4.1.1 Dust Removal Technology

Dust removal technology in industry will vary based on the use of the product gas. For example, gas engines will require different standards compared to gas turbines or a simple gas burner as shown in Table 19.

**Table 19.** Comparison of particle limit specifications (Anis and Zainal 2011).

	Unit	IC engine	Gas turbine
Particles	mg/Nm <sup>3</sup>	<50	<30
Particle size	µm	<10	<5
Tar	mg/Nm <sup>3</sup>	<100	<5
Alkali metals	mg/Nm <sup>3</sup>	-	0.24 <sup>i</sup>

The conventional options for particle removal are:

- Gravity settling chambers
- Cyclone filters
- Fabric filters and membranes
- Flocculation agents

The preference of these options will depend on the particle size and operating temperature e.g. cyclones will be limited to ~300°C (Chibante, Fonseca et al. 2007, Sharma, Dolan et al. 2008, Richardson, Blin et al. 2012). Although fabric filters cannot withstand high temperatures, ceramic filters can be used in their place. Figure 25 shows expected separation efficiencies of equipment used for particle removal.

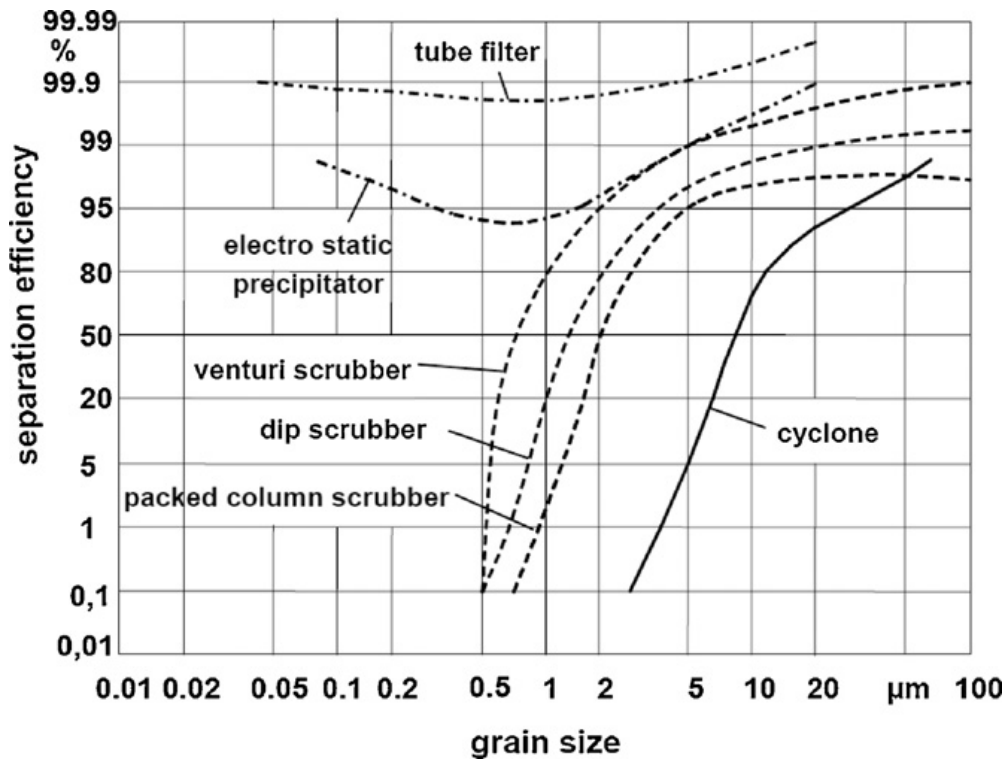


**Figure 25.** Separation efficiency with respect to particle grain size for a variety of equipment (Anis and Zainal 2011).

### 2.3.4.1.2 Further physical/ mechanical separations

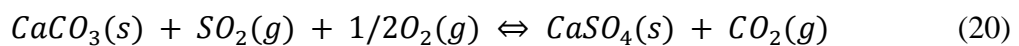
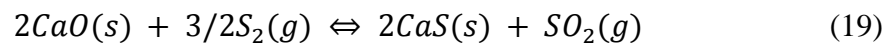
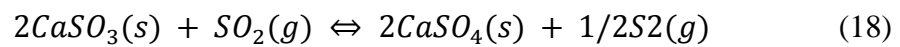
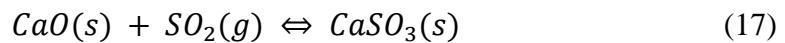
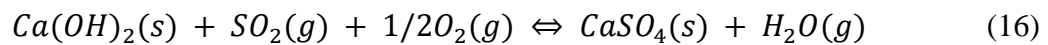
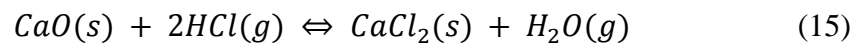
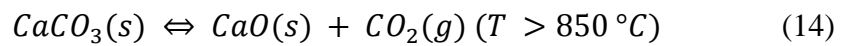
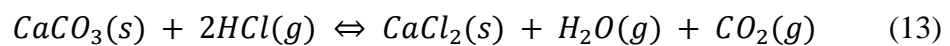
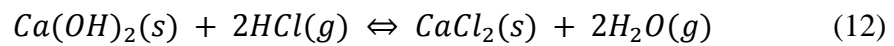
Apart from the removal of particulates, gas scrubbing is also deployed for the selective extraction of specific compounds from the gas stream. Mechanical/ physical gas scrubbing systems are typically classified as either dry or wet types.

**Table 20.** Physical/mechanical scrubbers.

Basic type	Equipment
Dry	Cyclone, rotating particle separators(RPS), Electrostatic precipitators (ESP), bag filters, baffle filters, ceramic filters, fabric/ tube filters, sand bed filters, adsorbers, etc.
Wet	Spray towers, packed column scrubber (wash tower), impingement scrubbers, venture scrubbers, wet electrostatic precipitators, OLGA systems, wet cyclones, etc.

Dry scrubbing can be used at higher temperatures, prior to any gas cooling (Rezaiyan and Cheremisinoff 2005, Sharma, Dolan et al. 2008, Ohtsuka, Tsubouchi et al. 2009, Anis and Zainal 2011, Richardson, Blin et al. 2012). Dry techniques are preferred to wet because they lower capital and operating costs and

requiring less space , with acid removal efficiencies higher than 90% (Chibante, Fonseca et al. 2007) For example fine dispersed powder is fed into the gas stream in one end of the vessel and specific compounds including tars in the gas react and adsorb onto the particle surface. The high temperature promotes reactivity of the powder and compounds and the products are removed via a cyclone at the exit. Alternatively, through task integration, the cyclone can be used as a reactor. Liu et al (2002) provides a list of reactions that can be used to describe dry scrubbing of acid gasses using  $\text{Ca(OH)}_2$ .

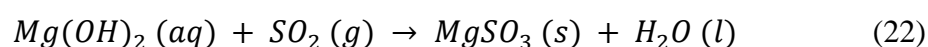


Wet scrubbing is generally more effective at particle and tar removal due to the higher rates of mass transfer associated with a liquid medium compared to a solid. They work using the principle of solubility (Sharma, Dolan et al. 2008). Water, being relatively cheap is the generic scrubbing fluid used, however, this is normally associated with poor performance due to saponification, poor regeneration efficiency, low solubility of hydrocarbon compounds, clogging of apparatus and high expense of wastewater treatment of the sludge product. These can usually be countered by using an organic fluid as the scrubbing medium. Emulsions containing cooking oil or diesel oil are good alternatives as the oil additives support the solvent's tar cleaning properties and reduce fouling (Sharma, Dolan et al. 2008, Anis and Zainal 2011).

Wet scrubbing can also use aqueous solutions which may contain alkaline salts or amino-based compounds (Kapdi, Vijay et al. 2005). The ions in these solutions react with impurities and the products are precipitated and separated from the liquid phase. As in the case with flue gas desulphurisation (FGD) systems,  $\text{Ca}(\text{OH})_2$  (lime) slurry, the reaction also produces  $\text{CaSO}_3$  (calcium sulfite) and can be expressed as:



In the case where a  $\text{Mg}(\text{OH})_2$  (magnesium hydroxide) slurry is used, the reaction produces  $\text{MgSO}_3$  (magnesium sulfite) and can be expressed as:



Prospective mediums for extraction of contaminants include:

- Water
- Oil water emulsions
- Monoethanolamine (MEA)
- Diethanolamine (DEA)
- Digylcolamine (DGA)
- Methyldiethanolamine (MDEA)
- Sodium hydroxide
- Potassium hydroxide
- Calcium hydroxide
- Magnesium hydroxide

#### **2.3.4.2 Catalytic Cracking**

Cracking is the process by which tars are broken down from heavier organic molecules into lighter ones. Catalytic cracking works on the principle of introducing another chemical either during the bio-syngas production stage or after to facilitate the formation of smaller molecules from heavier ones. When present in the production stage a catalyst might also inhibit the formation of tars to an extent and promote the selectivity of syngas components.



Sutton et al (2001) provides the following specifications for catalysts:

1. The catalysts must be effective for removing tar
2. If the desired product is syngas, the catalysts must be capable of reforming methane
3. The catalysts should provide a suitable syngas ratio for the intended process
4. The catalysts should be resistant to deactivation as a result of carbon fouling and sintering
5. The catalysts should be easily regenerated
6. The catalysts should be strong
7. The catalysts should be inexpensive

There has been a lot of research on potential catalysts for tar removal from syngas. Anis and Zainal (2011) have done a very good review on the use of catalytic cracking and has classified them into six groups

1. Nickel-based catalysts
2. Non-nickel metal catalysts
3. Alkali metal catalysts
4. Basic catalysts
5. Acid catalysts
6. Activated carbon catalysts

The last category should be noted because the production of char. Char is predominantly made of carbon; therefore it will have similar properties. However, activated carbon has a higher pore density compared to normal char.

Anis and Zainal (2011) go further and lists some equipment used for catalytic cracking of tar, highlighting the normal operating conditions and performance (Table 21).

**Table 21.** Catalytic cracking equipment (Anis and Zainal 2011).

	Temperature (°C)	Particle reduction (%)	Tar reduction (%)
Sand bed filter	10 – 20	70 – 99	50 – 97
Wash tower	50 – 60	60 – 98	10 – 25
Venturi scrubber			50 – 90
Rotational atomizer	<100	95 ± 99	
Wet electrostatic precipitator	40 – 50	>99	0 – 60
Fabric filter	130	70 – 95	0 – 50
Rotational particle separator	130	85 - 90	30 – 70
Fixed bed tar adsorber	80		50
Catalytic tar cracker	900		>95

### 2.3.4.3 Thermal Treatment

#### 2.3.4.3.1 Thermal Cracking

Thermal cracking involves holding the tars at high temperatures of 700 – 1250°C for a specified residence time. The high temperature excites the tar molecules reducing the stability of the molecules, favouring the formation of the smaller compounds (Ohtsuka, Tsubouchi et al. 2009, Anis and Zainal 2011). It is fairly obvious to see why this technique is seldom used because it will require the product gas to be held at temperatures much higher than those used in the pyrolysis reactor for long periods of time. With increased residence time the volume of the reactor will need to increase..

#### 2.3.4.4 Other Syngas Recovery Design Concerns

This section considers other aspects related to syngas recovery past the need to keep it clean and reliable. these include; processing characteristics such as pressure and flow regulation; and hazard management of fires, explosions, toxic gas emissions and material handling concerns. Pressure and Flow Regulation

The decomposition rate of the feedstock varies based on the residence time and its instantaneous temperature. This means that the production of volatiles will vary, therefore post processing of the syngas will need to account for this. A buffer system, such as a pressurised holding tank, can be used to minimise the effects of fluctuating production rates, and release the gas at a controlled flow rate (Apt, Newcomer et al. 2008).

### **2.3.5 Hazard Management**

The pyrolysis process, by definition should be designed to ensure that no air enters the system. Having an air-tight system will ensure there are only minute product losses. However, achieving this may not be feasible, therefore the plant should be designed to cater for any spillage or escape of materials in a safe manner (Peters 1991, Moyers. and Baldwin 1999, Branan 2005, Rezaiyan and Cheremisinoff 2005). The main hazards associated with the process in order of likelihood are; fires, explosions and toxic release. They are ordered in this way because even though toxic release is potentially more dangerous to life than an explosion which in turn might injure more people more severely than a fire, fire is the most frequently occurring hazard and that explosion certainly and toxic release possibly are usually consequences of serious fires (Thompson 1995).

#### **2.3.5.1 Fires**

The pyrolysis system will operate under anaerobic conditions. This means there is a higher risk of fires being caused by extreme temperatures and flammable gas escape from the reactor. Pipeline pressures can be monitored continuously to assess for any leaks.

#### **2.3.5.2 Explosions**

Other than fires, there are two main contributors to explosions in pyrolysis units are dust and syngas instability. Fine particles from the char dust can spontaneously combust and explode. Gas clean-up technologies such as cyclonic filters can be installed to minimise this risk.

#### **2.3.5.3 Toxic Gas Emissions**

Pyrolysis of biomass at temperatures below 600°C has been known to produce PAHs, PCBs, dioxins and other toxic compounds that will pose a threat to human health and can also be classified as greenhouse gases. These can be directly oxidised via combustion in the burner or extracted using a scrubber.

#### **2.3.5.4 Material Handling Issues**

Traditionally most of the required hazard management systems are integrated into the system design. This makes the system slightly more complex but also cheaper to run in the long run. The aim of the integration is to allow as much automation of the process as practically feasible so that the plant operators are not put in a scenario where they have to come in contact with toxic compounds. E.g. gas recovery systems are designed to be airtight. Any pressure vessels used for storage will have pressure release valves and also be designed to leak before explosion. More details of material handling practices can be found in the Appendix under MSDS for fine sawdust.

### **2.4 Process Economics**

Pyrolysis has been the focus of many ventures in industry; however, many plants usually end up unsuccessful due to the endothermic demands overwhelming the economic feasibility of the process.

Capital costs will mainly comprise of equipment used to set up the plant. Other costs will include resource consents, working capital that will be used to commission the plant and technology licenses.

The economic model for the pyrolysis process is based the cash-flow streams shown in Figure 26.

The effects of the specified cash-flow streams will be dependent on the feedstock type being considered. This is because the independent variables have different boundary conditions for each feedstock (Sichone 2012). Charts can be plotted for a number of cases which will include sensitivity analyses of variables that affect the highlighted cash-flow streams to determine the conditions needed to achieve an economically viable pyrolysis process.

A flexible economic model will provide information on the fixed and independent variables. This will allow for easy adjustment of the variables to determine which variables can be manipulated in order to achieve economic feasibility. Following

list shows the main variables that affect the pyrolysis process cash-flow streams as identified in the author's previous studies (Sichone 2012).

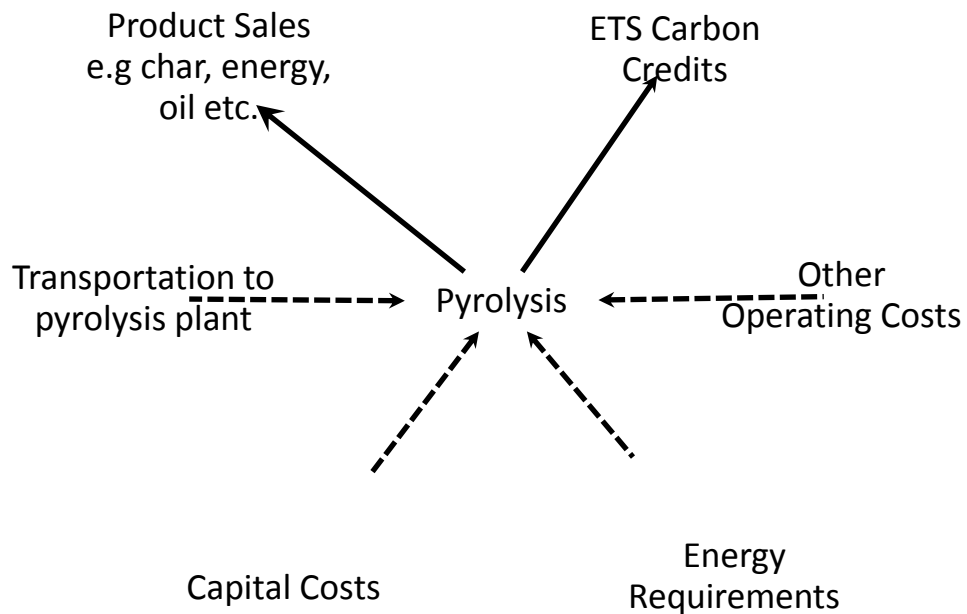


**Figure 26.** Directional schematic of cash-flow streams that can be associated with economics of pyrolysis (Sichone 2012).

### **Independent Variables**

- Initial moisture content – This will determine whether the feedstock needs to go through any dehydration processes prior to being fed into the reactor. Drying is an expensive process therefore it would be preferred
- Pre-dried moisture content – in combination with the initial moisture content this will determine the amount of energy used to pre-dry the feedstock and also determines how much moisture is allowed into the reactor.
- Annual feedstock consumption – This will determine the scale of operation. Previous studies such as the Waikato Regional Council and partners' pyrolysis project have shown that the scale of operation will

affect the profitability of the process. The larger the plant capacity, the more likely it is to be economically viable.

- Reactor operating temperature – This will affect the quality of the products, the yields and costs incurred in terms of heat demand. The options for heat delivery can also be affected by the reactor operating temperature.
- Process efficiencies – Process efficiencies are generally limited by technology and processing parameters. The economic model will be designed to use a range of process efficiencies reported by literature and compare them to those of the pilot plant. This way the feasibility assessment will provide results for the pilot plant setup and show the maximum and minimum predicted by literature values.
- Biochar price – the biochar selling price is still unknown but a market scan focussing on biochar produced from woody biomass will be conducted to show the potential revenue that could be generated.
- Energy pricing rates – these rates will be based on current energy rates but can be adjusted for future calculations using the marketing trends.
- Procurement costs – The sawdust currently has a value of \$4 per tonne. This procurement cost will be weighed up against the revenue potential of the pyrolysis products. To assess the profitability of pyrolysis as a means of maximising the value of the sawdust. This cost does not consider the cost of transportation.
- Effluent Disposal costs – The process will deploy recycling as much as possible to reduce the amount of waste produced. However in the case where waste such as processing water needs to be disposed. Disposal costs such as material handling and resource consents will be incurred.

### **2.4.1 Current Market Scan**

There has been little evidence of commercial biomass pyrolysis ventures. The few ventures cited typically give little information. However, based on the literature viewed a number of active pyrolysis projects that have been started or are in the start-up process are listed in Table 22.

**Table 22.** Current commercial pyrolysis ventures.

Company	Technology	Market Cap	Description
<b>Best Energies Inc</b>	Pyrolysis/ Gasification		Wide range of domestic, industrial and agricultural residues/wastes for Char and Syngas, (no oil) Demonstration 300kg/hour
<b>International Environmental Solutions Corp</b>		n/r	All types of biomass, Electricity and other saleable by-products, Demonstration 50 tonne/day
<b>Taylor Biomass Energy Recycling Pacific Pyrolysis</b>	Gasification	n/r	Construction and demolition debris, waste wood, MSW for Syngas product, Unknown scale
		n/r	Industrial/Agricultural residues and wastes by Agrichar Syngas for electricity and heat , Demonstration at Somersby, NSW
<b>Renewable Oil Corporation Pty Ltd</b>	Pyrolysis/ Gasification	n/r	Woody biomass to BioOil 70%, Electricity, heat, char, value added chemicals for Dynamotive
<b>Crucible Carbon</b>		n/r	Lignocellulosic feedstocks (Agri and forestry residues) Energy (Syngas) and char for Demonstration 100-400 kg/hr
<b>KIOR</b>	BFCC	~\$1 billion	“Biomass Fluid Catalytic Cracking” is 2 step continuous process. Pilot unit – 9000 hours, .025 BDT/day, 250 catalyst systems tested . Demo unit – 3000 hours, 10 BDT/day, produced 32k g (762 bbl) RCO. First Commercial Unit – 500 BDT/day, \$222MM (including hydrotreater). - Originally targeted at \$190MM and delayed from early 2011 to mid 2012
<b>Ensyn</b>	Pyrolysis	Private	Patented Rapid Thermal Processing (RTP™) Technology. Renfrew, Ontario Plant - 100 TPD Capacity. Upgrading UOP partnership called Envergent
<b>Rentech</b>	Gasification/Fischer-Tropsch	\$450 million	Patented Technology To Produce Synthetic Fuels (Primarily Petcoke Feedstock But Can Use Biomass). Sand Creek, Colorado - Demonstration Plant In Operation . Natchez, Mississippi - Announced Plans In June 2008 To Build 1,600 BPD in 2011 to date there is no update on progress

---

**Table 22. Current commercial pyrolysis ventures.**

---

Company	Technology	Market Cap	Description
<b>Dynamotive</b>	Pyrolysis	\$45 million	Patented Technology Proven With 4 Plants (2 Pilot & 2 Commercial). West Lorne, ON – 130 TPD / Guelph, ON– 200 TPD Capacity. Upgrading IFPen / Axens Partnership! Most advanced value chain / market reach through AXENS worldwide with oil refiners.
<b>Choren</b>	Gasification/Fischer - Tropsch	Private	3.9 Million Gallons / Year Synthetic Diesel Plant Commissioned in Dec 2009. Feedstock Is Forest Residue And Wood Wastes



## 2.4.2 Pyrolysis Technology Patent Citation Report

In addition to the market scan, a patent search will also provide a good understanding of progressive trends in the field of biomass pyrolysis development. The patent search was conducted using the American Chemical Society (ACS) database.

Initially, English and patents options were used as limiters, the following key-word phrases were used:

- ‘biomass pyrolysis’
- ‘biomass gasification’
- ‘biomass torrefaction’
- ‘biomass conversion’

The search results were categorized yearly to give a general indication of the trend of interest in biomass conversion technology. Language limiters were removed to give a broad global understanding of the development of the technology.

The patent search showed that biomass gasification has twice the number of patents as biomass pyrolysis despite the former being noted as less environmentally friendly (Table 23). Biomass gasification has proven to have higher economic favourability as the products are normally gas and electricity which are easily marketable. Biomass pyrolysis has been noted to provide environmental benefits via carbon sequestration and other soil related bioremediation approaches and alternative liquid fuels such as biodiesel. However, the market for these products has not been established and as a result cannot compete with gasification products market.

**Table 23.** Patent search hits for a combination of keywords.

Keyword	References containing keyword as entered		References containing the concept of the keyword	
	1	1,2	1,	1,2
Biomass pyrolysis	170	494	434	1,439
Biomass gasification	217	1,248	599	2,801
Biomass torrefaction	63	83	63	83
Biomass conversion	214	157	822	459

1: Only English text

2: No Language limiters

Biomass torrefaction received the least number of patent applications. This is because torrefaction is a very simple process. It is commonly used for coffee roasting and wood processing for furniture. In the case of coffee roasting the coffee beans are dried and lightly roasted to enhance their flavour and brittleness for easier grinding. In the case of furniture wood processing, torrefaction is used to realign the fibrous structure as it dries. This allows for manipulation of shape/warping for aesthetic and more importantly mechanical benefits. Other applications for torrefaction include pellet production and manufacturing of wood based composite materials such as medium-density fibreboard (MDF).

Biomass conversion showed the least promising results despite having more than that of the preceding search. This is because a large majority of the patents cited see biomass conversion subject as a chemical/bio-chemical process where digesters and chemical solutions are used to break down the biomass. The patents were not necessarily relevant to the scope of the thesis. However, they add another dimension to alternative pathways for biomass conversion.

The overall trend showed an increase in the development of these technologies (Figures 27 to 30). The earliest relevant patent on record according to the ACS database was given in 1982, following the oil crisis of 1970s (Slesser. and Lewis. 1979, Boyles 1984). There seemed to be little interest in biomass pyrolysis technology up to the late 2000's.

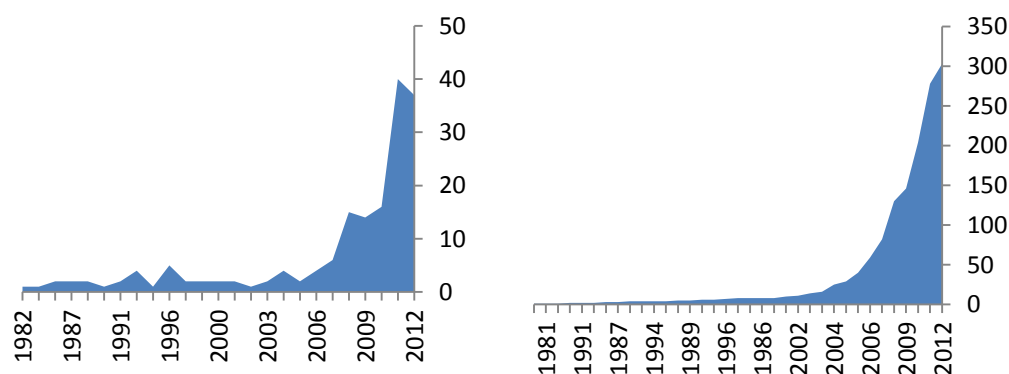


**Figure 27.** Biomass pyrolysis patent yearly application count (a) to the left English patents only (b) to the right all patent search results no language limiters.

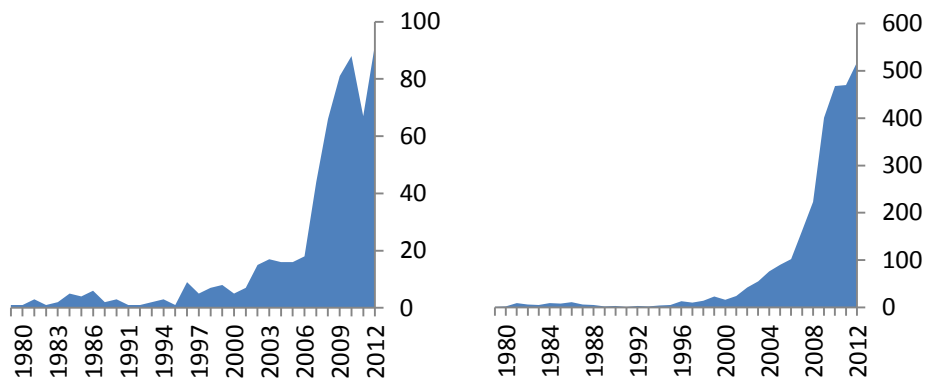


**Figure 28.** Biomass gasification patent yearly application count (a) to the left English patents only (b) to the right all patent search results no language limiters.

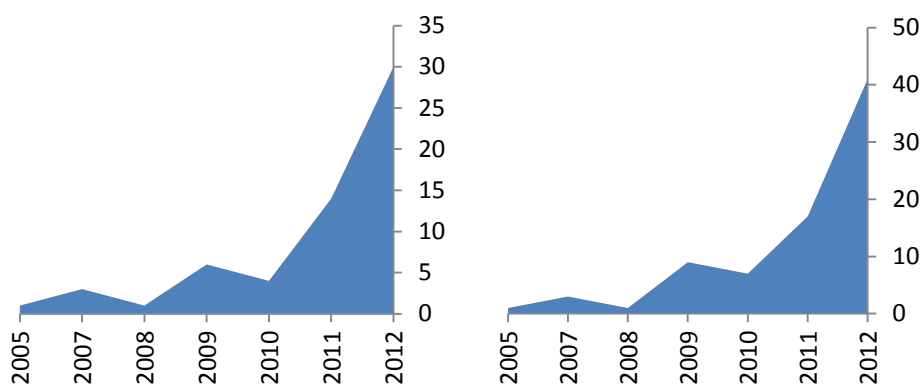


**Figure 29.** Biomass torrefaction patent yearly application count (a) to the left English patents only (b) to the right all patent search results no language limiters.

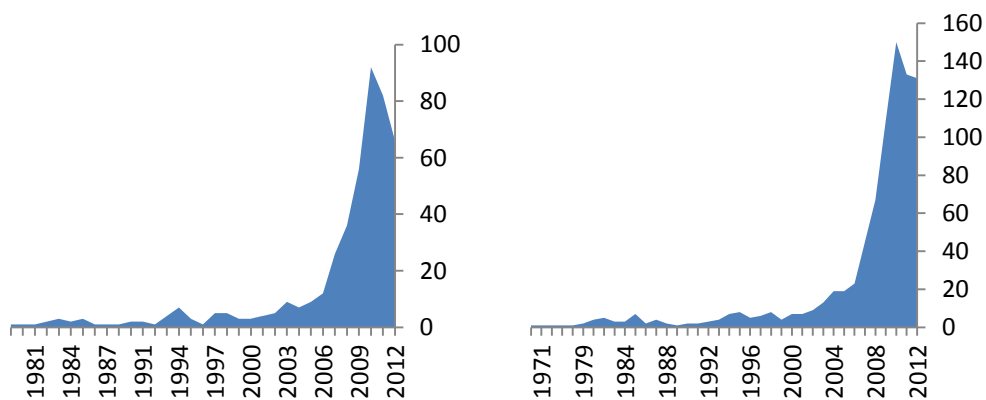


**Figure 30.** Biomass conversion patent yearly application count (a) to the left English patents only (b) to the right all patent search results no language limiters.

Biomass pyrolysis and gasification have been around for centuries however, it was rendered unviable by the discovery of fossil fuel reserves which initiated the industrial age. The oil shortage crisis of the 1970's initiated an interest in the commercialisation of this technology as fossil derived fuel prices increase and the perceived limited abundance of fossil fuel reserves. The Kyoto protocol was signed in 1997 and scheduled to be in effect in 2005 might have boosted interests in green energy technology and thus government and private institutions funded a lot research in this topic.

Based on the observation of global events and trends at the critical points in time during the development of biomass pyrolysis technology thus far, it is obvious that political views play a huge role in the perception of this technology.

The patent search has shown a dip or plateau after the year 2010. Although it might be too early to comment on this, the following reasons might explain this:

- It appears the delay in implementing Kyoto protocol legislation and a carbon trading market has reduced the investment in this sector.
- The number of successful commercial ventures upscaled from research and lab scale findings is limited. Many patents have been demonstrated on lab scale and sometimes even up to a pilot plant scale. A saturation of unproven technology in the intellectual property market might be discouraging to potential investors.
- The current economic recession which was declared mid-2008 might have caused a shift in focus for most governments. Finding quick and direct remedies to declining economies proved to be a higher priority.

The technology being presented in these patents is technically important for the growth of this sector. However, the next step logical move would be to develop a product that can be commercialised.

## **2.5 Summary**

The literature review has confirmed that there has been a lot of research done on biomass pyrolysis. A large part of this research is solely based on understanding

the nature of this complex process. Predicted energy demand forecasts have highlighted the need for the development of this technology.

Whilst this is meaningful, and technically important, the issue at hand remains to be the missing link which will aid in converting the knowledge gained from all this research into commercial schemes that are at par or at least comparable to the bar for clean energy set by schemes such as wind or geothermal.

Most of the equipment used in biomass pyrolysis processing plants is based on equipment used in coal, oil and gas plants.

The poor economics of the process are caused by a lack of market for the biochar and bio-oil. The stalling of the carbon trading scheme is proving to be a hindrance to the commercialisation of pyrolysis. Another aspect that has been identified is the sensitivity of the economics to the scale of operation. A number of preliminary economic feasibility assessments have theoretically proven that by increasing the scale of a process the profits increase at a higher rate than the operating costs. Based on the ethanol production scheme in Brazil, it is clear that a large scale will improve process economics. Social integration of the plant could also improve chances for economic feasibility. Social integration relates to collaborative efforts such as waste heat being sold to neighbouring plants.

# **Chapter 3.**

## **Methodology**

### **3.1 Introduction**

This chapter presents the methods used for the experiments reported in this thesis.

There are three main areas of experimental work:

1. Feedstock characterisation – This included determining characteristic properties of the feedstock such as, moisture content, ash content, calorific value, and elemental composition analysis. The drying characteristics and decomposition reaction kinetics were also investigated.
2. Pilot plant trials – This involved pyrolysis of sawdust using the Lakeland Steel pilot plant at different processing conditions by manipulating moisture content, reaction temperature and auger speed. The product yields for the different configurations were collected to investigate the main effects and compound effects using a three factor-three level experiment approach.
3. Product characterisation – this was similar to feedstock characterisation and involved determining product characteristics such as, moisture content, ash content, calorific value, and elemental composition analysis.

### **3.2 Reagents**

Pine sawdust provided by Lakeland Steel was used as the feedstock. This was directly used in feedstock characterisation experiments and the pilot plant trials. The product characterisation experiments used the biochar, and syngas. A batch of oil was also analysed. The analysis techniques did not need the addition of other reagents with the exception of pure nitrogen and a standard used for calibration of the GC.

### **3.3 Equipment**

In addition to the pilot plant provided by Lakeland Steel limited, the following equipment was used:

- Contherm digital series oven

- Jetlow Shimaden SR53 Furnace
- TA Instruments SDT 2960 Simultaneous DTA-TGA
- Perkin Elmer Autosystem Arnel gas chromatography system
- Perkin Elmer Ramanstation 400F series raman spectrometer
- Third party institutions – Campbell Labs, Otago University
- Lakeland Steel Ltd kiln
- Picolog thermal data log

## **3.4 Feedstock Characterisation Experiments**

### **3.4.1 Proximate Analysis**

#### **3.4.1.1 Moisture Content**

Samples were placed in pre-weighed crucibles and mass measured using a 4 d.p. balance. Moisture content analysis of the samples was determined by drying at 105°C until the sample was a constant mass. The total moisture content was calculated by the difference between wet and dry weight divided by the wet weight.

#### **3.4.1.2 Ash Content**

Pre-dried samples were placed in pre-weighed crucibles and mass measured using a 4 d.p. balance. Ash content was determined by heating the samples up to 600°C for three hours in a Jetlow Shimaden SR53 Furnace. The change in mass was recorded and ash content was calculated by dividing the ash weight by the initial weight.



### 3.4.2 Ultimate Elemental Analysis

Elemental analysis of sawdust was performed by Campbell Labs at Otago University, New Zealand. The analysis determined C, H, N, S and O was calculated by difference. Campbell Labs were also able to provide calorific values.

### 3.4.3 Sawdust Drying Curves

Sawdust drying curves were determined using a Contherm digital series oven. The drying was performed at three different temperatures and mass loss with time was recorded. The sample surface area was also recorded to determine the water loss flux with respect to cross section area. The drying curves were fitted using four different drying models:

$$\text{Newton} \quad MR = \exp(-C_1 t) \quad (23)$$

$$\text{Page} \quad MR = \exp(-C_1 t^{C_2}) \quad (1949) \quad (24)$$

$$\text{Henderson and Pabis} \quad MR = C_1 \exp(-C_2 t) \quad (1998) \quad (25)$$

$$\text{Simpson and Tschernitz} \quad MR = \exp(-t/\tau) \quad (1979) \quad (26)$$

Where;  $MR$  is moisture ratio,  $C_1$  is a constant,  $t$  is time,  $C_2$  is another constant and  $\tau$  is the time constant.

Quality of fit was determined by measuring the sum of squared errors. The most accurate model was used to calculate the required drying time for the large scale dryer.

### 3.4.4 Thermogravimetric Analysis

Thermo-gravimetric analysis of sawdust was performed up to 900°C at three different heating rates using the TA instruments SDT 2960. The analysis was performed under an argon atmosphere with a purge flowrate of 150mm<sup>3</sup>/min. Analysis of the data was performed in Matlab using gaussian distribution activation energy models (further described in section 4.2.4).

## **3.5 Pilot Plant Trials**

### **3.5.1 Design of Experiments**

Pyrolysis of biomass can be a very broad assignment because of the versatility of the products. As a result, the products can be used for a number of applications. The process can be modified by identifying the driving variables and manipulating them to optimise a desired result.

Studies of biomass pyrolysis are yet to define a universal model for pyrolysis therefore each feedstock case has to be treated individually. Pseudo reactions are currently being used to generalise the pyrolytic process, however, there may lie variation within the feedstock options based on source of origin. This would mean extensive experimental setup would have to be set up to investigate the effect of the driving variables on the pyrolysis process.

The design of experiment will look at systematically reducing the number of variables to be investigated based on the main effects they can have on the process.

### **3.5.2 Variables for Pilot Plant Trials**

From previous studies done on organic wastes such as biosolids, paunch waste and chicken DAF sludge (Berg., Sichone. et al. 2011, Sichone 2012), it had been determined that the main driving variables are pyrolysis temperature, feedstock moisture content and feed rate. The effects of these factors were investigated on:

- Char, syngas, and oil yields
- Fixed carbon in char
- Syngas composition

A three level-three factor experiment was carried out using the parameters shown in Table 24.

**Table 24.** Three factor-three level range assignment.

Level	Moisture (%)	Temperature (°C)	Throughput (hertz)
0	15%	400	15
1	30%	450	20
2	60%	500	25

The number of trials needed to produce enough data to investigate these factors using three levels is 27. Table 25 shows the possible combinations required.

**Table 25.** Three factor-three level combination setup.

		Factor A		
Factor B	Factor C	0	1	2
0	0	000	100	200
0	1	001	101	201
0	2	002	102	202
1	0	010	110	210
1	1	011	111	211
1	2	012	112	212
2	0	020	120	220
2	1	021	121	221
2	2	022	122	222

With the cost and time required per experiment each setup was repeated once. This means there will be a total of 54 trials.

This experiment model was designed under the assumption that the cost of syngas analysis was fixed due to the procurement of an gas chromatography unit for syngas analysis. This is because the cost of analysis via CRL proved to be outside the budget for the project. The availability of the department's GC equipment meant the three level analysis could be afforded.

### **3.5.3 Experimental Setup and Procedure**

The pilot plant trials involved:

- Processing the feedstock at nominal conditions.
- Repeating the pilot plant trials at conditions different from nominal conditions as described in the experimental procedure for the three factor-three level approach.
- Collection of mass and energy balances
- Collecting and characterising products for composition and energy content.

## **3.6 Product Characterisation**

Proximate and ultimate analysis of products was performed using the same methods used in feedstock characterisation.

### **3.6.1 Syngas Gas Chromatography Analysis**

Gas chromatography analysis was performed for the syngas samples to evaluate their composition and calorific value. The analysis was predominantly performed using a Perkin Elmer Autosystem Arnel gas chromatography system, capable of measuring H<sub>2</sub>, CH<sub>4</sub>, O<sub>2</sub>, N<sub>2</sub>, CO<sub>2</sub> and CO. The system was calibrated using Scotty Analysed Gases.

A software malfunction and shortage of time prompted the need of a third party. When this occurred, CRL Energy Limited, Lower Hutt, was used for gas analysis.

Syngas samples were collected from pilot plant trials using 1 L tedlar bags provided by CRL Energy Limited. The gas was analysed within 48 hours of collection to ensure integrity of the samples.

### **3.6.2 Raman Spectroscopy**

Raman analysis of char produced by pyrolysis and TGA was used to verify the maximum temperature reached by the feedstock as it went through the auger.

Samples were analysed using a Perkin Elmer Raman Station 400F Raman Spectrometer at a spectral range of 200-3200  $\text{cm}^{-1}$ .

Raman works on the basis of a laser striking the char sample and plotting a spectrum depicting the alignment of the molecules present in the char. A method developed by McDonald-Wharry (2012) was used that characterises char using graphite as the datum (John McDonald-Wharry 2012). Char samples are analysed for graphene likeness based on the position of the G band, D band and the valley between them. These bands have been identified as the most prominent features that change within temperature ranges.

The comparative analysis method assumes the following parameters (John McDonald-Wharry 2012):

- Batch mode operation
- Isothermal degradation
- 12 minute mean residence time at maximum temperature
- Spectral range of 200 – 3200  $\text{cm}^{-1}$

# **Chapter 4.**

## **Results and Discussion**

## **4.1 Introduction**

Experimental work to obtain empirical data for a large scale mobile pyrolysis plant design is presented in this chapter. Pilot plant data was combined with lab-scale analysis to determine characteristics of the associated feedstock and products. Mass and energy balances were also collected to provide a basis for the large scale process. Results are discussed in terms of individual main effects of variables and compound effects of multi-variable conditions on product yields and composition.

## **4.2 Feedstock Characterisation**

### **4.2.1 Introduction**

Pyrolysis is generally considered to be a distillation process where large complex organic molecules are thermally cracked into wide-spectrum of smaller molecules (Slessor and Lewis 1979, Antal and Varhegyi 1995, Moyers and Baldwin 1999, Rezaiyan and Cheremisinoff 2005, Basu 2010, White, Catallo et al. 2011). As described in the literature review, the yields will depend on processing parameters and also the feedstock being used.

In some cases feedstock pre-treatment techniques such as the use of catalysts and pre-drying is performed to lower heating demands and/or promote the selectivity of certain products (Lédé 1994, Antal and Varhegyi 1995, Xu, Matsumura et al. 1996, Moyers and Baldwin 1999, Rezaiyan and Cheremisinoff 2005, Li, Wang et al. 2008, Basu 2010, French and Czernik 2010, Anis and Zainal 2011, Bulushev and Ross 2011, Butler, Devlin et al. 2011, White, Catallo et al. 2011).

In other cases such as Municipal Solid Waste (MSW) treatment where feedstock composition is not consistent, pre-treatment will be required for monitoring purposes.

### **4.2.2 Composition Analysis**

The sawdust being used as the feedstock is from New Zealand grown pinus radiata softwood. This has a lignocellulose structure and has a mean particle

diameter of 1.5mm. Table 26 and Table 27 show the proximate and ultimate analyses of dry pinus radiatta sawdust from the client R.H. Tregoweth Sawmills. The later includes a comparison to other biomass sources.

**Table 26.** Proximate analysis composition for pine sawdust.

Moisture (%)	Ash (%)	Organic matter (%)	HHV <sup>a</sup> (kJ/kg)
59.88	0.78	99.22	25,543

**Table 27.** Comparative ultimate analysis of pinus radiatta sawdust and other organic feedstock.

Ultimate analysis of dry feedstock (Dry basis) of some biomass and other fossil fuels * <sup>dwb</sup>								
Fuel	C (%)	H (%)	N (%)	S (%)	O † (%)	Ash (%)	HHV (kJ/kg)	Source
Pinus Radiata	47.2	6.5	0.3	0.3	44.9	0.8%	25,543	Own work
Comparative Literature values								
Maple	50.6	6.0	0.3	0	41.7	1.4	19,958	Tillman,1978
Douglas fir	52.3	6.3	9.1	0	40.5	0.8	21,051	Tillman,1978
Douglas fir (bark)	56.2	5.9	0	0	36.7	1.2	22,098	Tillman,1978
Redwood	53.5	5.9	0.1	0	40.3	0.2	21,028	Tillman,1978
Redwood (waste)	53.4	6.0	0.1	39.9	0.1	0.6	21,314	Boley and Landers, 1969
Sewage sludge	29.2	3.8	4.1	0.7	19.9	42.1	16,000	
Rice Straw	39.2	5.1	0.6	0.1	35.8	19.2	15,213	Tillman,1978
Rice Husk	38.5	5.7	0.5	0	39.8	15.5	15,376	Tillman,1978
Sawdust	47.2	6.5	0	0	45.4	1.0	20,502	Wen et al., 1970
Paper	43.4	5.8	0.3	0.2	44.3	6.0	17,613	Bowerman, 1969
MSW	47.6	6.0	1.2	0.3	32.9	12.0	19,879	Sanner et al., 1970
Animal Waste	42.7	5.5	2.4	0.3	31.3	17.8	17,167	Tillman,1978
Peat	54.5	5.1	1.65	0.45	33.0	5.2	21,230	
Lignite	62.5	4.38	0.94	1.41	17.2		24,451	
PRB Coal	65.8	4.88	0.86	1.0	16.2		26,436	Bituminous coal research, 1974
Anthracite	90.7	2.1	1.0	7.6	11.4		29,963	Probstein and Hicks, 2006
Petcoke	86.3	0.5	0.7	0.8	10.5		29,865	

\* <sup>dwb</sup> = dry weight basis, † = calculated by difference

### 4.2.3 Drying Characteristics

Green sawdust is normally received with moisture levels higher than typical wood due to the use of water as a coolant for the saws. Previous work (Berg., Sichone.



et al. 2011) done by the author confirmed statements from literature review (Rezaiyan and Cheremisinoff 2005, Basu 2010, Jones 2010, Downie 2010-2011). The moisture content will need to be reduced before the feedstock is introduced into the reactor to prevent processing issues.

This section presents the results of drying trials conducted on the prospective feedstock. Drying experiments were set up in an attempt to obtain drying characteristics of the sawdust

#### 4.2.3.1 Aim

The aim of the drying trials is to investigate the drying characteristics of sawdust. Thermal efficiencies of rotary dryers are within the 45-80 % (Moyers. and Baldwin 1999). Rotary dryers are normally designed using empirical data from small/pilot scale trials. This is because they are normally for cases where the moisture is not free-moisture. Thus, the drying rates are based on diffusion of the liquid through the material. This function is very complex for heat sensitive materials such as sludge due to physical transformations caused by the heat. However the function can be made simpler for materials that are thermally stable within the operational temperatures especially when their water activity coefficient is known.

#### 4.2.3.2 Theory

Drying will occur while the moisture within the solid is not at equilibrium with the moisture in the drying medium (usually air).

$$N_w = k_c [a_w p_w^{sat}(T_s) - \phi p_w^{sat}(T_\infty)] \quad (27)$$

Where  $N_w$  is the mass transfer flux (drying rate), ( $\text{kg}\cdot\text{m}^{-2}\cdot\text{s}^{-1}$  or  $\text{mol}\cdot\text{m}^{-2}\cdot\text{s}^{-1}$ )

$k_c$  is mass transfer coefficient ( $\text{kg}\cdot\text{m}^{-2}\cdot\text{s}^{-1}$  or  $\text{mol}\cdot\text{m}^{-2}\cdot\text{s}^{-1}$ )

$a_w$  is the water activity coefficient

$p_w^{sat}$  is saturation pressure of the water ( $\text{kg}\cdot\text{m}^{-2}\cdot\text{s}^{-1}$  or  $\text{mol}\cdot\text{m}^{-2}\cdot\text{s}^{-1}$ )

$T_s$  is the temperature of the solids ( $^{\circ}\text{C}$ )

$T_{\infty}$  is the temperature of the air ( $^{\circ}\text{C}$ )

$\psi$  is the relative humidity

Since the solids content is assumed to remain constant, the drying rate  $N_w$  may be evaluated a number of different ways:

$$N_w A = \frac{dM}{dt} = \frac{dm_w}{dt} \quad (28)$$

Where  $A$  is the surface area of the sawdust

$dM/dt$  is the change in mass of the whole sample

$dm_w/dt$  is the change in mass of the water content for a given time period  $dt$ .

A plot of drying rate vs. time reveals a lot about the drying process. In particular, some key periods may be observed.

#### **4.2.3.2.1 Settling-Down Period**

Typically the sample to be dried is initially lower than the wet and dry bulb temperatures in the oven. During this period much of the heat arriving at the sample's surface is being used to heat the sample rather than evaporate water, so initially drying rates are low (Figure 31). As the temperature rises, the evaporation rate increases until the cooling effect of the evaporation matches the rate of heat transfer to the surface, at which point the constant-rate period begins.

#### **4.2.3.2.2 Constant-Rate Period**

During this period the surface water activity is close to unity and the rate of moisture evaporation matches the rate at which heat is arriving at the surface, and hence the surface temperature remains constant, approximately equal to the wet-bulb temperature. Assuming the humidity, oven temperature and heat and mass transfer coefficients remain relatively constant, the drying rate will also be approximately constant (hence its name).

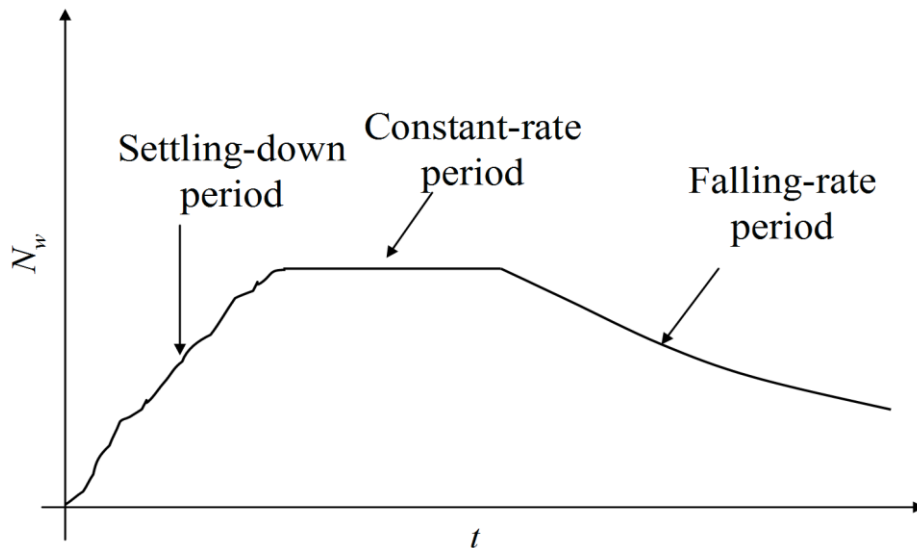


**Figure 31.** Drying rate vs time.

#### **4.2.3.2.3 Falling-rate period**

If the rate of moisture removal from the surface is greater than the rate at which water migrates to the surface from within the sample, the surface water activity will drop below unity and the evaporation rate will decrease, which will mean that the surface temperature will rise, which in turn will mean that the driving force for the drying process will decrease and the drying rate will fall (hence its name).

#### **4.2.3.3 Experimental**

Drying trials were performed on the selected feedstock for property characterisation purposes. The trials were performed at three different temperatures (80, 90 and 100°C) in an attempt to find an optimal drying temperature. The drying rate for the sawdust is expected to vary depending on the temperature, grain size and the relative humidity (Simpson and Tschernitz 1979).

#### **4.2.3.4 Results**

Data from the drying experiments was recorded and plotted to give mass loss curves (Figure 32).

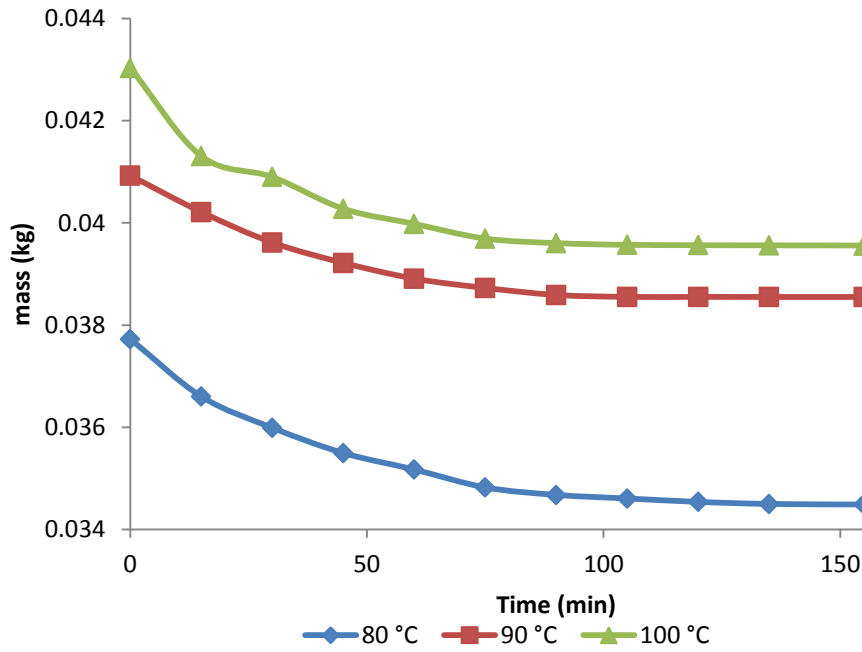


**Figure 32.** Mass vs. time for sawdust drying at 80, 90 and 100°C.

The rate at which wood dries depends upon a number of factors, the most important of which are the temperature, the dimensions of the wood, and the relative humidity (Simpson and Tschernitz 1979).

The mass loss curves were normalised for reliable comparisons to be made and the percentage of mass loss for each data set was calculated (Figure 33).

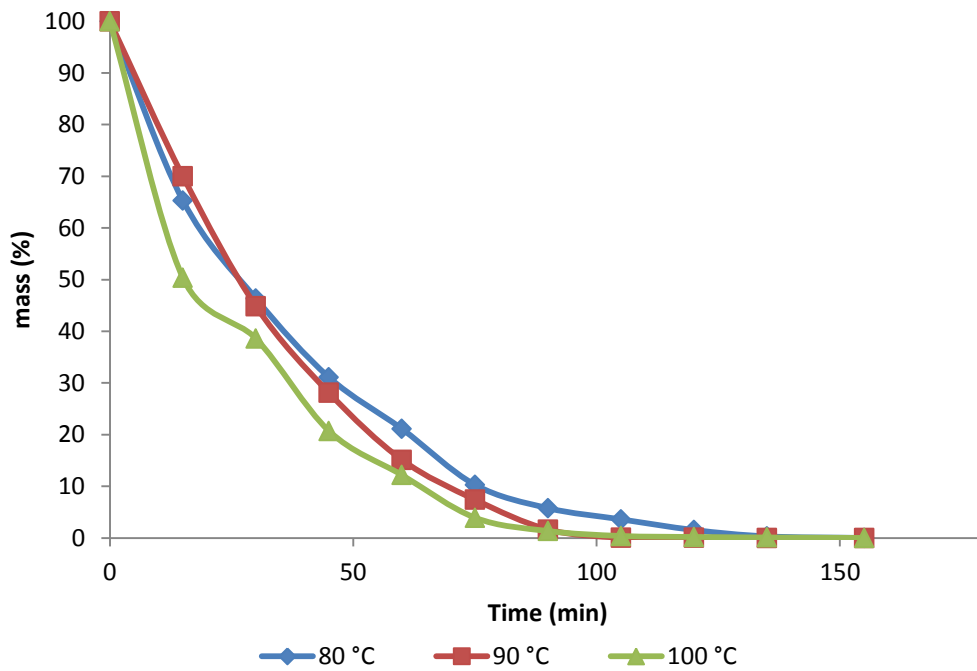


**Figure 33.** Mass fraction vs. time for sawdust drying at 80, 90 and 100°C.

The curves can be defined by the following expression

$$y(t) = \frac{M_t - M_f}{M_0 - M_f} \quad (29)$$

Where  $M_0$  is the initial mass;

$M_f$  is the final mass and

$M_t$  is the mass at a given time.

The water loss curves were converted into water loss flux curves (Figure 34). The plots show an increase of mass loss for the first mass value reading. This was due to the driving force for surface water evaporation governing the mass transfer rates. The rate of mass loss decreased with time for all samples until the sawdust reached equilibrium moisture conditions. This behaviour is characteristic of the falling rate period. It appears that the drying experiments at all three temperatures do not exhibit the first two stages of drying as predicted by theory. This is because the theory is based on tray drying of materials of larger size. The small grain size means the bulk load has a higher surface area to volume and this accelerates

evaporation from the surface. Once surface moisture is evaporated the drying rate is controlled by the moisture diffusion through the sawdust.

The sawdust dried at 100°C reached equilibrium within the shortest time. This was caused by the higher thermal gradient between the feedstock initial temperature and the drying air. The higher drying temperature accelerates the rates of mass loss because the higher thermal gradient provides a higher driving force for water diffusion. Higher temperatures will yield faster drying times, but they will also create greater stresses in the wood due because the moisture gradient will be larger (Simpson and Tschernitz 1979).

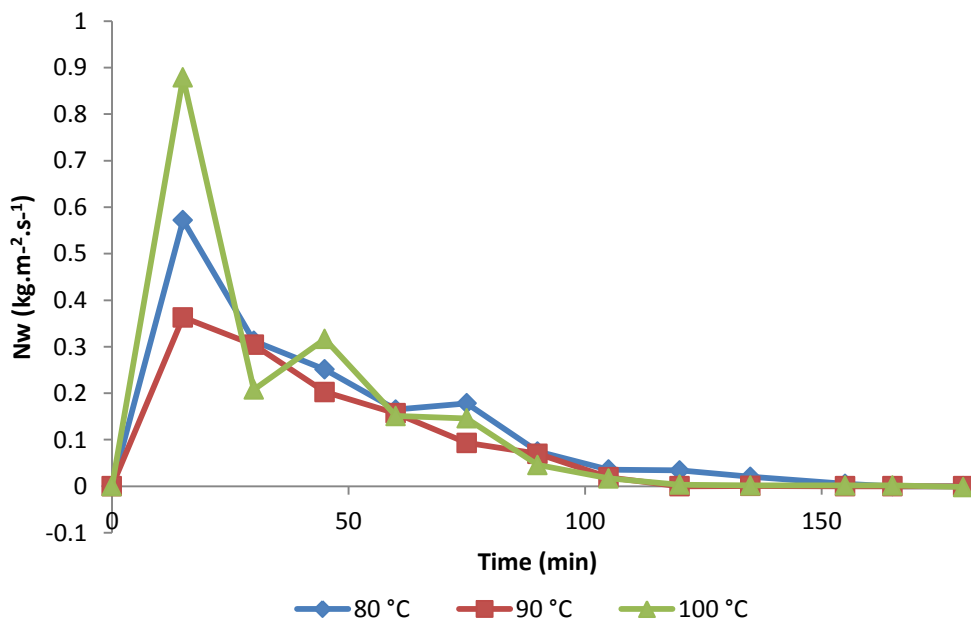


**Figure 34.** Mass loss flux vs. time for sawdust drying at 80, 90 and 100°C.

For the sake of designing the large scale dryer, attempts to fit the drying data to modelled curves were made using four models described in Table 28.

**Table 28.** Drying models.

Model name	Model	Reference
Newton	$MR = \exp(-C_1t)$	Lewis, 1921
Page	$MR = \exp(-C_1t^{C_2})$	Page, 1949
Henderson and Pabis	$MR = C_1\exp(-C_2t)$	Henderson, 1952; Pabis, 1998
Simpson and Tschernitz	$MR = \exp(-t/\tau)$	(Simpson and Tschernitz 1979)

The Page model appeared to be the most appropriate as it had the lowest residual sum of squares value for each of the drying temperatures as shown in Table 29.

**Table 29.** Quality of fit assessment for drying curves.

Drying Temperature	80 °C	90 °C	100 °C
Newton	0.041	0.070	0.031
Page	0.006	0.005	0.015
Henderson and Pabis	0.021	0.027	0.025
Simpson and Tschernitz	0.069	0.103	0.071

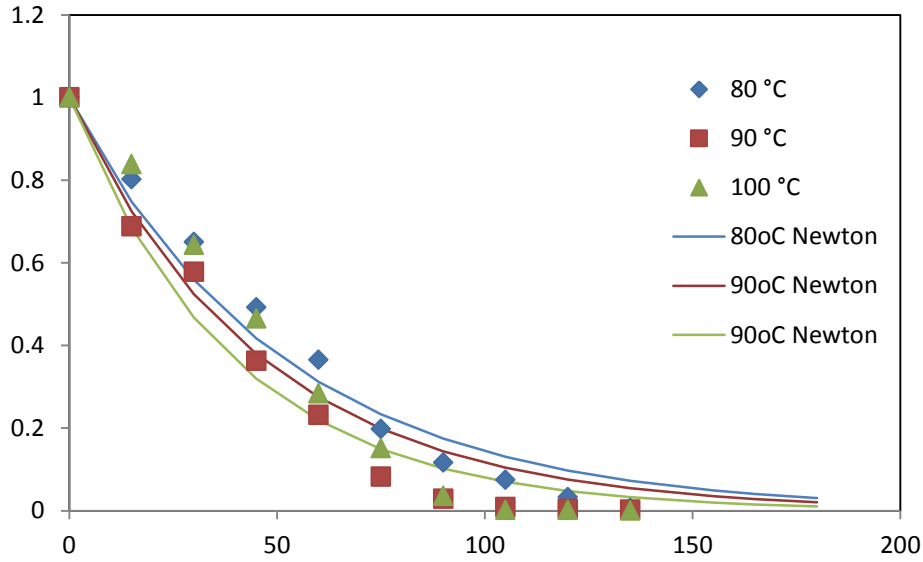


**Figure 35.** Newton model.

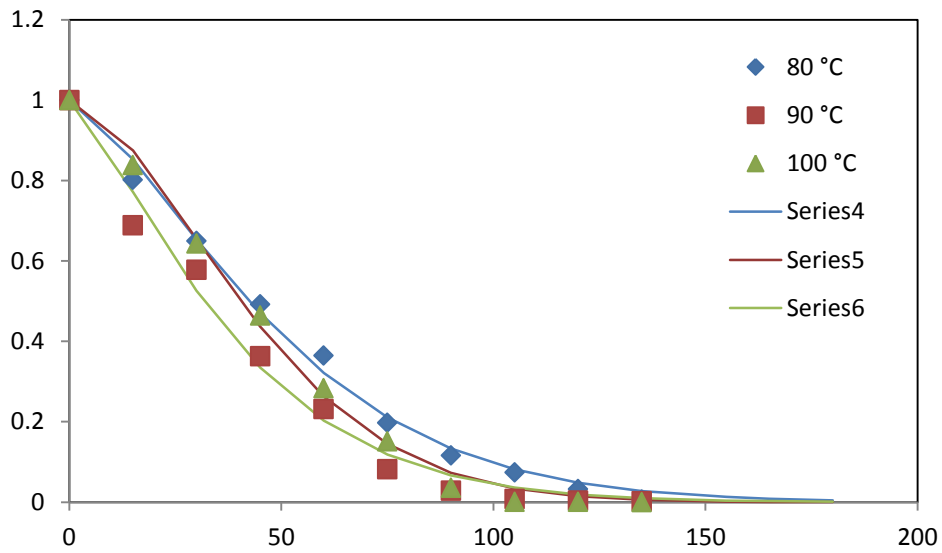


**Figure 36.** Page model.

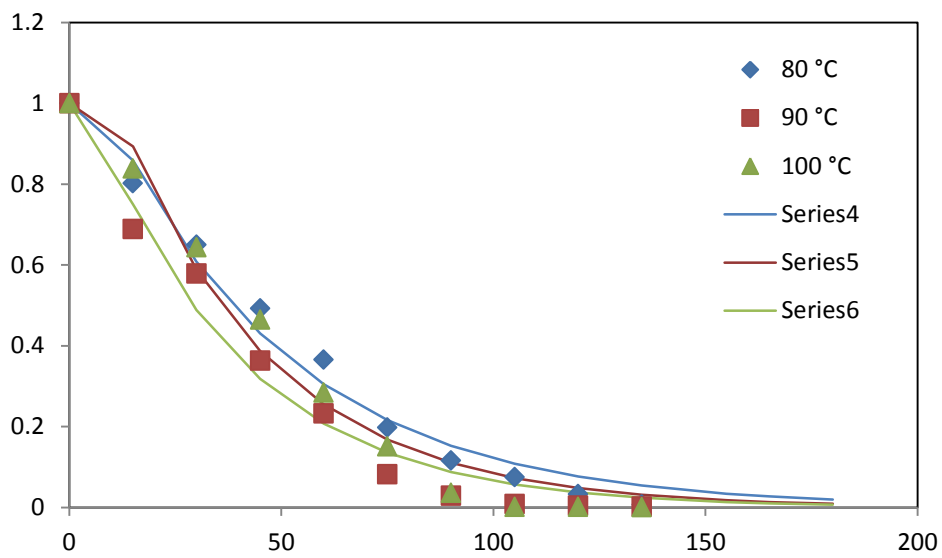


**Figure 37.** Henderson and Pabis model.



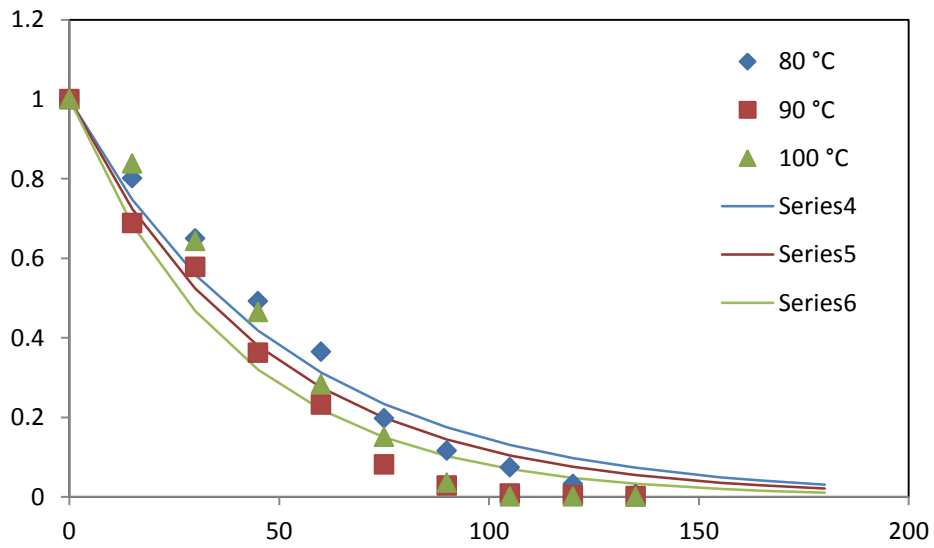


**Figure 38.** Simpson and Tschernitz model.

The Page model was used to calculate the required time for drying. This will be used in the dryer design section.

#### 4.2.4 Reaction Kinetics Model Development

Reaction kinetics of the pyrolysis can be quite complicated to model. There are currently a lot of models available for the modelling of wood pyrolysis. The majority of the kinetics are based on Arrhenius law with some sort of adjustment to accommodate for heating rate or any other variable.

The lab-scale simulations using thermo-gravimetric analysis (TGA) can be used to predict the behaviour of the feedstock as it is processed in the pilot plant.

A few steps were taken to ensure that the simulation has similar processing conditions as the pilot plant. These included:

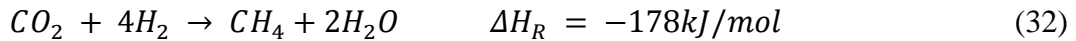
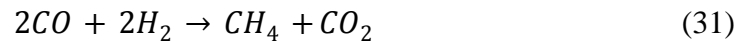
- Using argon as the inert medium, ensuring that no combustion occurs.
- Controlling the heating rate and using similar to that determined from preliminary energy balances around the reactor.
- The pilot plant operates at a maximum of 680°C, however, to understand the thermal properties of the feedstock the lab-scale experiments will be performed up to 900°C.

Sawdust, being a ligno-cellulosic biomass has a heterogeneous composition comprising of three components which have different temperature ranges for the initiation of pyrolysis as described in (Rezaiyan and Cheremisinoff 2005).

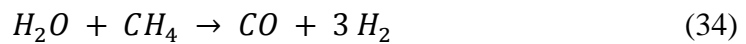
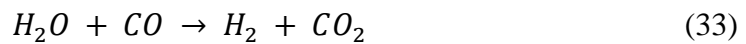
- Hemicellulose: 150-350 °C
- Cellulose: 275-350 °C
- Lignin: 250-500 °C

Water is the fourth component which can be considered as negligible at low level analysis. TGA curves suggest that water is removed by 400° K~130°C. This is because for lab-scale DTA/ TGA experiments it is expected that the water is normally removed from the biomass before any of the three main constituents begin decomposing. However, in practice the water vapour might interact with decomposition products (either the char or the evolved volatile gas). This is evident in the synthesis reactions responsible for the creation of methane or hydrogen.

Methanation reactions (Apt, Newcomer et al. 2008):



Water- gas reactions using carbon monoxide and methane as feedstock (Kaneko, Derbyshire et al. 2000):



Some of this water is initially present in the feedstock whilst some of it is a product of pyrolysis. However, by using a lumped semi-global model the origin and presence of the free water can be regarded as irrelevant.

#### 4.2.4.1 TGA Analysis

TGA analysis of sawdust was performed upto 1273 °K (900 °C). Mass loss curves were obtained for sawdust at 10, 20 and 30 °K/min. Due to the initial masses of the samples being slightly different the curves have to be converted to mass fraction vs temperature curves to enable meaningful comparison as shown in Figure 39.

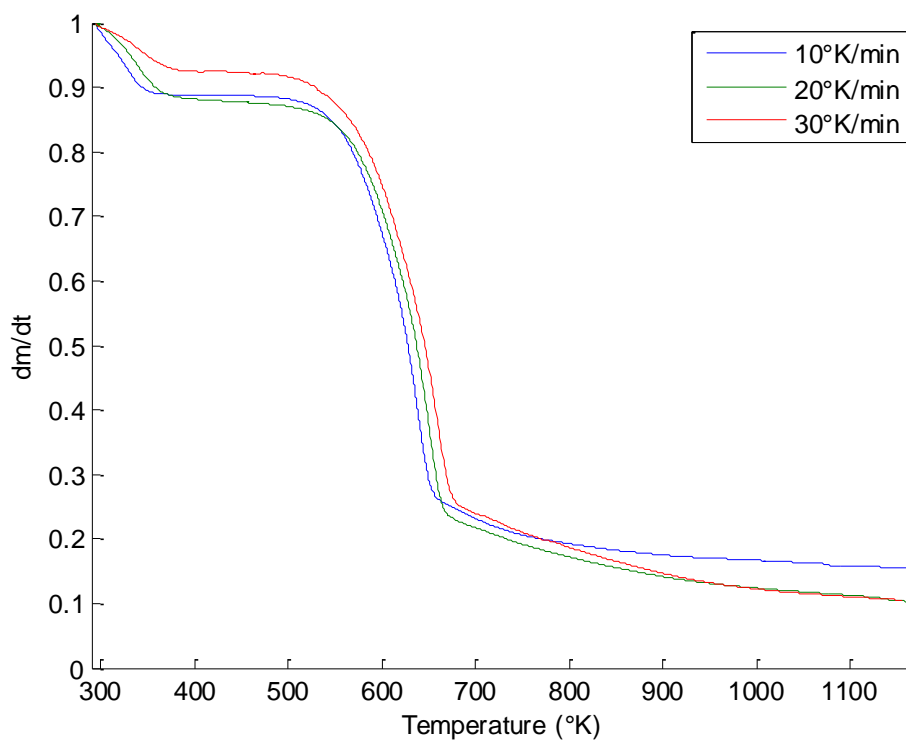


**Figure 39.** Normalised mass loss curves mass % vs temperature.

The mass loss curves each give a sinusoidal shape typical of non-isothermal decomposition. These curves suggest that the sawdust being processed at 10°C produces the most char 15% whilst the other two trials appear to converge at 11%. The first drop in mass can be credited to water loss. The sample mass remains constant before decreasing in what appears to be two-step decomposition. To have a closer view of the decomposition the curves will need to be converted into mass loss rate vs. temperature curve.

#### 4.2.4.2 Distributed Activation Energy Model (DAEM) Reaction Model

The mass loss rate vs temperature curves show two main peaks and a side peak attached to the second main peak (Figure 40). The first peak can be attributed to the evaporation of any free moisture. The second main peak and the side peak can be attributed to devolatilisation of cellulose and hemi-cellulose. After the second main peak, at approximately 650-700 °K, a shallow gradual slope is observed.

This slope suggests a slow release of another component. Using decomposition characteristics highlighted in literature, this fourth component is lignin.

The different component peaks and ranges were highlighted for each heating rate sample in the following order:

- water
- lignin
- hemi-cellulose
- cellulose

The order was used because it proved to be a relatively straight forward approach to lumping volatile components which showed similar decomposition profiles.

The water fraction was by far the easiest to map due to its outlying position. The lignin was used first because it had the longest decomposition temperature range and thus provided a better basis for the other components. Hemi-cellulose and cellulose were mapped after that.

It is important to note that despite the organic components being labelled as lignin, hemicellulose and cellulose, the corresponding Gaussian curves are only approximate as each of the pseudo components can comprise of a mixture of decomposing lignin, hemi-cellulose, cellulose and unstable char. Gaussian curves can be described by the following relationship

$$f(x) = ae^{-\frac{(x-b)^2}{2c^2}} \quad (35)$$

Where;  $a$  is the height of the DTG curve's peak;

$b$  is the temperature corresponding to the centre of the peak;

$c$  controls the width of the "bell" .

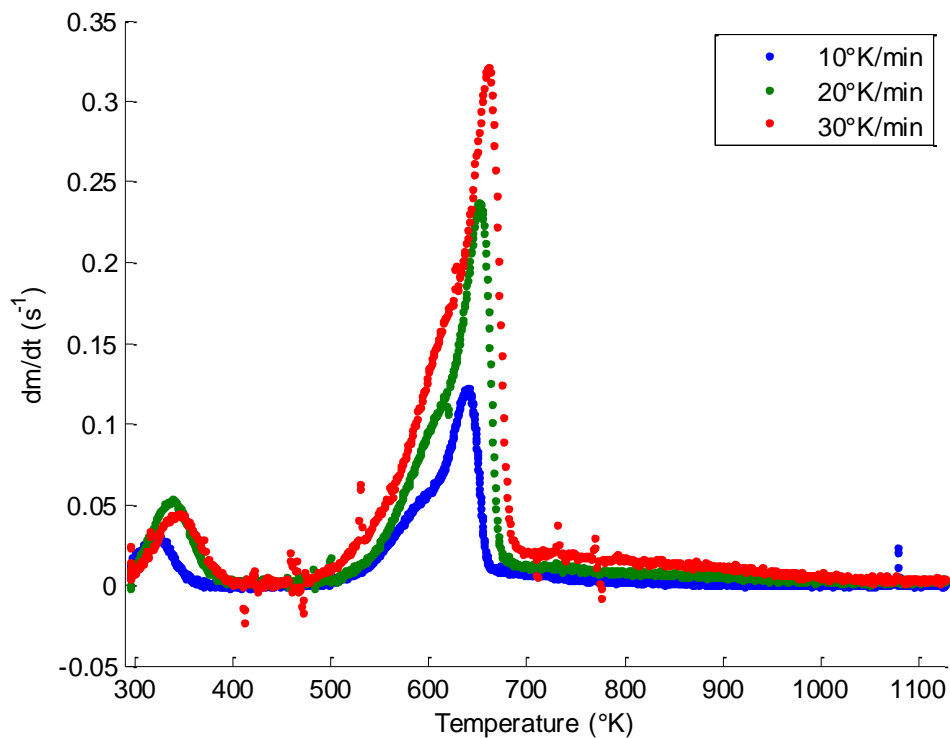


**Figure 40.** Mass loss rate vs temperature curves.

For simplicity, consider the curve for sawdust analysed at 10°K/min (Figure 41). The first peak is observed at 321.5°K with a value of  $9.871 \times 10^{-4} \% \text{ s}^{-1}$ . This peak is attributed to water content. The second main peak appears to be a sum of multiple curves because it does not have the typical bell curve. It shows a slight step/shoulder at temperature value of 607°K to the left of the main peak and gradual decreasing slope at temperatures greater than 675°K. These characteristics are used as the basis for the pseudo component allocation. The determination of the organic pseudo components involved:

- Identification of the background curve which is attributed to lignin decomposition but could in reality involve char degradation too. The mean was located at the middle of the base curve.
- The hemi-cellulose curve which had a mean at the slight step at 607°K.
- The cellulose curve was derived from the second main peak.

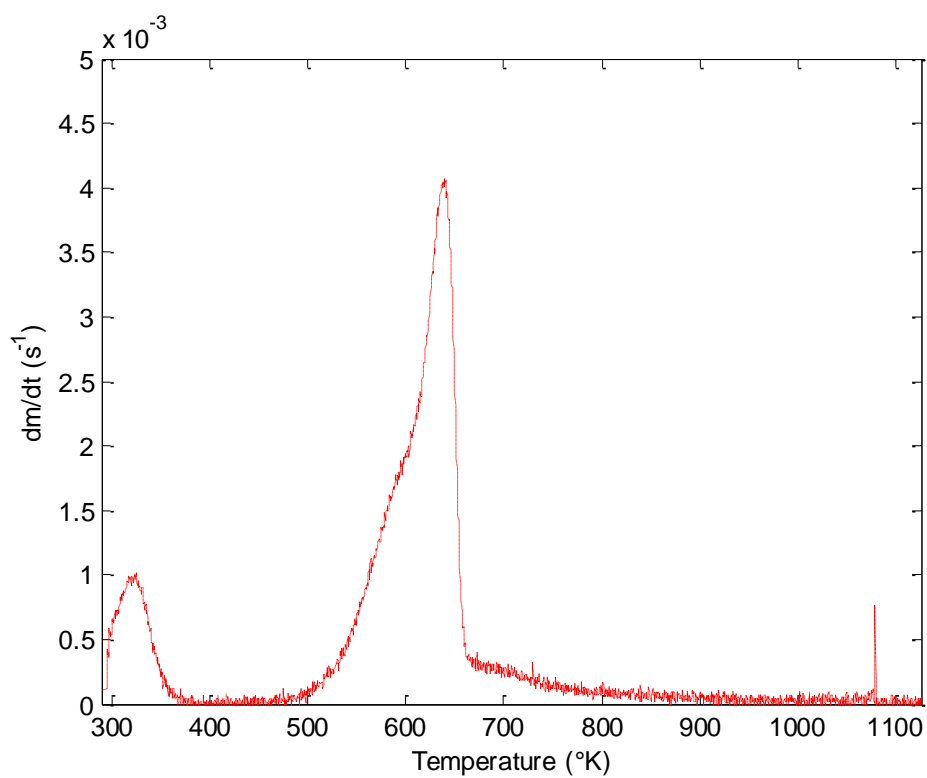


**Figure 41.** Derivative thermogravimetric (DTG) analysis curve for sawdust at  $10^{\circ}\text{K}/\text{min}$ .

Using trial and error it was found that the order in which the pseudo component curves were determined affected the quality of fit for the organic components. This is shown in Figure 42 and which are both trying to predict the decomposition rates of the sawdust at  $10^{\circ}\text{K}$ .

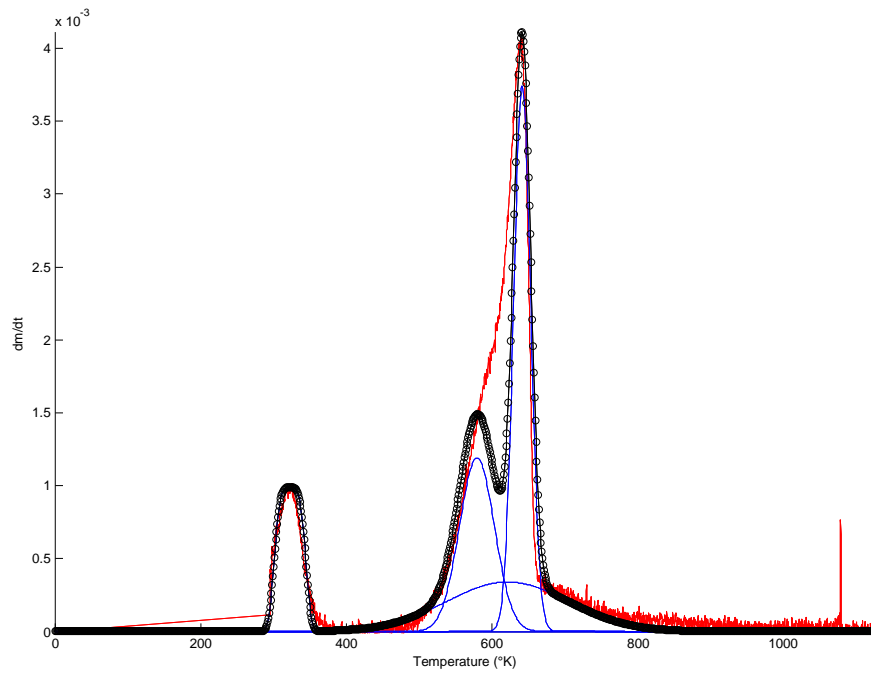


**Figure 42.** First attempt at pseudo component mapping for sawdust at 10°K/min.

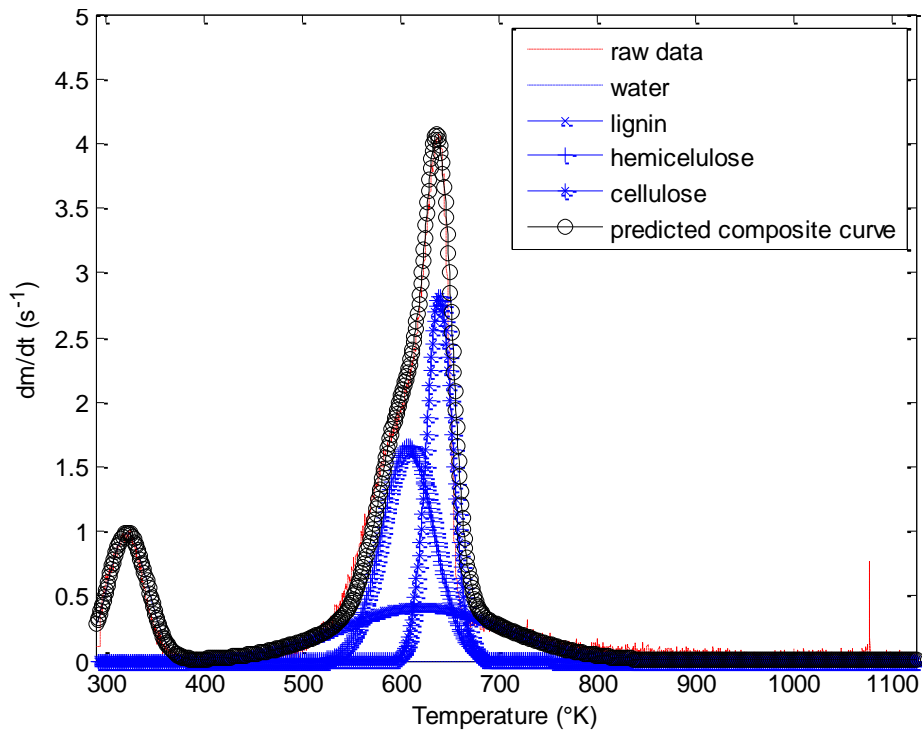


**Figure 43.** Gaussian distribution fitting for sawdust mass loss rate curve for sample heated at 10°K/ min.



The curve fitting assuming a first order decay relationship and this assumption holds very well for the moisture. However the fit accuracy dropped slightly for the section describing the organic volatiles evolution. The discrepancies might be caused by complex interactions which can not be mapped easily by the assumption of three pseudo components. This method was repeated for sawdust analysed at 20 and 30° K/min and the graphs are presented in Figure 44 and 45 respectively.

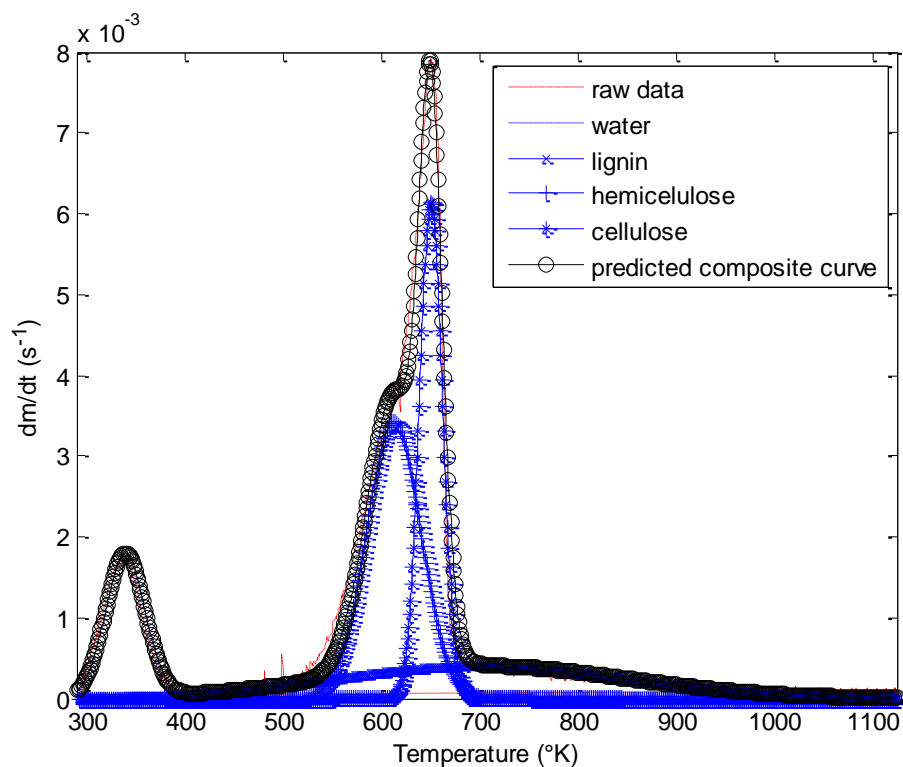


**Figure 44.** Gaussian distribution fitting for sawdust mass loss rate curve for sample heated at 20°K/ min.

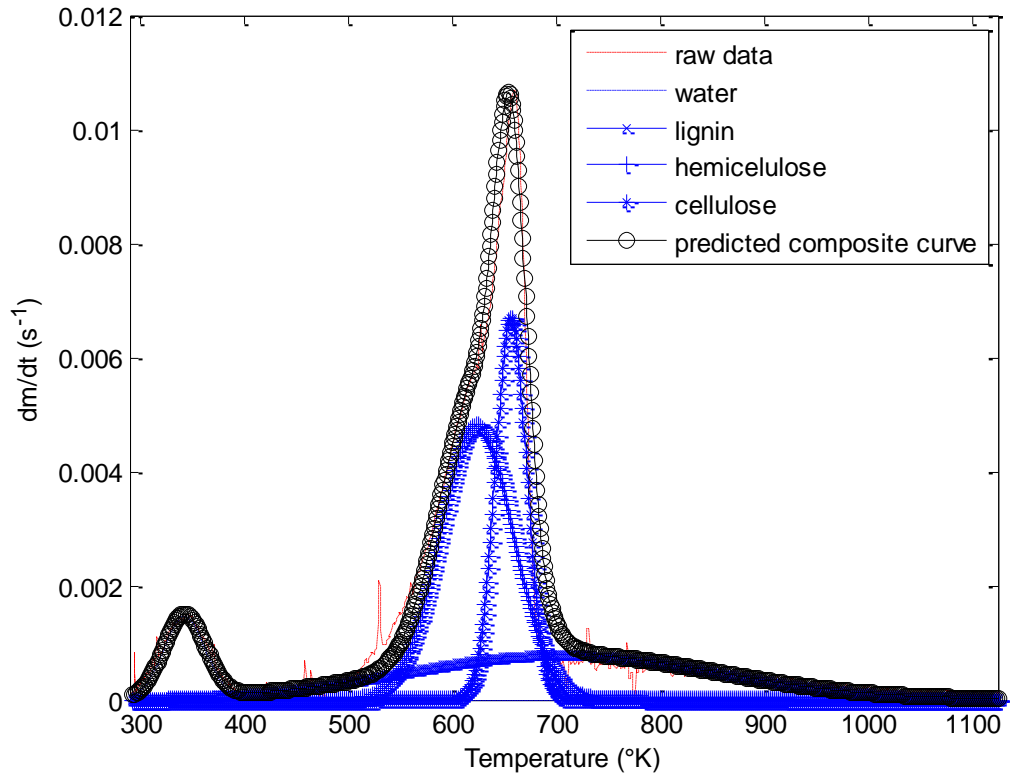


**Figure 45.** Gaussian distribution fitting for sawdust mass loss rate curve for sample heated at 30°K/ min.

#### 4.2.4.2.1 Determination of Kinetic Triplet

The mass loss rate curve fitting using Gaussian distribution proved to be a great means of predicting the liberation of the volatiles. However, this did not provide much information on the kinetic parameters ( $A$ ,  $E_a$  and  $k$ ).

$$\frac{d\alpha}{dT} = \frac{k(T)}{\beta} \cdot f(\alpha) = \frac{A}{\beta} \exp\left(\frac{E_a}{RT}\right) \cdot f(\alpha) \quad (36)$$

#### 4.2.4.2.2 Determination of Reaction Constants ( $k$ )

Using the reaction order model, the previous equation can be simplified to

$$\frac{d\alpha}{dT} = k(T)(1 - \alpha)^n \quad (37)$$

Rearranging this for  $k$  gives

$$k(T) = \frac{\frac{d\alpha}{dT}}{(1-\alpha)^n} \quad (38)$$

Where  $n$  is =1 for first order reaction modelling. Figure 46 shows a plot of  $k$  vs temperature, for the three heating rates. The plot shows a peak for each heating rate trial within the range associated with organic volatile release. Maximum reaction rate constants were 0.52 , 0.943 and 1.182 ( $s^{-1}$ ) for heating rates of 10, 20 and 30 ° K/min. The maximum reaction rate constant increases with increase in heating rate. The increase in heating rate also increased the temperature range of the main set of decomposition reactions. The plot exhibits some strange results which indicate a scattered exponential increase in reaction constant with increase in temperature after the main organic matter decomposition. These results are inconsistent with the mass loss curves shown in Figure 39 which show a slow mass loss rate after the main organic matter decomposition region.

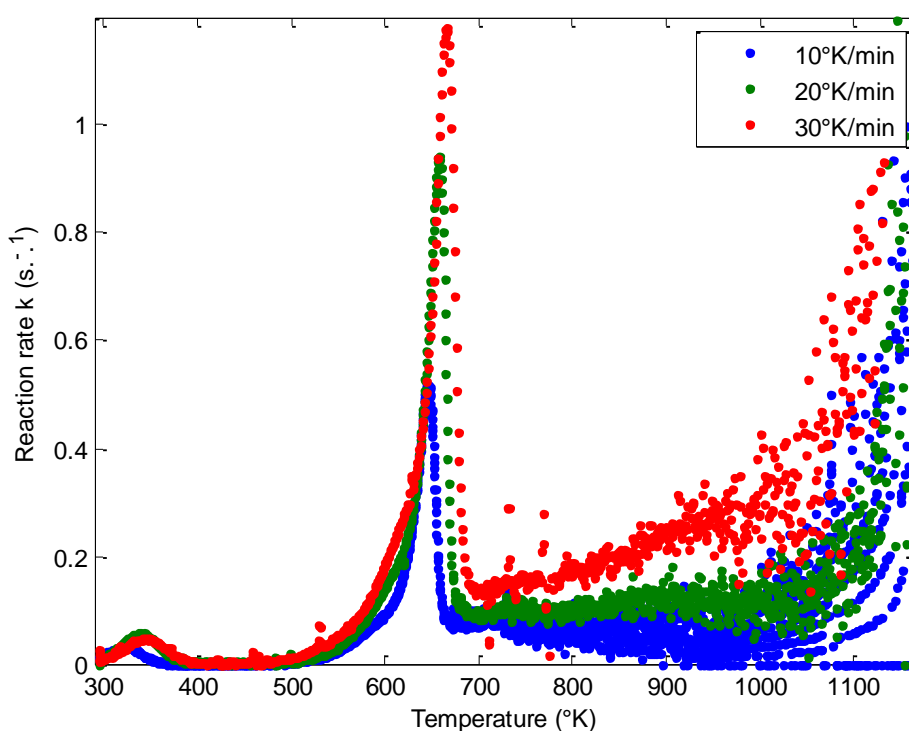


**Figure 46.** Reaction rate vs. temperature.

#### 4.2.4.2.3 Determination of Activation Energy

Figure 47 shows a plot of the activation energy vs. temperature for all three samples. The graph shows a peak within the same temperature ranges associated with organic volatile liberation for trials performed using each of the heating rates. Maximum activation energy values of 180.1, 169.6 and 145.2 (kJ/mol) for heating rates of 10, 20 and 30 ° K/min. The maximum  $E_a$  for the global organic matter reaction decreased with increase in heating rate. The increase in heating rate also shifted the peak to the right showing that the decomposition temperature range was prolonged with increase in heating rate.

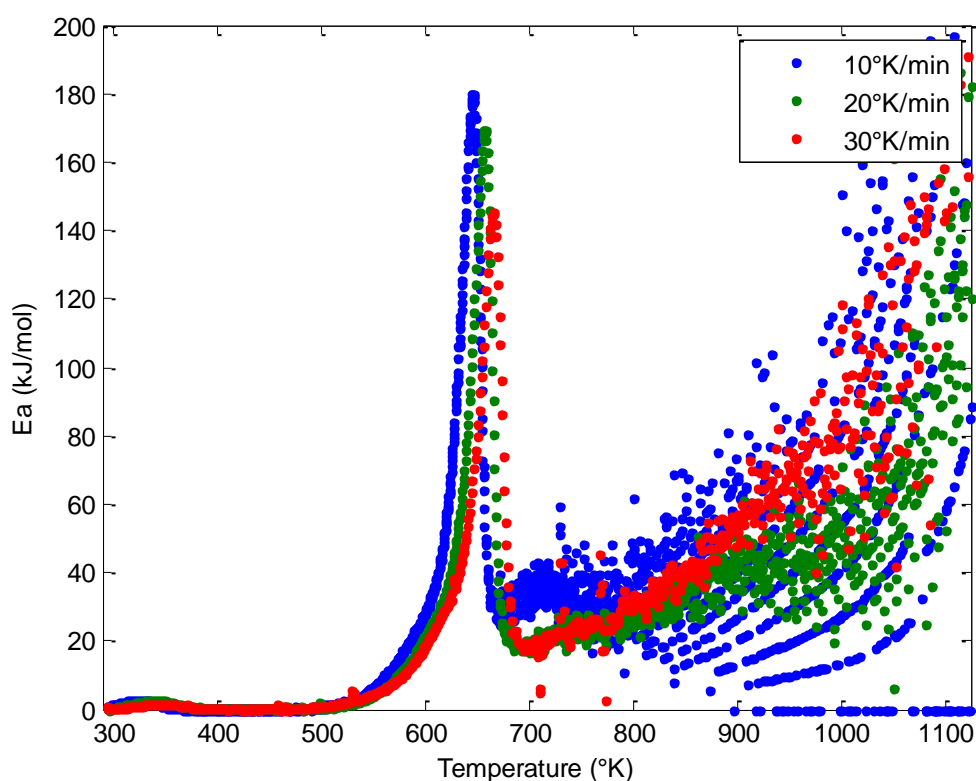


**Figure 47.** Rate constant  $k$  vs. Temperature ( $^{\circ}$ K).

The individual  $E_a$  vs. temperature for the sawdust analysed at 10°K/min in Figure 48 shows that the distribution of the activation energy required for the main organic matter devolatilisation can be mapped using two composite curves. However, the plot also shows a degree of variation for the activation energy levels at temperatures between 665 and 800 °K with values ranging from ~20 -

~50kJ/mol. A strange pattern is observed for temperatures greater than 800 °K. However the overall trend of the strange pattern shows that the activation energy increases exponentially as the temperature approaches 1125 °K. This exponential increase can be credited to the reduction in volatile matter. Most organic matter is now converted to char and although char can be burnt, it can be very difficult to devolatilise in absence of oxygen.

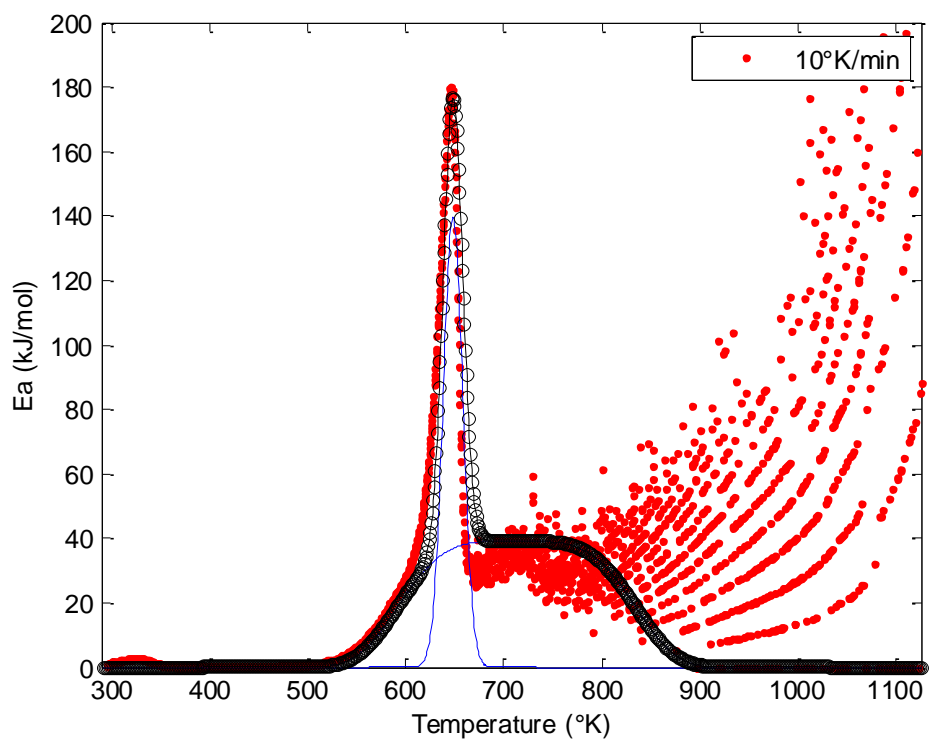


**Figure 48.** Activation energy vs temperature for sawdust at 10°K/min.

#### 4.2.4.2.4 Determination of Pre-Exponential Constant

The pre-exponential constant was determined using an approximate method by Braun and Burnham (1987) using the following relationship:

$$\ln\left(\frac{\beta}{(T_{max})^2}\right) = \frac{E_0}{RT_{max}} + \ln\left(\frac{AR}{E_0}\right) \quad (39)$$

Rearranging to make  $A$  the subject yields

$$\ln A = \ln\left(\frac{\beta}{(T_{max})^2}\right) \ln(E_0) - \ln(R) - \frac{E_0}{RT_{max}} \quad (40)$$

Taking the exponential of both sides gives  $A$ .

$$A = e^{(\ln\left(\frac{\beta}{(T_{max})^2}\right) \ln(E_0) - \ln(R) - \frac{E_0}{RT_{max}})} \quad (41)$$

Where  $A$  is the pre-exponential constant;

$E_0$  is the maximum activation energy level;

$T_{max}$  refers to the temperature value for  $E_0$ ;

$R$  is the universal gas constant;

$\beta$  is the heating rate.

Using this equation pre-exponential constant values of  $1.42627 \times 10^{-15}$ , 0.000914 and 0.001151 were obtained for sawdust TGA at heating rates of 10, 20 and 30 ° K/min.

## 4.2.5 Modelling Overview

Table 30 and Table 31 give the pseudo-component Gaussian distribution models for the three heating rates and a summary of the kinetic parameters respectively.

**Table 30.** Mass loss rate prediction using Gaussian prediction.

	10°K/min	20°K/min	30°K/min
<b>Water</b>			
<b>Peak Temp</b>	323	340	342
<b>Peak alpha</b>	0.0009875	0.001797	0.001457
<b>Temperature range (° K)</b>	290-390	290-400	295 – 389
<b>Power</b>	2	2	2
<b>Pseudo lignin</b>			
<b>Peak Temp</b>	621	699.7	703
<b>Peak alpha</b>	0.00042	0.0004028	0.0007896
<b>Temperature range (° K)</b>	397 – 864	612 – 788	405 - 1001
<b>Power</b>	2	2	2
<b>Pseudo Hemi-cellulose</b>			
<b>Peak Temp</b>	608	613	624
<b>Peak alpha</b>	0.001659	0.003429	0.004813
<b>Temperature range (° K)</b>	521 – 695	518 - 708	521-727
<b>Power</b>	2	2	2
<b>Pseudo cellulose</b>			
<b>Peak Temp (° K)</b>	634	651	657
<b>Peak alpha</b>	0.002818	0.006139	0.006701
<b>Temperature range (° K)</b>	597 -683	603 -697	609 -705
<b>Power</b>	2	2	2

**Table 31.** Global kinetic parameters.

	10°K/min	20°K/min	30°K/min
<b><math>E_{a \max}</math></b>	180.1	169.6	145.2
<b><math>T_{\max}</math> for <math>E_{a \max}</math></b>	646.1	657.7	665.8
<b><math>k_{\max}</math></b>	0.52	0.943	1.182
<b>A</b>	$1.42627 \times 10^{-15}$	0.000914	0.001151

Gaussian distribution proved to be a very convenient approach to modelling the decomposition rates of the sawdust at all three temperatures. However quality of fit assessment gave  $R^2$  values of 1.16, 1.13 and 1.01 for the sawdust treated at 10, 20 and 30 °K/min respectively.  $R^2$  value is best suited to linear regression so adjusted  $R_{bar}^2$  were equal to  $R^2$  values when rounded to 3 decimal places.

## 4.3 Pilot Plant Trials

### 4.3.1 Experimental Data

The pilot plant trials were run from 14<sup>th</sup> August 2012 to 6<sup>th</sup> November 2012. The Nominal conditions were assigned as:

- 15% moisture feedstock – This moisture content had theoretically demonstrated autogenesis for paunch grass pyrolysis in previous studies. of a higher moisture content
- Pyrolysis at 400 °C – this appears to be the lower end of the most commonly used temperature range (400 – 600°C) for slow pyrolysis without the aid of catalysts.
- An auger speed of 15rpm – This was the lowest speed used in previous studies.

**Table 32.** Processing parameter level assignment.

Level	Processing parameters		
	Moisture (%)	Temperature (°C)	Throughput (hertz)
0	15%	400	15
1	30%	450	20
2	60%	500	25

### 4.3.2 Pilot Plant Pyrolysis Process Description

The feedstock is force fed into an auger kiln using two augers from the hopper, the kiln is heated to temperatures between 400 -500°C. Once the reactor reaches the specified temperature the augers are started and sawdust is fed into the system. The products leave as hot volatiles and char. The char goes down a small cyclone whilst the hot volatiles are passed through a flash tank, which separates the heavy oils. The vapour then flows through a condenser where the remaining water vapour and oil condenses leaving the syngas to go through.



### 4.3.3 Feedstock Performance

Qualitative observation of the pilot plant trials was used to determine the processing attributes of the pilot plant and the feedstock highlighting issues that might need consideration for the large scale design.

The sawdust generally flowed consistently through the augers for two of the moisture content levels (15% and 30%) identified for analysis. The green sawdust with a high moisture content of (60%) caused blockages on several attempts regardless of reactor temperature or auger speed.

As the sawdust was conveyed through the first couple of augers (Figure 49), it experienced compressional forces which built a firm plug (Figure 50). This was needed to eliminate the possibility for addition of oxygen via entrapped air in the system. The compressional and shear forces in combination with the moisture which acted as a lubricant caused an increase in density of the feedstock as it was conveyed to the reactor.



**Figure 49.** Loose sawdust being fed through bulk density  $280 \text{ kg/m}^3$ .



**Figure 50.** Dry compacted sawdust prior to decomposition, bulk density 1,202 kg/m<sup>3</sup>.

Hot volatiles were produced in as little as 45 – 80 minutes after feeding was started using the motors. Based on visual interpretation, the effects of manipulating the three variables (moisture content, reaction temperature and auger speed) on the process showed characteristics similar to results predicted by theory.

Increase in temperature showed an increase in flame height and reduced the char yield volumes. This suggests higher volumetric flow rates of syngas due to a larger degree of volatilisation. This was confirmed by the rotameter readings which at times exceeded the maximum scale of 2500 ml/min. Generally the pilot plant results showed more tar formation at 400°C, more oil formation at 450°C and more syngas formation at 500°C.

For a fixed temperature and fixed motor speed the increase of moisture content in the sawdust showed a reduction in feedstock flow properties. This is because the moisture could have acted as a lubricant which allowed the sawdust a higher degree of shear strain. This in turn caused an increase in density of the sawdust, thus causing a need for a larger mechanical driving force. The lower moisture feed generally produced more volatiles.

For a fixed temperature and fixed moisture content increase in feed rate via an increase in motor speed increased the amount of char produced. The char also appeared to be cooked less compared to slower feed rates.

A peculiar observation was made during a randomised run. It was noticed that starting the pyrolysis at a slow auger speed and increasing the motor speed to

ranges of 30 – 50 rpm enhanced gas flow properties. This could have been caused by the agitation of the solids in the reactor which allowed for more evenly distributed exposure times for different particles in a given channel. The agitation could have inhibited carbon fixing thus more gas was evolved from each particle because they had slightly more time to be transferred

Bio oil, bio-char and syngas yields were determined for the specified range of operating conditions and are shown in Table 33 and Table 34. The green sawdust could not be processed properly due to blockages. This was probably caused by increased shear strength of the sawdust due to high moisture (60%). The higher moisture allowed the sawdust to deform plastically which resulted in higher density of the sawdust plug. The high density plug required a large force to be conveyed through the reactor. Thus the pilot plant data was only collected from trials performed at two moisture levels.

**Table 33.** Raw data collected from pilot plant.

<b>Trial</b>	<b>Sample I.D</b>	<b>Moisture content (%)</b>	<b>Temp. (° C)</b>	<b>Auger speed (rpm)</b>	<b>Feed rate (kg/hr)</b>	<b>Char mass (kg/hr)</b>	<b>Oil mass (kg/hr)</b>	<b>Syngas mass (kg/hr)</b>
1	000	15	400	15	1.54	0.59	0.25	0.71
2	001	15	400	20	1.75	0.77	0.32	0.67
3	002	15	400	25	0.63	0.32	0.17	0.14
4	010	15	450	15	1.74	0.26	0.36	1.11
5	011	15	450	20	1.39	0.56	0.18	0.67
6	012	15	450	25	1.15	0.46	0.23	0.46
7	020	15	500	15	0.77	0.28	0.12	0.36
8	021	15	500	20	1.41	0.52	0.24	0.65
9	022	15	500	25	1.96	0.43	0.39	1.13
10	100	30	400	15	n/r	n/r	n/r	n/r
11	101	30	400	20	n/r	n/r	n/r	n/r
12	102	30	400	25	n/r	n/r	n/r	n/r
13	110	30	450	15	1.19	0.53	0.19	0.48
14	111	30	450	20	0.90	0.33	0.24	0.32
15	112	30	450	25	0.89	0.34	0.23	0.32
16	120	30	500	15	0.80	0.16	0.12	0.52
17	121	30	500	20	1.06	0.29	0.14	0.64
18	122	30	500	25	n/r	n/r	n/r	n/r

**Note:** Syngas mass was calculated by difference

**Table 34.** Pilot plant trial product distribution.

Trial	Sample I.D	Moisture content (%)	Temperature (° C)	Reactor auger speed (rpm)	Char yield (%)	Oil yield (%)	Syngas yield (%)
1	000	15	400	15	38	16	46
2	001	15	400	20	44	18	38
3	002	15	400	25	51	27	22
4	010	15	450	15	15	21	64
5	011	15	450	20	40	13	48
6	012	15	450	25	40	20	40
7	020	15	500	15	37	16	47
8	021	15	500	20	37	17	46
9	022	15	500	25	22	20	58
10	100	30	400	15	23	36	41
11	101	30	400	20	15	67	18
12	102	30	400	25	44	22	33
13	110	30	450	15	44	16	40
14	111	30	450	20	37	27	36
15	112	30	450	25	38	26	36
16	120	30	500	15	20	15	65
17	121	30	500	20	27	13	60
18	122	30	500	25	42	8	50

**Trials 19 – 27** Blocked reactor auger due to the use of green sawdust.

#### 4.3.4 Effects of Processing Parameters on Product Yields

The main effects of “reaction temperature” variation were determined using data from experiments 000, 010, 020 and can be viewed in Figure 51. This ensured that the other two variables were kept at nominal levels. The nominal yields are 38%, 16% and 46% for char, oil and syngas, respectively.

The char yield appears to decrease from 38% to 15% as the reaction temperature is raised from 400 to 450 °C causing an increase of liberated volatiles (62% - 85). It is observed that the syngas production rate has a higher increase (46%-64%) compared to that of the oil yield (16% - 21%).

The second increase in in temperature, displays similar yields to the nominal setup. This shows a reduction of volatiles liberated from 85% at 450°C to 63% at 500°C. The syngas yield drops to 47% whilst the oil yield is 16%.

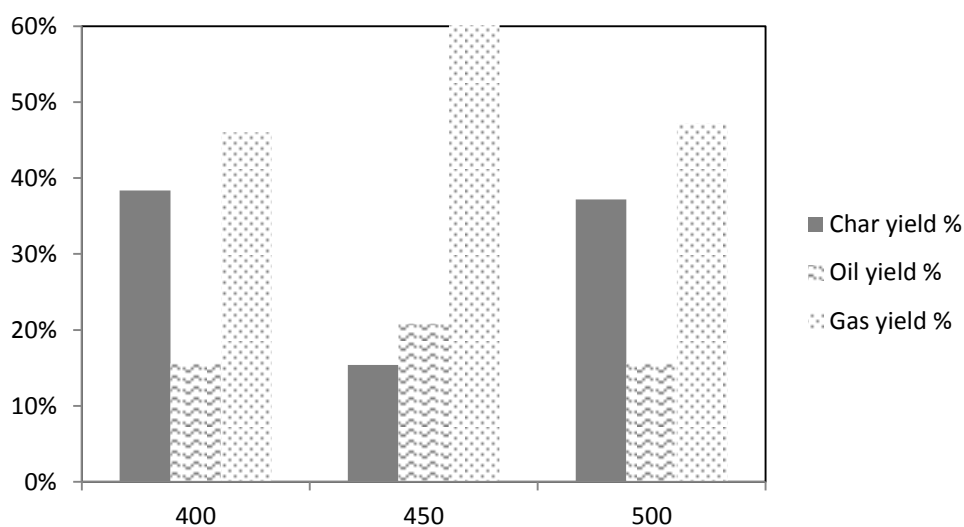


**Figure 51.** Product yields with respect to change in temperature.

The main effects of sawdust moisture content were determined using data from experiments 000 and 100. Yields from trial 200 could not be determined due to blockages caused by processing 60% moisture feedstock. Similar to the analysis of the main effect/s of temperature, the other two variables were kept constant at nominal conditions.

Using the nominal trial as a basis, the char yield is reduced from 38% to 23 % for sawdust at 30% moisture (Figure 52). A simple mass balance from the yield fractions might suggest this decrease is related to the increase of moisture. The change in distribution of volatile matter between oil and gas might confirm this too. The higher water content in the oil will demand a higher organic matter content in emulsions to reach equilibrium in the condensation step.

When the phenomena dictating the mass transfer is considered; one can note that drier sawdust will have a higher tendency to carbonise due to a lower heat capacity compared to the wetter. Therefore the apparent reactive surface for the

wetter feedstock is higher since the absence of this promotes movement of volatile matter.

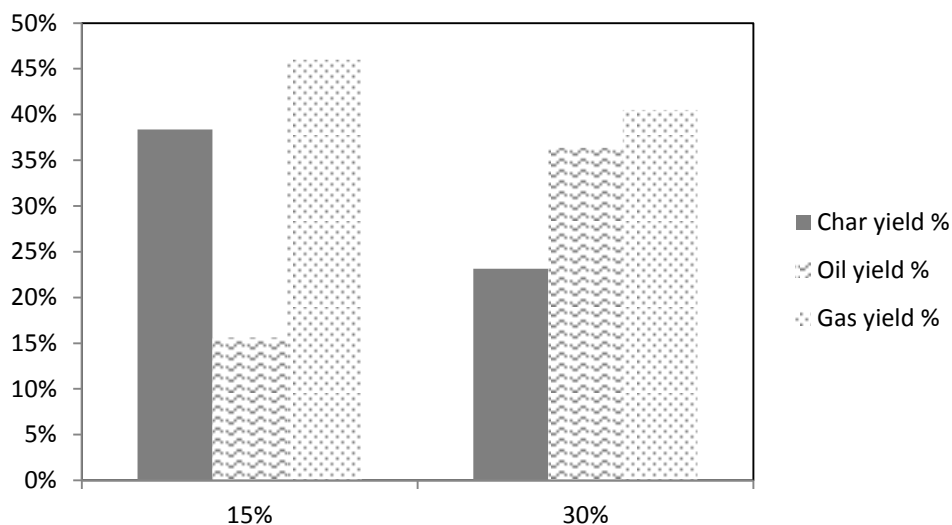


**Figure 52.** Product yields with respect to change in moisture.

The main effects of “reactor auger speed” variation were determined using data from experiments 000, 001, 002 and can be viewed in Figure 53. This ensured that the other two variables were kept at nominal levels. The nominal yields are 38%, 16% and 46% for char, oil and syngas, respectively as stated previously.

The char yield appears to increase from 38% to 44% as the auger speed is raised from 15 rpm to 20 rpm causing an decrease of liberated volatiles (62% - 55). It is observed that only the syngas production rate was decreased (46%-38%) while the oil yield increased (16% - 18%).

The second increase in in temperature, holds a similar trend char yields continue to increase when auger speed is increased from 20 – 25 rpm. Volatiles are reduced from 55% at 20rpm to 49% at 25 rpm. The syngas yield drops to 22% whilst the oil yield increases to 27%.

These effects confirm literature predictions. This can be simplified by considering the variables directly affected by the auger speed. Increasing the auger speed will typically alter the heating rates due to the lower contact times. Shorter contact time at constant temperature will have a lower degree of volatilisation thus char

yields are increased. A shorter contact time will inhibit the completion of devolatilisation reactions thus produce a higher solid residue.

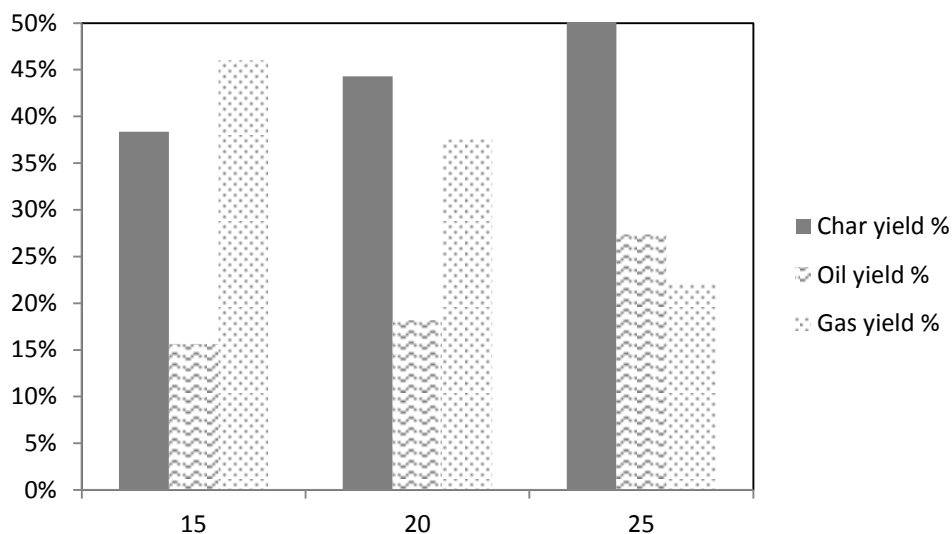


**Figure 53.** Product yield with respect to change in auger speed.

#### **4.3.4.1 Compound effects of processing parameters on product yields**

Compound effects of variables are normally hard to predict theoretically. This is because the variables might have complex interactions. These interactions could either be competitive or synergistic by nature. Synergistic interactions are interactions which produce higher effects than what might be predicted by a simple addition of the two main effects of the variables. Regardless of this, Table 34 shows different product yields for the other possible combinations of the three variables with the exception of those involving green sawdust.

### **4.4 Product Characterisation**

#### **4.4.1 Char Characterisation**

To simplify the interpretation of the pilot plant results the trials were analysed in two groups determined by the two moisture contents used. Case A includes all trials using 15% moisture content sawdust and Case B includes those of 30%



moisture. Step change of a processing parameter refers to a change in value based on the processing parameter key in Table 34.

The pilot plant trials showed that biochar yields varied with the experimental set up. Proximate and ultimate analyses of the different chars are presented in Table 35 and Table 36 respectively.

**Table 35.** Proximate analysis of biochars.

<b>Case</b>	<b>Moisture (% wt<sub>wb</sub>)</b>	<b>Dry solids (% wt<sub>wb</sub>)</b>	<b>Total ash (% wt<sub>wb</sub>)</b>	<b>Total organic matter (% wt<sub>wb</sub>)</b>	<b>Char yield</b>
<b>000</b>	36.74	63.26	9.77%	53.49	38%
<b>001</b>	28.19	71.81	6.83%	64.98	44%
<b>002</b>	26.30	73.70	4.90%	68.80	51%
<b>010</b>	72.86	27.14	2.81%	24.33	15%
<b>A 011</b>	23.14	76.86	3.55%	73.32	40%
<b>012</b>	21.86	78.14	21.33%	56.82	40%
<b>020</b>	20.38	79.62	4.94%	74.68	37%
<b>021</b>	5.61	94.39	8.00%	86.39	37%
<b>022</b>	3.34	96.66	3.05%	93.60	22%
<b>100</b>	10.15	89.85	2.45%	87.40	23%
<b>101</b>	25.95	74.05	1.93%	72.12	15%
<b>102</b>	10.58	89.42	8.07%	81.36	44%
<b>110</b>	47.79	52.21	1.27%	50.94	44%
<b>B 111</b>	47.79	52.21	4.94%	47.27	37%
<b>112</b>	3.24	96.76	5.13%	91.63	38%
<b>120</b>	43.66	56.34	7.22%	49.12	20%
<b>121</b>	13.81	86.19	7.06%	79.13	27%
<b>122</b>	6.01	93.99	7.29%	86.70	42%

Samples 000, 010, 020 were used to explore the main effects of temperature on the char proximate composition. No apparent trend is shown as the residual organic matter fraction decreases from 53.49 % to 24.33% with the first step increase in temperature from 400 to 450°C then it increases from 24.33% to 74.68% with increase in temperature from 450°C to 500°C.

Char elemental analysis revealed that carbon, hydrogen and nitrogen contents increased from 68.88 %, 2.82% and 0.38%, to 77.90 %, 3.36%, and 0.48% respectively with the first step increase in temperature. The second step increase

in temperature causes a slight drop in content levels of carbon, hydrogen and nitrogen from 77.90 %, 3.36%, and 0.48% to 76.25%, 3.07% and 0.35%.

**Table 36.** Ultimate elemental analysis for biochar.

Case	Sample I.D	C (%)	H (%)	N (%)	S (%)	O (%)*	HHV (MJ/kg)	L HV (MJ/kg)	H/C ratio	Residual carbon (%)
A	000	68.88	2.82	0.38	<0.40	27.53	27.71	27.10	0.04	22.25
	001	74.90	3.23	0.41	<0.40	21.07	30.36	29.67	0.04	28.01
	002	75.92	3.26	0.27	0.40	20.16	30.77	30.07	0.04	32.91
	010	77.90	3.36	0.48	<0.40	17.86	31.58	30.86	0.04	9.93
	011	77.50	2.84	0.31	<0.40	18.96	30.70	30.09	0.04	26.35
	012	69.78	3.19	2.74	<0.40	23.90	28.55	27.87	0.05	23.72
	020	76.25	3.07	0.35	<0.40	19.94	30.60	29.94	0.04	23.98
	021	79.52	2.62	0.31	<0.40	17.16	31.07	30.50	0.03	25.01
	022	81.43	2.58	0.39	<0.40	15.21	31.66	31.11	0.03	15.23
B	100	80.92	3.38	<0.30	<0.40	15.28	32.65	31.92	0.04	15.82
	101	78.41	3.14	0.54	<0.40	17.52	31.44	30.76	0.04	10.00
	102	78.93	2.96	0.31	<0.40	17.41	31.36	30.73	0.04	29.52
	110	73.10	3.40	0.66	<0.40	22.45	29.99	29.26	0.05	27.34
	111	71.54	3.41	0.41	<0.40	24.25	29.47	28.74	0.05	22.50
	112	77.99	2.83	0.42	<0.40	18.37	30.85	30.24	0.04	25.19
	120	75.24	2.71	0.47	<0.40	21.19	29.73	29.15	0.04	12.79
	121	83.06	2.59	0.34	<0.40	13.63	32.24	31.69	0.03	19.06
	122	80.10	3.10	0.37	<0.40	16.04	31.96	31.30	0.04	28.59

**Residual carbon** = Carbon sequestration potential assuming total carbon in char is fixed in soils

The heating values follow suit with HHV increasing from 27.71 to 31.58 before dropping to 30.60 MJ/kg respectively as they depend on the carbon and hydrogen contents. Oxygen contents were calculated from difference and show opposing trends to those of the other elements.

The main effect analysis from samples 000, 001, 002 with auger speeds at 15, 20, 25 rpms respectively, proximate analysis shows that total organic matter increases with increase in auger motor speed. This confirms that increasing the reactor auger speed will lead to a decrease in degree of devolatilisation of organic matter. The total ash content is reduced as a result mostly due to dilution effect.

Char elemental analysis revealed that carbon and hydrogen contents increased from 68.88 % and 2.82% to 74.90% and 3.23% then 75.92% and 3.26% respectively. Nitrogen contents initially increase from 0.38%, to 0.41% for the

first auger speed step increase but decrease to 0.27% for the second auger speed step increase.

The heating values are a function of mainly the carbon and hydrogen content increase from 27.71 to 30.36 then 30.77 MJ/kg respectively with increase in reactor auger speed.

Oxygen contents calculated from difference and are shown to increase with increase in reactor auger speed opposing the trends observed for carbon and hydrogen.

For case B, with moisture content of feedstock at 30% wet weight basis the main effects of temperature were observed using samples 100, 110, 120. The data showed that increase in temperature lead to a decrease in total organic matter content in the char. The total organic matter for the samples were 87.40%, 50.94%, 49.12% respectively. This confirms an increase in degree of devolatilisation of biomass as reaction temperature is increased.

Char elemental analysis revealed that carbon was decreased from 80.92% to 73.10% in the first step change, hydrogen, nitrogen and oxygen contents increased from, 3.38%, <0.30% and 15.28% to 3.36%, 0.66% and 22.45% respectively. The second step increase in temperature causes a slight increase in carbon content levels from 73.10% to 75.24% of carbon. Hydrogen, nitrogen and oxygen contents decrease from 3.40%, 0.66% and 22.45% to 2.71% 0.47% and 21.19% respectively. The heating values of the chars decrease with increase in reaction temperature with HHV values of 32.65, 29.99 and 29.73 MJ/kg respectively.

The main effects of auger speed for case B were observed using samples 100, 101, 102. The data showed that the total organic content of the char decreased from 87.4% to 70.12% with the first step increase in reactor auger speed from 15rpms to 20rpms. The next step increase in temperature from 20 to 25rpms shows an increase of total organic content of the char from 70.12% to 81.36%.

Char elemental analysis revealed that carbon and hydrogen contents were decreased from 80.92% and 3.38% to 78.41% and 3.14% in the first step change, nitrogen and oxygen contents increased from, <0.30% and 15.28% to 0.54% and

17.52% respectively. The second step increase in auger speed causes a slight increase in carbon content levels from 78.41% to 78.93% of carbon. Hydrogen, nitrogen and oxygen contents decrease from 3.14%, 0.54% and 17.52% to 2.96% 0.31% and 17.41% respectively.

The heating values are shown to decrease from 32.65 to 31.44 then 31.36 MJ/kg respectively with increase in reactor auger speed.

#### **4.4.1.1 Summary of effects process parameters on char**

##### **4.4.1.1.1 Feedstock moisture content**

An increase in feedstock moisture also showed an increase in total organic matter in chars from 000, 100 which correspond to 15%, 30% moisture content respectively. Similar to the preceding subset, the total ash content decreases with increase in moisture content due to the dilution effects.

It appears that the feedstock moisture does not appear to have a significant effect on the moisture content of the char. The residual moisture in the char will depend on the water retention properties of the char product (Taylor 2010). Therefore, it appears there is no direct correlation between the feedstock moisture and the moisture content of the chars.

Using a global energy balance on the process based on the rule of mixtures, it is clear to see that for a specific reaction temperature, sawdust of higher moisture content will have higher heating demands (3 kJ/kg compared 2.75 MJ/tonne assuming dry wood has  $C_p$  of 2.5 MJ/tonne (The\_Engineering\_Toolbox)). However, considering the pilot plant yields it appears that the 30% moisture sawdust trials had a higher degree of devolatilisation. This might have been a result of the water enhancing heat transfer within the saw dust bulk. The excess water meant the sawdust contained 30% moisture has a higher heating capacity compared to that which contained only 15%. Steam performs as a heat carrier, therefore, increasing the amount of moisture will increase the amount of heat needed to raise the temperature of the feedstock however it will increase the driving force for heat exchange between the combustion gas and the feedstock through the reactor walls. Literature states that increase in heating rate will

increase volatile product yields (Antal and Grønli 2003, Branan 2005, Rezaiyan and Cheremisinoff 2005, Mohan, Pittman et al. 2006, Lu, Li et al. 2009, Basu 2010).

#### **4.4.1.1.2 Reactor Temperature**

Basic pyrolysis theory states that increase in temperature will increase the fraction of volatiles released. However, pilot plant trials such as 000,010,020 which were inconsistent with trends predicted by theory cannot be explained at first glance. The deviation from trends predicted by basic theory can be explained inspecting the nature of pyrolytic reactions, the yields obtained suggest that the two extremes, 400°C and 500 °C favour different phenomena.

1. Increase in temperature a constant moisture content level and auger speed will increase the rate of devolatilisation.
2. Increasing the temperature will also increase the tendency of case hardening which inhibits liberation of volatile matter thus promoting carbonisation. Case hardening effects can be minimised by inducing agitation.

The two phenomena are the principle limiting mechanisms and the product yields of any configuration will depend on the higher driving force available. An avenue that might be of great interest is the investigation of the heat transfer scheme of the reactor which monitors the heat transfer from combustion gases into the feedstock. This would be very useful in quantifying the heating rate experienced by the feedstock. Accurate monitoring of the feedstock heating rate has proven to be a big challenge for pyrolysis at pilot scale levels because the cost could not be justified.

#### **4.4.1.1.3 Auger Speed**

Auger speed manipulation consistently demonstrated a strong relationship with the extent of devolatilisation. This was proven in both case A and B by a consistent increase in char yields and residual organic matter content of chars with increase in auger speeds. This inconsistent behaviour might be explained if you

consider the reactor auger speed to have two main responses to the processing conditions.

1. Increasing the auger speed causes agitation of the bulk sections. This enhances volatile discharge from sawdust particles. This promotes higher volatile yields.
2. Increasing the auger speed reduces the contact time for the sawdust particles and the heating walls. This reduces the extent of decomposition thus promotes char formation.
3. Increase in auger speed enhances even temperature distribution.

If one is to consider a variant reactor auger speed as shown in samples 100, 101, 102 from case B, The amount of organic matter in the char can be credited to these two responses. The first response is dominant in the first step change from 15rpms to 20 rpms, whilst the second is dominant in the change from 20rpms to 25 rpms. The third response is expected to be active in both steps but from the experiment it appears to be a background/recessive response.

#### **4.4.1.2 Raman spectroscopy**

Multiple spectra of the samples were collected and mean values were analysed. A summary of the spectral analysis is shown in Table 37. The samples are referred to using the same naming code defined in the design of experiments (Table 34).

##### **G band Position**

G band position appears to be one of the most sensitive features in terms of thermo-induced structural morphology. Figure 54 shows the increase of the G band wavelength position with an increase in heat treatment temperature (HTT) for batch process char. This scale will be used as a basis for comparison for the char produced from Lakeland Steel's continuous process.

**Table 37.** Summarised spectra analysis results.

Code	Moisture content (%)	Temperature (° C)	Reactor auger speed (rpm)	G band position
000	15	400	15	1572
001	15	400	20	1573
002	15	400	25	1568
010	15	450	15	1572
011	15	450	20	1576
012	15	450	25	1572
020	15	500	15	1576
021	15	500	20	1577
022	15	500	25	1577
100	30	400	15	1570
101	30	400	20	1576
102	30	400	25	1578
110	30	450	15	1572
111	30	450	20	1534
112	30	450	25	1575
120	30	500	15	1579
121	30	500	20	1580
122	30	500	25	1578

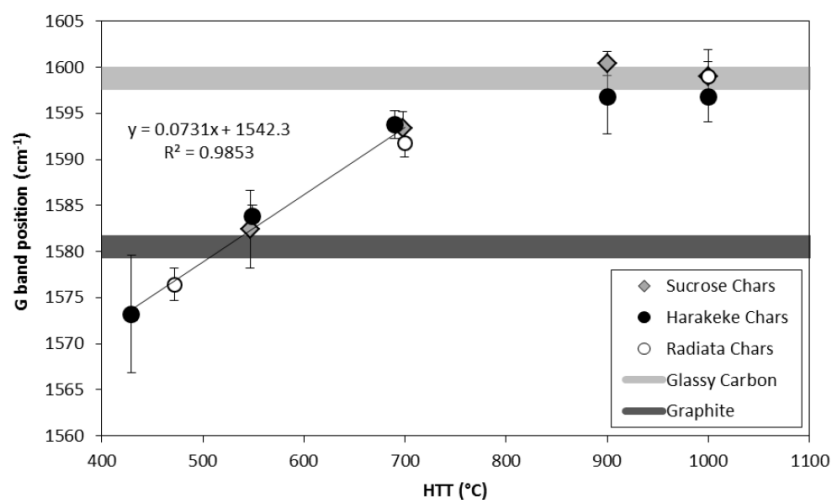


**Figure 54.** Plot of G band position as a function of heat treatment temperature for chars. Broad horizontal guide lines represent approximate G band positions measured for glassy carbon and graphite samples. Linear trend line and correlation based on mean data points (from chars derived from all three precursors) between  $HTT \approx 420 \text{ }^\circ\text{C}$  and  $HTT \approx 700 \text{ }^\circ\text{C}$  (John McDonald-Wharry 2012).

The chars being analysed have been produced within the limits of the linear range. Figure 55 shows the G band positions for the char samples. With the exception of sample 111, all the position of the G band for the samples appears to confirm comparable results. Discrepancies can be attributed to the difference in heating scheme. The batch process allows for a heat up time and a known retention time at the reaction temperature whilst the continuous process allows a transient heating profile for most of the reaction.

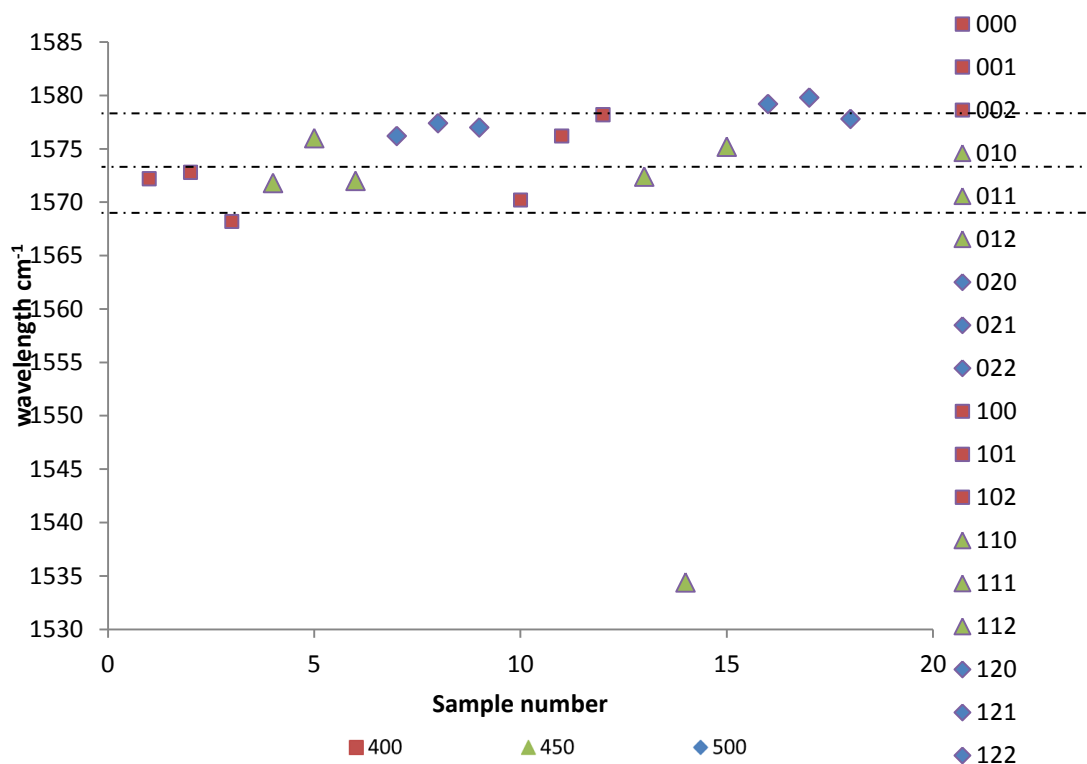


**Figure 55.** G band position for different pine char samples (sample number along the x axis refers to the sample ordered vertically on the right end).

The comparison of G band positions verified that the char produced from the continuous process had temperature comparable to char produced in a batch experiment performed by McDonald-Wharry (2012).

While, sample 111 does not show predicted G band position, minor discrepancies observed for other samples might have been due to the limitations of the Raman method which include:



- Inability to directly distinguish main effects of other parameters such as moisture content and reactor auger speed.
- Quantification of a direct correlation of batch operation maximum feedstock temperature vs continuous mode non-isothermal temperature profile.

Understanding the similarities between char produced under different conditions for example batch vs continuous will allow for a better evaluation in terms of marketing potential of the product.

#### **4.4.2 Syngas Characterisation**

Syngas characterisation was performed using two chromatography units as described in the methodology section. The department's chromatography method was only able to detect was not able to detect CH<sub>4</sub>, CO<sub>2</sub>, H<sub>2</sub>, O<sub>2</sub>, N<sub>2</sub>, CO. therefore; C<sub>2</sub>H<sub>4</sub> and C<sub>2</sub>H<sub>6</sub> will not be discussed. From observation of the data presented in Table 38, Syngas calorific values range from 5.07 - 12.38 MJ/dscm. The earlier was obtained from pilot plant running at 400°C whilst the later at 500°C. This confirms pyrolysis theory which predicts that increasing the temperature increases the calorific value of the syngas. This prediction assumes that the higher degree of volatilisation will promote the formation of methane and hydrogen.

#### **4.4.3 Bio-Oil Characterisation**

Bio-oil was highlighted as the least marketable pyrolysis product in New Zealand at the moment, despite the huge global interests it has received. This is because New Zealand has a relatively small infrastructure for liquid fuel refining. Whilst biochar is sought after for its environmentally friendly properties and syngas is used to lower processing costs. Thus, characterisation was only performed for concentrated samples obtained in the first trial (000) and is presented in Table 39. The sample was concentrated by decanting.

**Table 38.** Syngas characterisation for pilot plant trial samples.

Trial	Composition (%)								HHV (MJ/dscm)
	CH <sub>4</sub>	CO <sub>2</sub>	C <sub>2</sub> H <sub>4</sub>	C <sub>2</sub> H <sub>6</sub>	H <sub>2</sub>	O <sub>2</sub>	N <sub>2</sub>	CO	
000	9.40	32.70	0.76	0.81	16.80	5.20	20.60	13.60	8.21
001	9.40	39.90	0.00	0.00	11.55	5.14	30.36	3.66	5.37
002	9.06	31.62	0.00	0.00	13.55	7.21	29.83	31.62	6.10
010	8.26	24.70	0.00	0.00	12.38	8.48	32.85	13.32	6.21
011	11.40	15.60	0.18	0.69	9.30	12.00	45.90	5.00	6.57
012	Not recorded								
020	Not recorded								
021	7.60	18.50	0.41	0.65	10.30	11.30	45.40	5.90	5.50
022	15.50	30.10	0.61	1.11	27.50	1.60	6.00	17.50	12.38
100	6.27	28.70	0.00	0.00	5.35	7.45	35.05	17.18	5.07
101	9.85	34.95	0.00	0.00	4.90	7.38	26.19	16.72	6.31
102	13.00	38.36	0.00	0.00	8.18	4.51	22.93	13.03	7.45
110	15.29	43.92	0.00	0.00	10.65	2.13	8.30	19.71	9.41
111	10.27	51.22	0.00	0.00	17.78	2.06	8.05	127.87	7.29
112	11.50	31.90	0.37	0.87	15.40	4.30	25.40	10.20	8.23
120	9.90	33.50	0.78	0.58	24.00	4.20	15.90	11.10	8.80
121	17.00	24.50	0.63	0.95	20.50	4.40	17.00	15.00	11.70
122	Not recorded								

Trials 012, 02, 122 were not analysed due to technical issues with GC equipment

**Table 39.** Bio oil ultimate analysis.

C (%)	H (%)	N (%)	S (%)	O* (%)	HHV (MJ/kg)	LHV (MJ/kg)
49.09	7.71	1.56	<0.40	41.24	27.96	26.31

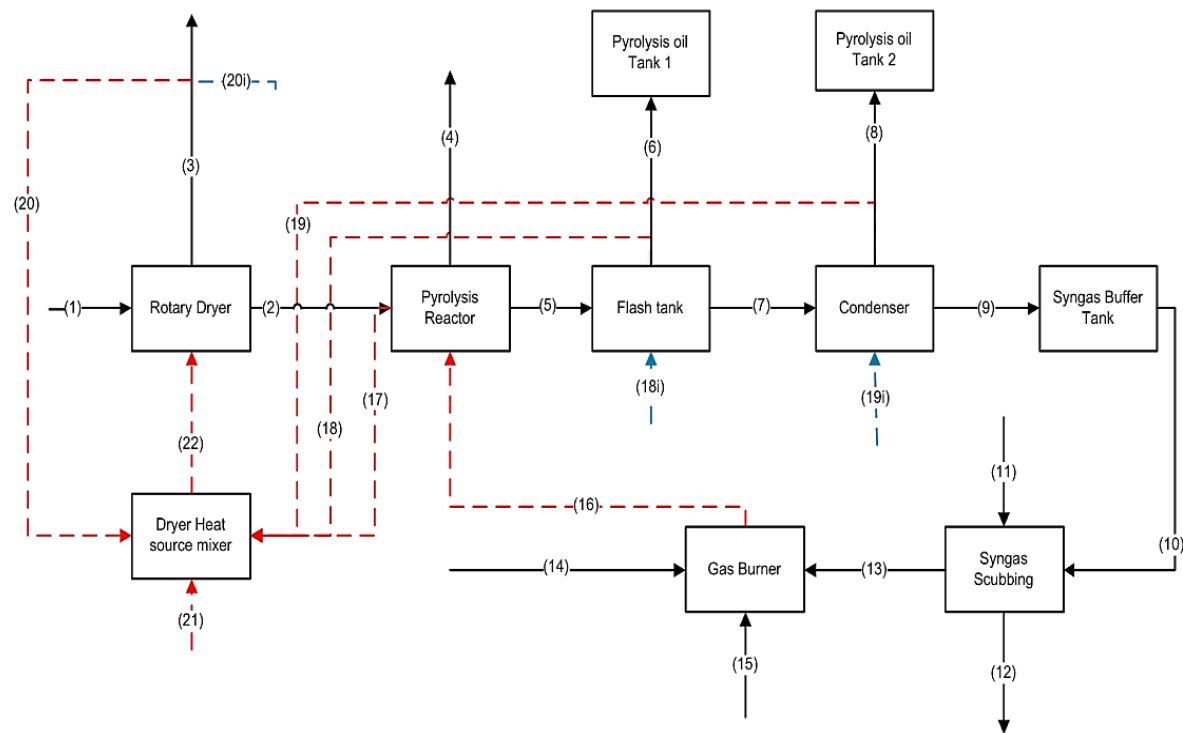
O\* calculated by difference

**Chapter 5.**  
**Large Scale Plant**  
**Design Concept**

## **5.1 Introduction**

### **5.1.1 Process Description**

The large scale concept will work on the same principles used in Lakeland Steel Ltd.'s pilot plant. The feedstock is force fed into an auger kiln using augers from the hopper. The kiln is heated to the desired reaction Temperature (400°C will be used as a basis) and the products leave as hot volatiles and char. The char goes down a small funnel (cyclone like) and conveyed to a collection vessel whilst the hot volatiles are passed through a flash tank, which separates the heavy oils. The vapour then flows through a condenser where the remaining water vapour and light oil condenses allowing the syngas to go through to the syngas buffer tank. The buffer tank regulates the syngas flow rate as it feeds it into the gas burner.



Stream	Description	Temp. (°C)
1	Wet feed	25
2	Dried feed	85
3	dryer exhaust	85
4	Char	50
5	Hot volatile gas	250
6	Heavy oil	60
7	Light oil & syngas	135
8	Light oil	30
9	Syngas	30
10	Syngas	30
11	Scrubbing fluid ( <i>optional</i> )	25
12	Scrubbing effluent ( <i>optional</i> )	25
13	Syngas	25
14	Supplementary fuel	25
15	Air	25
16	Combustion gases	$\geq 900$
17	Reactor stack	115
18	Condenser recovery	115
19	Flash recovery	115
20	Char cooling loop	85
21	Char heat recovery loop	65
22	Dryer exhaust recovery	65
23	Supplementary air	25
24	Drying air	115

Figure 56. Schematic for large scale pyrolysis process.

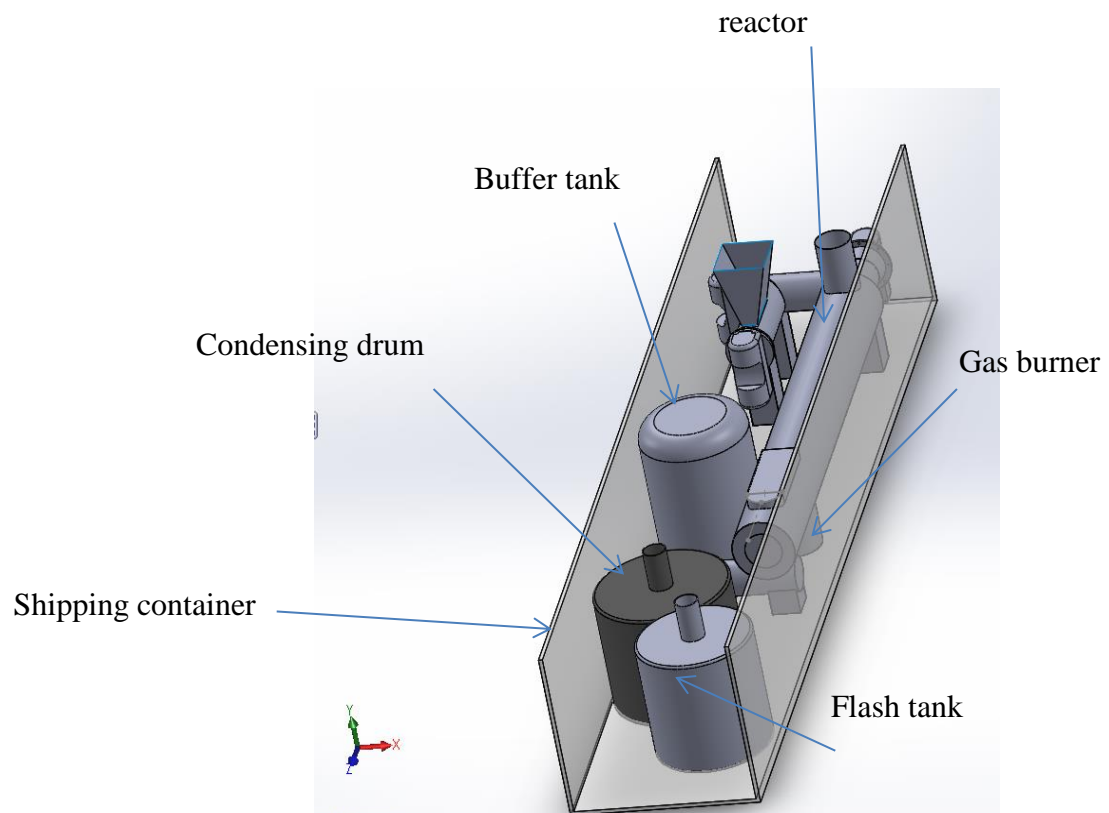


**Figure 57.** Arrangement of equipment in shipping container showing no space for dryer.

## 5.1.2 General Assumptions for Large Scale Plant Design

The large scale plant design is adapted from Lakeland Steel's pilot plant technology and uses an auger reactor. The large scale plant design concept was created based on the project brief specifications. The large scale plant was needs to handle 3.45 t/hr. which amounts to a yearly throughput of 28,980 tonnes. It also had to be able to fit in a 40 foot/ 12m standard shipping container. The size would effectively render this to be a mobile plant. The design will therefore be dimension driven.

## 5.2 Large Scale Plant Design

The design process will emulate the anatomy of the chemical process shown in Coulson and Richardsons Chemical Engineering handbook as shown in Figure 58.

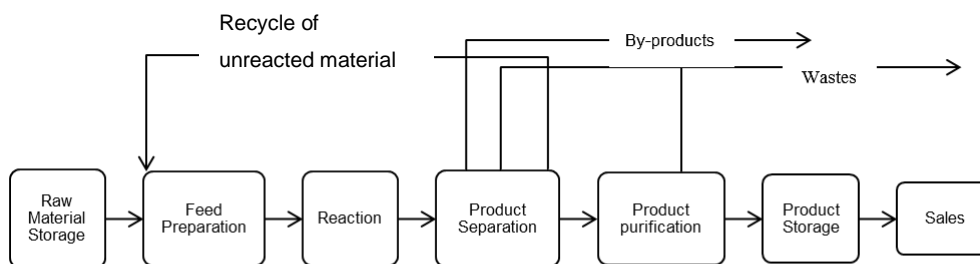


**Figure 58.** Generic Anatomy of Chemical Processes.

### 5.2.1 Feed Preparation

Pre-treatment refers to any processes prior to the main reaction which in this case refers to pyrolysis. Pre-treatment includes procedures such as drying, particle control. The later will not be considered an issue as the sawdust is generally small grains with diameters ranging from approximately 2 to 4mm on average with trace of fines and chips which are up to 15mm long, 4mm

wide and 2mm thick. The chips do not pose much threat in terms of mass conveying but they introduce a slight risk in affecting the even heat distribution. A simple grate can be used to prevent the inclusion of wood chips into the hopper.

### **5.2.1.1 Dryer Design Selection Criteria**

Appropriate drying technology is normally selected based on the criteria shown in the ratings table. All ratings are out of 10, with 10 being the best and 0 being the worst.

#### ***5.2.1.1.1 Operating Cost / Energy Demands***

The two technology options being considered have slightly different dependencies when it comes to operating costs. The rotary dryer operating costs are generally dependent on the drying duty, whilst the multiple effect evaporators use pressure swings to take advantage of the heat in the steam from the evaporated water in the feedstock. This normally means the heat is being recycled, with each cycle. This means the multiple effect dryer earns a higher score of 9 while the rotary dryer has greater energy demands and thus will be rated 7 in this category.

#### ***5.2.1.1.2 Compatibility with Feedstock***

Some dryers require the feedstock to be pre-formed into specific shapes in order for the drying to be processed. The rotary dryer gets 8 out of 10 based on the fact that it can handle the sawdust really well. There are usually no problems with blockages or any other material flowing characteristics. The generic multiple effect evaporator normally requires feedstock to be presented in a thin film. However by using augers with small spacing, the thickness of the sawdust layer can be controlled. A heating jacket can be used to indirectly heat the feedstock. The fact that the multiple effect evaporators being used won't be the conventional type gives it a rating of 5.



#### **5.2.1.1.3 Capital Cost**

Some technologies are generally more expensive and thus, using them can only be justified at high production rates. The multiple effect evaporator is given a rating of 5 because it is generally known to be expensive. The number of cycles needed to dry the feedstock will typically determine the capital cost as each effect will require pressure swing equipment and housing for the feedstock. The sizing and costing of the rotary dryer is based on the feedstock occupying around 10 - 15% of the dryer volume for air circulation purposes. The simplicity of this design results in lower capital compared to the multiple effect evaporators and this gives it a capital cost rating of 7.

#### **5.2.1.1.4 Maintenance**

The main issue that arises with the maintenance of dryers is the ease of cleaning in terms of residue sticking to walls. The rotary dryer gets a rating of 8 because an optimal combination of installation angle and rotational speed will ensure the feedstock doesn't stick to the walls. The multiple effect evaporators will require cleaning of the auger channels as the wet sawdust can cause blockages. This earns the MEE a maintenance rating of 4.

#### **5.2.1.1.5 Heating Method**

The two methods being compared are direct and indirect heating. The direct heating method being used in the rotary dryer is more efficient as the heat is directly put into the feedstock. This gives it a rating of 8. The multiple effect evaporator works on the principle of recycling heat but it also requires the steam to be at a higher temperature than the air in the rotary dryer so this gives it a rating of 6.

#### **5.2.1.1.6 Versatility**

The versatility of the dryer can be seen as its ability to handle a range of feedstock and dry them to a range of moisture levels. The rotary dryer has been rated 7 based on how easy it would be to process a range of feedstocks or dry to different moisture contents and also handle a range of sawdust

particle sizes. The multiple effect evaporators will need to be resized to account for the different flowing properties of the feedstock. This earns the MEE a versatility rating of 5.

#### **5.2.1.1.7 Conclusion**

Based on this literature review, the most appropriate dryer types for the project are rotary dryer and multiple effect dryers. This is because the Rotary dryer is the most appropriate for the feedstock being considered and the multiple effect evaporators have the potential to have the lowest operating costs. The most applicable between the two can be determined after modelling the two designs for the up-scaled plant model. Experimental data from drying curves will be needed to facilitate the modelling.

The following table shows the rating of the two prospective drying technologies.

**Table 40.** : Prospective dryer ratings.

	<b>Maximum weighting</b>	<b>Rotary Dryer</b>	<b>Multiple Effect Dryer</b>
<b>Operating cost/ energy demands</b>	10	7	9
<b>Compatibility with feedstock</b>	10	9	5
<b>Capital Cost</b>	10	7	5
<b>Maintenance</b>	10	8	4
<b>Heating method</b>	10	7	6
<b>Versatility</b>	10	7	5
<b>Total (out of 60)</b>	10	45	34

The ratings show that the rotary dryer is the best option for pre-drying the sawdust.

#### **5.2.1.2 Rotary Dryer Design**

The rotary dryer design was based on sawdust

The design of the rotary dryer was performed using data collected from drying characteristics obtained in lab-scale experiments. Feedstock drying trials performed at 80, 90 and 100°C as described in the ‘Methodology’

section. Drying curves were used to determine the required residence time of the sawdust for a 100% efficient dryer.

The total energy needed to perform the drying was calculated using

$$Q_t = U_a V (t)_m \quad (42)$$

Where  $Q$  is the total energy;  $U$  the volumetric heat transfer coefficient;  $t$  is the temperature difference of the solids.

The volumetric heat transfer coefficient is calculated by:

$$U_a = 0.247 \left( \frac{M_s}{\rho_s V} \right)^{0.5} G^{0.16} \quad (43)$$

Where  $M$  is the dry solids mass,

$\rho_s$  is the density of the solids

$V$  is the volume of the sawdust,

$G$  is the mass velocity of the air.

Assuming that the charge only takes up 10% of the volume and that the L/D is within the 4-10 range as recommended by Perry's (Moyers. and Baldwin 1999), the dimensions of the dryer can be solved simultaneously.

Calculations were performed (Figure 59) using a spread sheet to produce dryers of the specifications in Table 41.

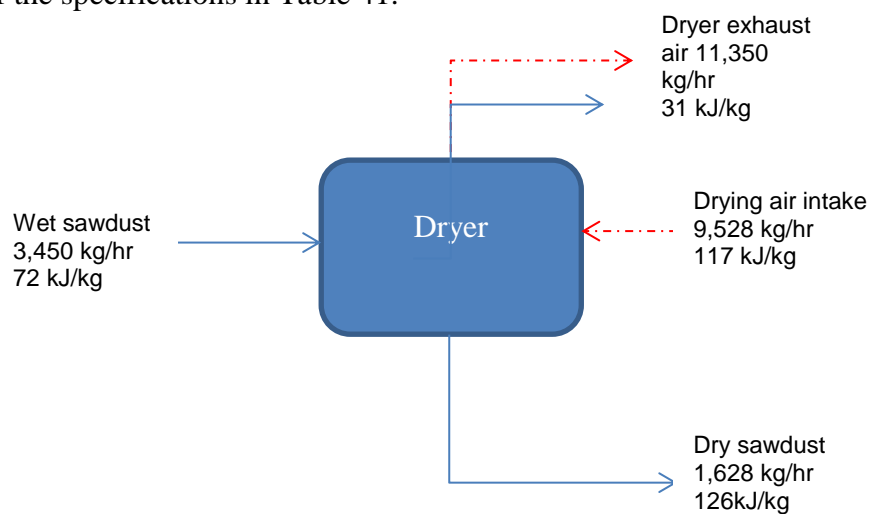


**Figure 59.** Mass and energy balance for sawdust drying.

**Table 41.** Rotary dryer specifications.

<b>Sawdust feed rate (kg/h)</b>	3,450
<b>Density (kg/m<sup>3</sup>)</b>	250
<b>Volume produced (m<sup>3</sup>)</b>	12.3
<b>Dry solids (kg/h)</b>	1,380
<b>Total moisture removed (kg/h)</b>	2,070
<b>Allowable moisture (@15% dry solids) (kg/h)</b>	248
<b>Pyrolysis charge (kg/h)</b>	1,628
<b>Water removed (kg/h)</b>	1,821
<b>Air needed (kg/hr)</b>	9,528
<b>Residence time(h)</b>	1.65
<b>Volume of dryer assuming feed is 10% vol (m<sup>3</sup>)</b>	203
<b>Length (m)</b>	16.2
<b>Diameter (m)</b>	4
<b>L/D ratio</b>	4
<b>Operating temperature (°C)</b>	85
<b>Q (MJ/h)</b>	5,000

## **5.2.2 Reaction stage**

### **5.2.2.1 Reactor design**

The reactor is the heart of the process and requires a flexible approach to design a unit which delivers the best aspects of a number of styles currently available. Thus flexible design morphology can be used to design the large scale unit.

#### ***5.2.2.1.1 Design Morphology***

The variables considered for reactor design include:

- Heating approach
- Heat type
- combustion, dielectric, electric– segmental vs. single input
- Feeding considerations – pressure control: gravity assisted, excess torque on auger,
- Volatile gas extraction
- Char extraction

- Heat recovery - including preheating feedstock, accounting for heat losses.

**Table 42.** Reactor design morphology overview.

Design variable	Options			
<b>Heating Approach</b>	Direct Hot combustion gases	Indirect through walls – temperature limited	Partial combustion of feedstock (more a gasification)	
<b>Heat type</b>	Combustion gases	Dielectric	Electric Resistance	Steam
<b>Feeding Considerations</b>	Stationary feed	Moving bed	Fluid assisted	Mechanically assisted
<b>Volatile Gas extraction</b>	Buoyancy effect	Post reactor vacuum/ blower	Pre- reactor pressure build using compressed inert gas	
<b>Char Extraction</b>	Gravity	Auger		
<b>Heat Recovery</b>	Heat exchange with air	Heat exchange with water		

### **5.2.2.1.2 Reactor Concept Selection Criteria**

Using this design morphology a strategic combination of the options can be used to design a range of reactors. However, the reactor concept selection will weigh two gas fired options a indirectly heated auger kiln vs. an indirectly heated rotary kiln reactor. As stated earlier the auger kiln is an adaptation of Lakeland Steel’s pilot plant whilst the rotary kiln was chosen due to it being similar to the auger technology. The main difference is the rotary kiln conveys the feedstock using a combination of gravity feeding and flights along the reactor walls. Another difference worth noting is that the rotary kiln relies a lot more on convection and has a higher void fraction of about 45% reactor volume whilst the effective void fraction of the auger is ~ 9%. The auger reactor does not actually have any void areas but the effective void fraction is a result of the auger flights which displace ~9% the volume. This value could change depending on the pitch and number of flights being used (the auger in this thesis uses a double flight design).

### **5.2.2.1.3 Compatibility with Feedstock**

Sawdust can be easily handled by either reactor concepts. Its physical properties exhibit low fouling tendencies. Both reactors can be expected to handle the feedstock well.

### **5.2.2.1.4 Capital Cost**

Both concepts have been chosen due to their exceptional capital cost compared to other reactors. They are relatively simple when compared to other options such as microwave reactors or fluidised bed reactors.

### **5.2.2.1.5 Heating Method**

The prospective concepts are both indirectly heated. However the auger reactor can be expected to have a higher heat flux per unit area of the reactor wall. This is because the rotary kiln has a high void fraction which effectively causes difference in driving forces for the heat transfer mechanism for the two sections of the reactor.

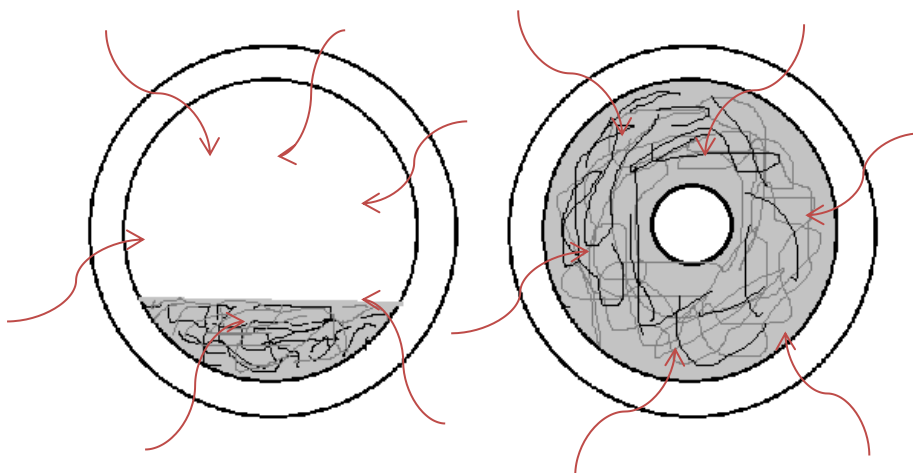


**Figure 60.** Schematic of heat transfer to feedstock.

The bottom will have a higher heat transfer coefficient whilst the top will be lower due to the difference in thermal conductivity between the sawdust and the air/void (Figure 60).

The rotary kiln would be more effective with directly fired heating approach however; this can lead to a change of process from pyrolysis to gasification.

#### **5.2.2.1.6 Versatility**

The two reactors work well with feedstock types that have low caking tendencies. However, the rotary kiln has an advantage as it can be easily modified for caking materials by incorporation of flights and detachable chains that clean the walls during processing. This is evident in gypsum processing where slurries can be conveyed without much difficulty in calcination processes. The auger kiln has shown tendencies to block when feedstock of high moisture is fed through. For a fixed diameter, this can be countered by increasing the linear flight density and increasing the torque from the motor.

#### **5.2.2.1.7 Operating Cost / Energy Demands and Maintenance**

The two reactors appear to have low maintenance costs with non-caking materials such as sawdust. This is because caking materials have a high tendency to foul reactor walls and this can lower corresponding heat transfer efficiencies.

The reactors both require the use of motors and deploy indirect heating. Whilst the difference in operating cost of the motors might not be easily distinguished without the aid of tedious sizing calculations, it can be noted that the higher heating flux from the auger reactor is expected to give it higher heat transfer efficiency. Therefore, the auger reactor can be expected to have lower energy consumption.

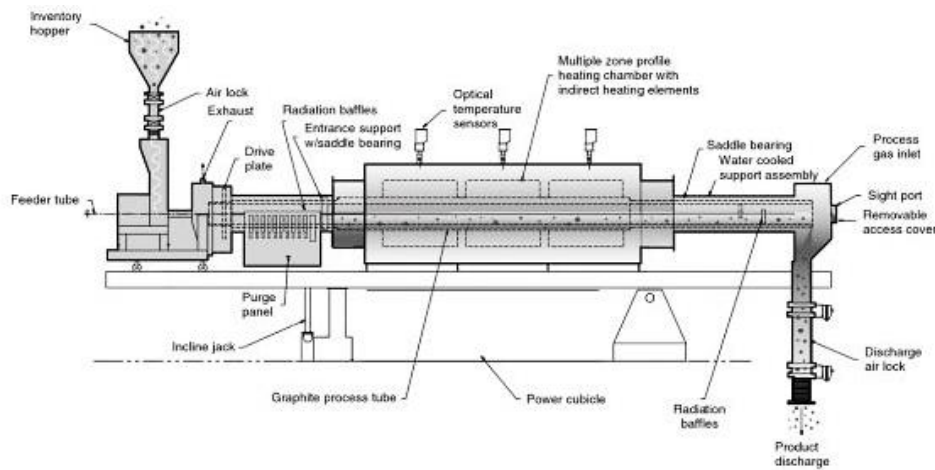


**Figure 61.** Indirect-fired small Rotary kiln reactor (Courtesy of Harper International, Lancaster, NY.).

**Table 43.** Reactor options ranking.

	Maximum weighting	Rotary kiln	Auger
<b>Operating cost/ energy demands and Maintenance</b>	10	7	8
<b>Compatibility with feedstock</b>	10	8	9
<b>Capital Cost</b>	10	6	7
<b>Heating method</b>	10	5	6
<b>Versatility</b>	10	8	7
<b>Total (out of 50)</b>	10	34	37

### 5.2.2.2 Conclusion

The auger reactor was chosen due to its superiority in terms of the selection criteria discussed. The rotary kiln appears to be almost as effective as the auger reactor. However, the auger kiln performance has already been proven at a pilot scale.

Based on the comparisons made the auger reactor can be expected to be a low cost and simple technology which can handle sawdust pyrolysis successfully.



### 5.2.3 Reactor Design

This section demonstrates the tasks that were involved in designing the large scale auger reactor. This design is based on a reactor operating at 400 °C and approximately atmospheric pressure.

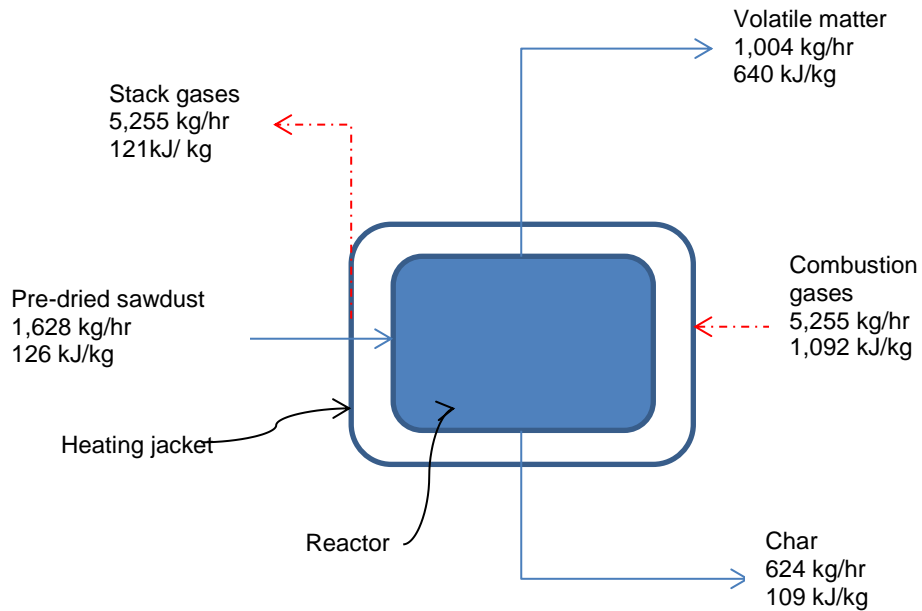


**Figure 62.** Reactor mass and energy balance.

**Table 44.** Reactor specifications.

<b>Feed rate (kg/h)</b>	1,628
<b>Density (kg/m<sup>3</sup>)</b>	250
<b>Volume produced (m<sup>3</sup>)</b>	12.3
<b>Dry solids (kg/h)</b>	1,380
<b>Allowable moisture (@15% ds) (kg/h)</b>	248
<b>Residence time(h)</b>	0.75
<b>Volume of reactor (m<sup>3</sup>)</b>	1.4
<b>Length (m)</b>	6.61
<b>Diameter (m)</b>	0.46
<b>L/D ratio</b>	13.2
<b>Operating temperature (°C)</b>	400 -600
<b>Q (MJ/h)</b>	2,400 – 2,700

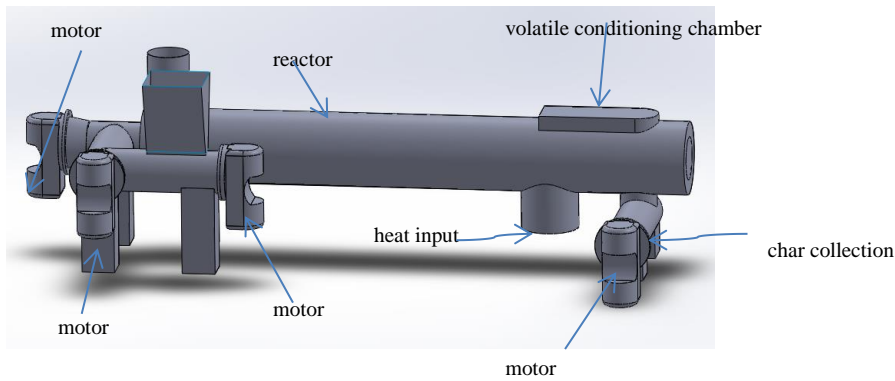


**Figure 63.** Large scale pyrolysis reactor.

## 5.2.4 Separation Phase

This section briefly describes the specifications of equipment used in the large scale plant. The separation phase approach is merely an adaptation of conventional oil and gas handling systems and is based on common steps applied in industry by technology such as OLGA (Könemann 2009). These steps can be classified using two groups:

- Dust/ particulate removal
- Separation train based on component volatility

### 5.2.4.1 Cyclone

Cyclones are commonly used in industry to remove particulates from gas streams. The syngas would normally require particulate removal, however, in an attempt to deploy task integration and minimise the cost of running the cyclone and space it will not be used.

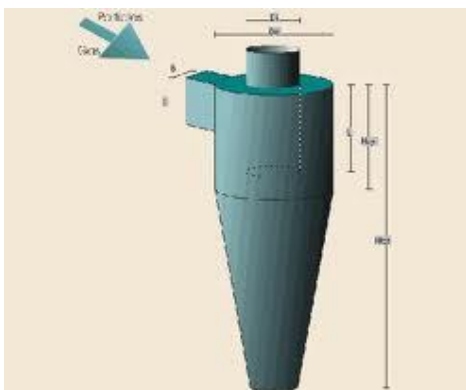


**Figure 64.** Gas cyclone design commonly used in industry.

However, the cyclone can be used in association with the rotary dryer to prevent release of fine particulates in the exhaust.

### 5.2.4.2 Flash Tank Design

The flash tank was designed to operate at atmospheric pressure, and temperature of 135°C as determined from pilot plant trials. Temperature will be maintained using a cooling jacket and air will be used as the heat exchange medium. The flash tank will be tasked with extracting heavy volatile organics and flocculating dust particulates from the hot volatile gas stream due to the elimination of the cyclone.

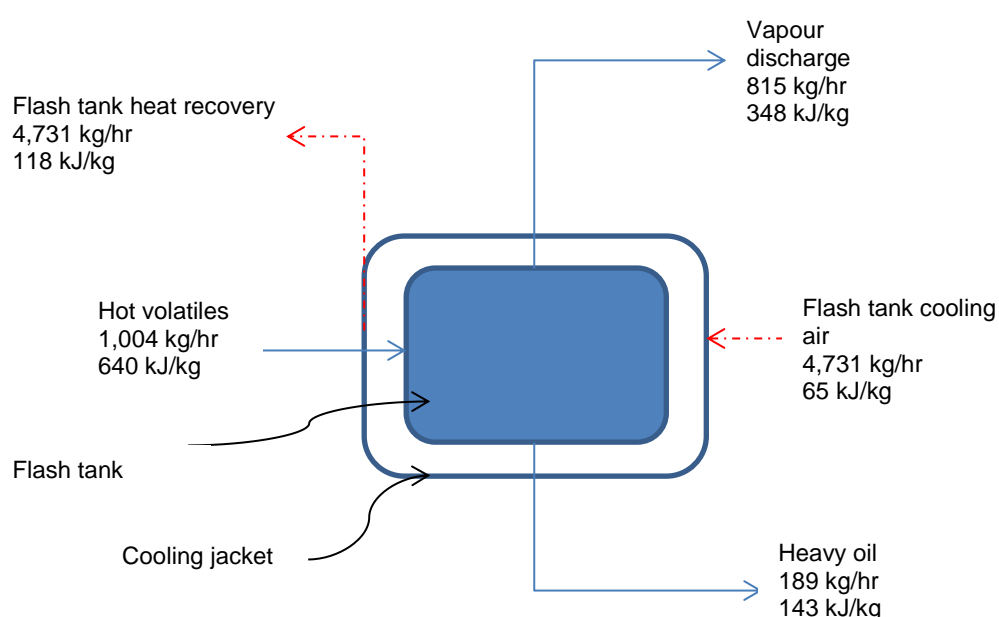


**Figure 65.** Mass and energy balance for flash tank.

**Table 45.** Flash tank specification sheet.

<b>Feed rate (kg/h)</b>	1,004
<b>Density (kg/m<sup>3</sup>)</b>	1.2
<b>Volumetric input (m<sup>3</sup>)</b>	842
<b>Liquid product (kg/h)</b>	104
<b>Vapour product (kg/h)</b>	1,071
<b>Residence time(seconds)</b>	5
<b>Volume of vessel (m<sup>3</sup>)</b>	2.57
<b>Hieght (m)</b>	1.45
<b>Diameter (m)</b>	1.5
<b>L/D ratio</b>	0.97
<b>Operating Temperature (°C)</b>	135

### 5.2.4.3 Condensing Drum Design

The condenser was designed to operate at atmospheric pressure, and temperature of 30°C. Temperature will be maintained using a cooling jacket and water as the heat exchange medium. The condenser drum will be tasked with extracting light volatile organics and water vapour from the syngas stream.

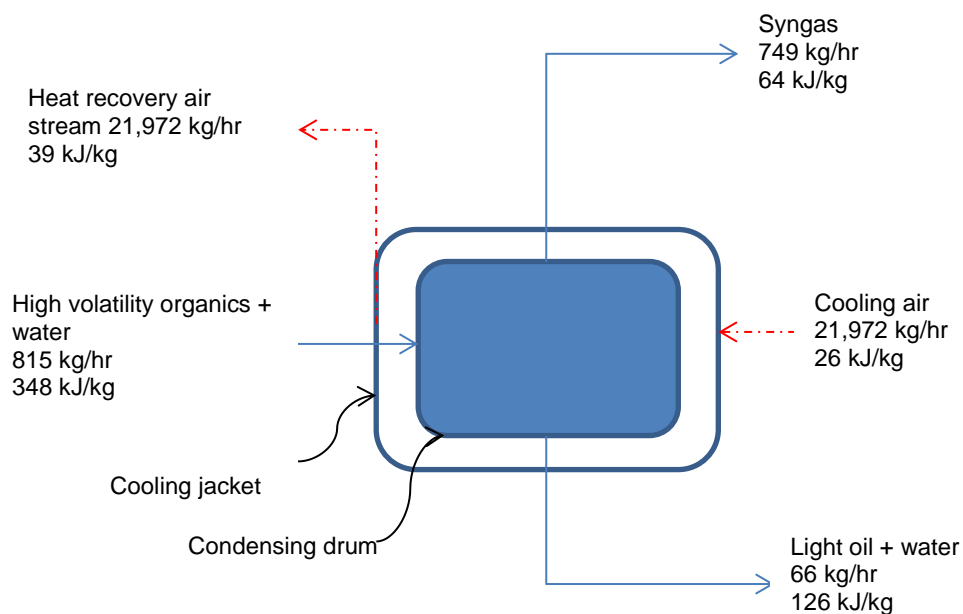


**Figure 66.** Mass and energy balance for condensing drum.

**Table 46.** Condensing drum specifications sheet.

<b>Feed rate (kg/h)</b>	815
<b>Density (kg/m<sup>3</sup>)</b>	0.99
<b>Volumetric input (m<sup>3</sup>)</b>	820
<b>Liquid product (kg/h)</b>	66
<b>Vapour product (kg/h)</b>	749
<b>Residence time(seconds)</b>	5
<b>Volume of vessel (m<sup>3</sup>)</b>	3.71
<b>Hieght (m)</b>	1.45
<b>Diameter (m)</b>	1.75
<b>L/D ratio</b>	0.83
<b>Operating temperature (°C)</b>	30

## **5.2.5 Product Handling**

This section describes the methods used in product storage and effluent treatment. The three products of pyrolysis are bio char, syngas and bio-oil. These products all have different destinations as a result of their market value.

### **5.2.5.1 Biochar**

Biochar storage has been very challenging due to its low density. This means a large volume will be needed to store or transport a given mass. The low density also affects the methods of application to soil. The char has to be placed at a certain depth below the surface to prevent being blown by the wind or being carried by water. This problem is usually solved by pelletizing the char using dense additives as adhesives. The char can also be explosive if allowed to dry, however the char being produced contains about 15% moisture, therefore, explosions are unlikely.

### **5.2.5.2 Gas Storage Tank**

The syngas does not get produced at a constant rate due to the complex kinetics of pyrolysis. Evolution of syngas does not only depend on fresh feedstock as the source, the other two products are also potential reactants. This means that the flow of syngas is always fluctuating. Since the process aims to recycle syngas to achieve autogenesis, the flow rate needs to be kept constant. This will be achieved by having a large tank that will act as a buffer. The gas can be stored in the tank and released at a constant flow once the tank pressure reaches a suitable level. The buffer tank can be made of low carbon steel with lining to prevent risk of corrosion.

### **5.2.5.3 Effluent Treatment**

Effluent streams such as the bio-oil can be recycled and mixed with the fresh feedstock. Water can be purged. In cases where the oil properties do not suit combustion due to corrosive nature or low heat content it can be disposed of depending on the most economically viable solution. This will

be investigated once the properties of the oil being produced have been assessed.

# **Chapter 6. Process Economics Modelling**

## **6.1 Introduction**

This section presents preliminary capital and operating cost estimations for the plant design presented in Chapter 5.

### **6.1.1 Assumptions for Base Case Economic model**

- Potential revenue streams include; char sales, landfill diversion savings.
- Carbon credits are not included in these case studies.
- Equipment cost is estimated by the main plant item cost (MPIC) method using quotes from SCENZ 2004 pricing and the New Zealand consumer capital goods pricing index for inflation rates.
- Commodity prices are based on market research performed using quotes from current suppliers in the market (Berg., Sichone. et al. 2011, Sichone 2012).
- All case studies are based on plant operation of 350 days/ 8400 hrs per year.
- All case studies are assumed to be operating at 80% plant capacity.

### **6.1.2 Base Case Economic model**

#### **6.1.2.1 Capital Cost**

This sub-section presents the capital cost estimates associated with the mobile large scale pyrolysis plant for sawdust described in the preceding chapter 5. Total plant direct costs were calculated to be \$460,306. Figure 67 gives an indication of the total plant direct cost distribution. The dryer is the most expensive component accounting for 23% of the total plant direct cost. The gas burner is follows at 21%.



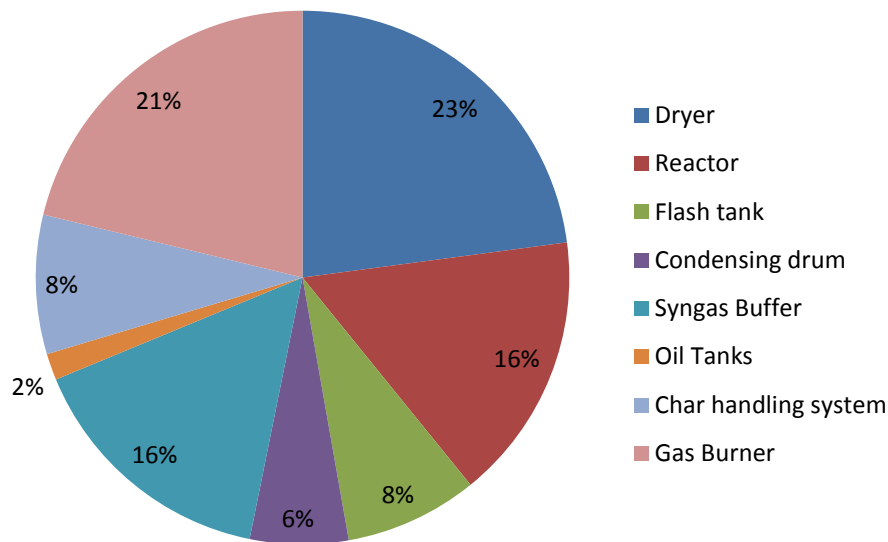


**Figure 67.** Main plant equipment cost distribution for mobile large scale design.

The total capital cost estimation was performed using steps recommended by Peters (1991). Total plant direct costs were assumed to account for 75% of the fixed capital investment. Indirect costs were assumed to account for 25% of the fixed capital costs, giving a value of \$153,435. Working capital was estimated at 15% of the fixed capital investment giving it a value of \$122,748. This brought the total capital investment to \$736,489.

**Table 47.** Total capital investment breakdown.

<b>Total Plant Direct Cost</b>	\$460,306
<b>Indirect Costs</b>	\$153,435
<b>Fixed Capital Investment</b>	\$613,741
<b>Working Capital</b>	\$122,748
<b>Total Capital Investment</b>	\$736,489

### 6.1.2.2 Operating Costs

The operating costs of the design model were estimated using the recommendations in Peters (1991). The total productions cost is estimated to be \$1,207,409 (Table 48). Considering an optimistic option where all the char was sold adds a revenue source of \$787,215 was obtained, leaving a yearly loss of \$420,194.

**Table 48.** Operating cost breakdown for mobile pyrolysis plant base case.

<b>Plant Capacity</b>	36,225 tonnes/yr		
<b>Operating capacity</b>	28,980 tonnes/yr		
<b>Manufacturing costs</b>			
<b>A direct production costs @ 65% of total production cost</b>			<b>Cost</b>
1 Raw materials			\$115,920
2 Operating labour			\$393,161
3 Direct Supervisory & clerical labour			\$58,974
4 Utilities			\$108,380
5 Maintenance and Repairs			\$42,962
6 Operating supplies			\$6,444
7 Lab charges			\$58,974
8 Patents & royalties			\$0.00
9 Supplementary fuel			\$0.00
<b>Total direct production costs</b>			\$784,816
<b>B. Fixed charges @15% of total product cost</b>			\$181,111
<b>C. General Expenses @ 20% total production cost</b>			\$241,481
<b>Total production cost</b>			\$1,207,409
<b>Gross earnings</b> (Assuming all char is sold)			
	<b>unit price</b>	<b>Production (Tpa)</b>	<b>Revenue</b>
<b>Char</b>	\$150/t	5,248	\$787,215
<b>Total gross earnings</b>			-\$420,194
<b>Payback (years)</b>			-1.8
<b>Minimum char price for Break even operation</b>			\$ 230.07

The char revenue was not enough to offset the operating costs and losses. The negative payback period means there is no achievable payback period for the process under these assumptions. The operating labour came at a cost of \$393,161 and appears to be the highest contributor to the total direct production cost. It was determined that the minimum char price for the base case to operate economically was \$207 per tonne (disregarding marketing mark-ups).

The syngas and oil were recovered and used as an energy source. It was determined that the pyrolysis plant would be self-sufficient once steady conditions were achieved. However, start-up would require the use of supplementary fuel such as natural gas or LPG as used in the pilot plant trials. The syngas and oil could not directly account for all heating

requirements. Therefore, heating of relatively low temperature process such as drying was done using heat recovered from product streams in condensation processes such as those in the flash tank and condensing drum.

### **6.1.2.3 Sensitivity Analysis Economic Models**

A sensitivity analysis of the preliminary economic model was performed in attempt to improve the process economics. The sensitivity analysis establishes a basis for optimistic and pessimistic scenarios based on probable scenarios.

#### ***6.1.2.3.1 Assumptions for Pessimistic Sensitivity Analysis***

- Capital costs – A syngas scrubber is needed. This might be the case if the product gas is very sour due to high content levels of hydrogen sulphide.
- Operating costs – No char is sold. This assumption is based on the limited bio char market in New Zealand.

#### ***6.1.2.3.2 Assumptions for Optimistic Sensitivity Analysis***

- Capital costs – The rotary dryer is not needed. This assumes the feedstock can be processed without the need of a dryer. This assumption ties in with the design limitations which do not allow for a rotary dryer of the required dimensions as estimated in Chapter 5
- Operating costs – A reduction of operating labour costs by 50% based on automated nature of mobile plant.

### **6.1.2.4 Capital Cost**

The capital cost sensitivity analysis is shown in Table 49. The analysis showed that the pessimistic total capital investment in the pessimistic case increases by 64% giving a value of \$1,204,669 while the optimistic case reduces capital investment by 19% with the value of \$595,783.

**Table 49.** Sensitivity analysis for capital costs.

	<b>Pessimistic</b>	<b>Base case</b>	<b>Optimistic</b>
<b>Total Plant Direct Cost</b>	\$752,918	\$460,306	\$372,364
<b>Indirect costs</b>	\$250,973	\$153,435	\$124,121
<b>Fixed capital investment</b>	\$1,003,891	\$613,741	\$496,486
<b>Working Capital</b>	\$200,778	\$122,748	\$99,297
<b>Total Capital Investment</b>	\$1,204,669	\$736,489	\$595,783

### **6.1.2.5 Operating Costs**

The sensitivity analysis for the operating cost estimations are shown in Table 50. The pessimistic case does not improve process feasibility and increases the deficit by three times. On the other hand, the optimistic case shows a gross net profit of \$153,226 before taxes. This allows for a payback period of approximately 4 years.

The sensitivity analysis showed that the even though the base case scenario is not economically feasible, the process economics can be improved by reduction of operating labour and reduction of the capital cost by excluding the dryer.

The minimum char price for a payback period of four years appears to be quite practical if the biochar market is established. Extensive agricultural activities have reduced the content of carbon in the soil and biochar might be sought after as a remedy. The minimum char price for break-even operations refers to the amount that can be charged for the char once the capital investment has been paid back. This assumes no profit is being generated from char sales.

Saw mills are normally located near kilns and it is possible that excess heat from the kilns and other onsite facilities could be used to dry the green sawdust. Other factors such as transportation costs might need to be considered. However in this case it is assumed that the plant will be driven to the site.

**Table 50.** Sensitivity analysis for operating costs.

<b>Plant Capacity</b>	36,225 tonnes/yr			
<b>Operating capacity</b>	28,980 tonnes/yr			
<b>Manufacturing costs</b>				
<b>A. Direct production costs @ 65% of total production cost</b>		<b>Pessimistic</b>	<b>Base case</b>	<b>Optimistic</b>
1 Raw materials		\$115,920	\$115,920	\$115,920
2 Operating labour		\$393,161	\$393,161	\$196,581
3 Direct Supervisory & clerical labour		\$58,974	\$58,974	\$19,658
4 Utilities		\$108,380	\$108,380	\$39,967
5 Maintenance and Repairs		\$70,272	\$42,962	\$34,754
6 Operating supplies		\$6,444	\$6,444	\$5,213
7 Lab charges		\$58,974	\$58,974	\$0
8 Patents & royalties		\$0.00	\$0.00	\$0
9 Supplementary fuel		\$0.00	\$0.00	\$0
<b>Total direct production costs</b>		\$812, 127	\$784,816	\$412,092
<b>B. Fixed charges @15% total product cost</b>		\$187,413	\$181,111	\$95,098
<b>C. General expenses @ 20% total production cost</b>		\$249,885	\$241,481	\$126,797
<b>Total production cost</b>		\$1,249,425	\$1,207,409	\$633,989
<b>Gross earnings</b>				
	<b>Production (Tpa)</b>	<b>Revenue</b>	<b>Revenue</b>	<b>Revenue</b>
<b>Char</b>	5,248	0	\$787,215	\$787,215
<b>Total gross earnings</b>		-\$1,249,425	-\$420,194	\$153, 226
<b>Payback (years)</b>		N/A	-1.8	3.9
<b>Minimum char price for Break-even operation</b>		\$238/t	\$ 230/t	\$120/t
<b>Minimum char price for payback period of 4 years</b>		\$295/t	\$265/t	\$149/t

# **Chapter 7.**

## **Conclusion and Recommendations**

## 7.1 General Findings

Lakeland Steel Limited developed a pilot plant for biomass pyrolysis based on sawdust. The pilot plant was based on an auger screw design which was indirectly heated using a double pipe heat exchange configuration to prevent oxidation (combustion) of the feedstock.

Proximate analysis of sawdust gave a moisture content of 60%. The dry solids had an organic matter content of 99.22% with ash making the balance. Ultimate analysis was used to determine content levels of elemental carbon, hydrogen, nitrogen sulphur and oxygen. The results on a dry basis were 47.2%, 6.5%, 0.3%, 0.3%, and 44.9 % respectively.

Drying models were also used to analyse the sawdust drying characteristics. Drying curves were obtained experimentally and four models (Newton, Page, Henderson and Pabis, Simpson and Tschernitz) were fitted to the data and their accuracy of fit was determined using residual squared sum of errors. Page's model was used to describe the sawdust behaviour in the dryer design as it had the highest accuracy.

The sawdust reaction kinetics were determined using data from thermogravimetric analysis (TGA) and analysed using distributed action energy model. The kinetics were observed at three heating rates of 10, 20 and 30 °C/min with a maximum temperature of 900°C under an argon atmosphere. Sawdust was modelled as a mixture of water, hemicellulose, cellulose and lignin. Good agreement between Gaussian distribution functions for each component and experimental data were observed.

Pilot plant trials were performed using a three factor-three level design of experiment. The factors under investigation were; feedstock moisture content with levels at 15, 30 and 60; reaction temperature with levels at 400, 450 and 500°C; and reactor auger speed with levels at 15, 20 and 25 rpm. Experiments at 60% moisture could not be performed to completion as the auger blocked repeatedly. The other two moisture contents showed that moisture content enhanced heat exchange properties of the feedstock and this generally increased the amount of

volatile organic matter released. It was observed that for 15% moisture sawdust increase of temperature did not consistently exhibit an increase in degree of devolatilisation of organic matter. However, the 30% moisture sawdust showed an increase in devolatilisation with increase in temperature. The effects of increasing reactor auger speed had the most consistent trend with which an increase in speed showed a decrease in degree of devolatilisation thus increasing char yield.

The empirical data collected from lab scale and pilot plant experiments were used to create mass and energy balances. These were the basis of the large scale mobile pyrolysis plant which was designed to process 3.45 tonnes per hour. Due to size restrictions the large scale dryer was not fitted in the container. It was then determined that the feedstock would either be dried using an onsite kiln or the reactor would process green sawdust.

A preliminary economic feasibility assessment was performed for the base case scenario which processed pre-dried sawdust of 15% moisture content at 400°C and a retention time of 45 minutes. The base case proved infeasible due to high operating costs and low revenue generation from char sales. It was determined that the base case scenario required char to be sold at a minimum of \$265/t for a four year payback period.

A sensitivity analysis based on predicted optimistic conditions showed that removal of a dryer and automation of the plant which reduced labour by 50% had the potential to increase the economic viability of the large scale process. This reduced the capital and operating costs to \$608,234 and \$636,559 respectively. The optimistic scenario ensured a payback period of 4 years.

The pessimistic case assumed the char had no value and the syngas required scrubbing. This increased the capital costs from \$748,940 to \$1,217,120 and operating costs from \$1,209,979.21 to \$1,251,995. The pessimistic scenario required char to be sold at a minimum of \$295/t for a four year payback period.

## **7.2 Recommendations for Future Work**

Future work would attempt to involve characterisation of compounds from the bio-oil fraction. This was not done because the oil fractions have been identified



to need extra processing steps before they can be used as a conventional liquid fuel. The literature review suggested that the bio-oil can be a source of numerous types of hydrocarbons and precursors. These organic compounds might improve the revenue generated from the processing plant.

A larger factorial study looking at a greater number of temperatures, feed rates and moisture contents could be beneficial to a greater understanding of the effects of these parameters on char, gas and oil yields observed.

The heating rate of the sawdust during pilot plant trials has been discussed briefly. It has been related to the reactor auger speed (analogous of sawdust feed rate), the maximum reaction temperature and the driving force for heat transfer from the combustion gases through the reactor wall. A temperature profile with data collected at five points on the reactor shell was used. However, a high resolution temperature profile which collects more data might give a better indication of the actual heating rate experienced by the sawdust.

Raman spectrometry was used to verify the maximum reaction temperatures for the produced char samples by tracking the position of the G band. This comparison is subjective to the residence time of the batch processed char samples used as calibration values. Raman spectroscopy could be used to provide more information on the char structural properties which might give a broader picture of the degree of carbonisation of the samples.

Online composition analysis of syngas would also be recommended. This is because syngas production rates were observed to vary for different times of the process. It was unknown whether the fluctuation of the production rates has an impact on the composition and therefore the calorific content of the syngas.

The thesis obtains reaction kinetics based on the devolatilisation of the organic matter. However an additional model that could predict the kinetics of carbonisation would help in creating a global model for the whole process.

# References

- Solids - Specific Heats, The Engineering Toolbox.
- (IBI), I. B. I. (2011). Standardized Product Definition and Product Testing Guidelines for Biochar That Is Used in Soil.
- (USA), D. o. E. C. (2013). "Lumber Pressure Treated With Chromated Copper Arsenate." Retrieved 07/02/2013, 2013.
- A.V.Bridgewater. (2004). "Biomass Fast Pyrolysis." Thermal Science **8**(2): 21-49.
- Aboyade, A. O., T. J. Hugo, M. Carrier, E. L. Meyer, R. Stahl, J. H. Knoetze and J. F. Görgens (2011). "Non-isothermal kinetic analysis of the devolatilization of corn cobs and sugar cane bagasse in an inert atmosphere." Thermochemica Acta **517**(1-2): 81-89.
- ACUSIM Shell and tube Heat exchangers.
- AG, V. P. S. (2011). "Range of VC999 Packaging Machines." Retrieved 05/12/2011, 2011, from <http://www.packaging-int.com/suppliers/inauen-maschinen-ag-vc999-packaging-systems.html>.
- Alden, N., Z. Humerick and A. Teixeira (2009). Molten Salt Gasification of Biomass, Worcester Polytechnic Institute.
- Anis, S. and Z. A. Zainal (2011). "Tar reduction in biomass producer gas via mechanical, catalytic and thermal methods: A review." Renewable and Sustainable Energy Reviews **15**(5): 2355-2377.
- Antal, M. J. and M. Grønli (2003). "The Art, Science, and Technology of Charcoal Production†." Industrial & Engineering Chemistry Research **42**(8): 1619-1640.
- Antal, M. J. and G. Varhegyi (1995). "CELLULOSE PYROLYSIS KINETICS - THE CURRENT STATE KNOWLEDGE." Industrial & Engineering Chemistry Research **34**(3): 703-717.

- Apt, J., A. Newcomer, L. B. Lave, S. Douglas, L. M. Dunn and M. Reed (2008). An Engineering-Economic Analysis of Syngas Storage. U. National Energy Technology Laboratory.
- Balat, M., M. Balat, E. Kırtay and H. Balat (2009). "Main routes for the thermo-conversion of biomass into fuels and chemicals. Part 1: Pyrolysis systems." Energy Conversion and Management **50**(12): 3147-3157.
- Balci, S., T. Dogu and H. Yucel (1993). "Pyrolysis kinetics of lignocellulosic materials." Industrial & Engineering Chemistry Research **32**(11): 2573-2579.
- Barrow, C. J. (2012). "Biochar: Potential for countering land degradation and for improving agriculture." Applied Geography **34**(0): 21-28.
- Basu, P. (2010). Biomass Gasification and Pyrolysis : Practical Design and Theory.
- Behrens, M. (2013). Solid State Kinetics, Fritz Haber Institute of the Max Planck Society Department of Inorganic Chemistry.
- Berg., L. v. d., K. Sichone. and H. Kay (2011). EW PYROLYSIS:Market and Technical Assessment, WaikatoLink.
- Boyles, D. (1984). Bio-Energy: Technology ,Thermodynamics and Costs.
- Bradley, D. (2006). European Market Study for BioOil (Pyrolysis Oil), Climate Change Solutions.
- Branan, C. R. (2005). 2 - Heat Exchangers. Rules of Thumb for Chemical Engineers (Fourth Edition). Burlington, Gulf Professional Publishing: 29-58.
- Branan, C. R. (2005). 8 - Separators/Accumulators. Rules of Thumb for Chemical Engineers (Fourth Edition). Burlington, Gulf Professional Publishing: 142-152.
- Branan, C. R. (2005). 12 - Gasification. Rules of Thumb for Chemical Engineers (Fourth Edition). Burlington, Gulf Professional Publishing: 201-212.
- Branca, C., A. Albano and C. Di Blasi (2005). "Critical evaluation of global mechanisms of wood devolatilization." Thermochimica Acta **429**(2): 133-141.

- Braun, R. L. and A. K. Burnham (1987). "Analysis of chemical reaction kinetics using a distribution of activation energies and simpler models." Energy & Fuels **1**(2): 153-161.
- Bridgwater, A. V. (1999). "Principles and practice of biomass fast pyrolysis processes for liquids." Journal of Analytical and Applied Pyrolysis **51**(1-2): 3-22.
- Bridle, T. (2011). Waste to Energy: Alternative uses for paunch waste and DAF sludge - Waste pyrolysis Review, Bridle Consulting.
- Brinkman, A. W. and J. Carles (1998). "The growth of crystals from the vapour." Progress in Crystal Growth and Characterization of Materials **37**(4): 169-209.
- Bulushev, D. A. and J. R. H. Ross (2011). "Catalysis for conversion of biomass to fuels via pyrolysis and gasification: A review." Catalysis Today **171**(1): 1-13.
- Butler, E., G. Devlin, D. Meier and K. McDonnell (2011). "A review of recent laboratory research and commercial developments in fast pyrolysis and upgrading." Renewable and Sustainable Energy Reviews **15**(8): 4171-4186.
- Cheremisinoff, N. P. (2000). Handbook of chemical processing equipment.
- Chibante, V., A. Fonseca and R. Salcedo (2007). "Dry scrubbing of acid gases in recirculating cyclones." Journal of Hazardous Materials **144**(3): 682-686.
- Choi, H. S., Y. S. Choi and H. C. Park (2012). "Fast pyrolysis characteristics of lignocellulosic biomass with varying reaction conditions." Renewable Energy **42**(0): 131-135.
- co.Ltd, C. H. B. m. e. (2011). "Products." Retrieved 05/12/2011, 2011, from <http://www.cnhengbo.com/en/index.asp>.
- Crocker, M., Ed. (2010). Thermochemical Conversion of Biomass to Liquid Fuels and Chemicals.
- D.Zhang. and S.Lilly. (2005). "Low-temperature Pyrolysis of Sewage Sludge and Putrescible Garbage for Fuel Oil Production." Fuel **84**: 809-815.
- Demirbaş, A. (2000). "Mechanisms of liquefaction and pyrolysis reactions of biomass." Energy Conversion and Management **41**(6): 633-646.

- Diebold, J. P. (1994). "A unified, global model for the pyrolysis of cellulose." Biomass and Bioenergy **7**(1–6): 75-85.
- Dominguez., A., J. A. Menendez, M. Inganzo and J. j. Pis (2006). "Production of bio-fuels by high temperature pyrolysis of sewage sludge using conventional and microwave heating." Bioresource Technology **97**: 1185-1193.
- Downie, A. (2008). Base Case in NSW, Au.
- Downie, A. (2010-2011). EW PYROLYSIS:Market and Technical Assessment. L. v. d. Berg. Hamilton City.
- Dupont, C., L. Chen, J. Cances, J.-M. Commandre, A. Cuoci, S. Pierucci and E. Ranzi (2009). "Biomass pyrolysis: Kinetic modelling and experimental validation under high temperature and flash heating rate conditions." Journal of Analytical and Applied Pyrolysis **85**(1–2): 260-267.
- Dutta, A. (2007). Bio-energy for achieving MDGs in Asia(Lecture 3), Asian Institute of Technology, School of Environment, Resources and development.
- Elliott, D. C. (2010). EW PYROLYSIS:Market and Technical Assessment. L. v. d. Berg, WaikatoLink.
- Exports, C. E. (2011). "Industrial Evaporation Technologies." Retrieved 05/12/2011, 2011, from <http://www.compevaporators.com/multi-effect-evaporators.html>.
- Fabrication, S. S. (2011). "Dryer." Retrieved 5/12/2011, 2011, from <http://www.indiamart.com/ss-fabrication/dryer.html>.
- Fake, D. M., A. Nigam and M. T. Klein (1997). "Mechanism based lumping of pyrolysis reactions: Lumping by reactive intermediates." Applied Catalysis A: General **160**(1): 191-221.
- FAO and N. R. M. a. E. Department (unknown). INTEGRATED ENERGY SYSTEMS IN CHINA - THE COLD NORTHEASTERN REGION EXPERIENCE... The research progress of biomass pyrolysis processes, , Natural Resources Management and Environment Department
- French, R. and S. Czernik (2010). "Catalytic pyrolysis of biomass for biofuels production." Fuel Processing Technology **91**(1): 25-32.

- Imam, T. and S. Capareda (2012). "Characterization of bio-oil, syn-gas and bio-char from switchgrass pyrolysis at various temperatures." Journal of Analytical and Applied Pyrolysis **93**(0): 170-177.
- Intelligence, G. M. (2012). Materials for Heat Exchanger Tubes.
- John McDonald-Wharry, M. M.-H., Kim Pickering (2012). Carbonisation of biomass-derived chars and the thermal reduction of a graphene oxide sample studied using Raman spectroscopy.
- Jones, D. J. (2010). EW PYROLYSIS:Market and Technical Assessment. L. v. d. Berg.
- Kaneko, T., F. Derbyshire, E. Makino, D. Gray and M. Tamura (2000). Coal Liquefaction. Ullmann's Encyclopedia of Industrial Chemistry, Wiley-VCH Verlag GmbH & Co. KGaA.
- Kapdi, S. S., V. K. Vijay, S. K. Rajesh and R. Prasad (2005). "Biogas scrubbing, compression and storage: perspective and prospectus in Indian context." Renewable Energy **30**(8): 1195-1202.
- Könemann, J. W. (2009). OLGA Tar Removal Technology, Dahlman.
- Kovács, T., I. G. Zsély, Á. Kramarics and T. Turányi (2007). "Kinetic analysis of mechanisms of complex pyrolytic reactions." Journal of Analytical and Applied Pyrolysis **79**(1-2): 252-258.
- Lédé, J. (1994). "Reaction temperature of solid particles undergoing an endothermal volatilization. Application to the fast pyrolysis of biomass." Biomass and Bioenergy **7**(1-6): 49-60.
- Lehmann, J. and S. Joseph (2012). Biochar for Environmental Management: Science and Technology.
- Lehmann, J., M. C. Rillig, J. Thies, C. A. Masiello, W. C. Hockaday and D. Crowley (2011). "Biochar effects on soil biota – A review." Soil Biology and Biochemistry **43**(9): 1812-1836.
- Li, G. Wang, X. Meng and J. Gao (2008). "Catalytic Pyrolysis of Gas Oil Derived from Canadian Oil Sands Bitumen." Industrial & Engineering Chemistry Research **47**(3): 710-716.

- Liu, Z.-S., M.-Y. Wey and C.-L. Lin (2002). "Reaction characteristics of Ca(OH)<sub>2</sub>, HCl and SO<sub>2</sub> at low temperature in a spray dryer integrated with a fabric filter." Journal of Hazardous Materials **95**(3): 291-304.
- Lu, Q., W.-Z. Li and X.-F. Zhu (2009). "Overview of fuel properties of biomass fast pyrolysis oils." Energy Conversion and Management **50**(5): 1376-1383.
- Made-in-China.com. (2008). "Forage Dryer." Retrieved 05/12/2011, 2011, from <http://cn2drying.en.made-in-china.com/product/uqVEBCgLAXcl/China-Forage-Dryer.html>.
- Made-in-China.com. (2011). "Screw Conveyor-GX-LS." Retrieved 5/12/2011, 2011, from <http://www.hellotrade.com/jyoti-engineering/rotary-drum-dryers.html>.
- Mcbirdle, T. (2011). EW PYROLYSIS:Market and Technical Assessment. L. v. d. Berg. Hamilton Cty.
- Mehrabian, R., R. Scharler and I. Obernberger (2012). "Effects of pyrolysis conditions on the heating rate in biomass particles and applicability of TGA kinetic parameters in particle thermal conversion modelling." Fuel **93**(0): 567-575.
- Mohan, D., C. U. Pittman and P. H. Steele (2006). "Pyrolysis of Wood/Biomass for Bio-oil: A Critical Review." Energy & Fuels **20**(3): 848-889.
- Moyers., C. G. and G. W. Baldwin (1999). Perry's, Chemical Engineers' Handbook.
- Müller-Hagedorn, M., H. Bockhorn, L. Krebs and U. Müller (2003). "A comparative kinetic study on the pyrolysis of three different wood species." Journal of Analytical and Applied Pyrolysis **68–69**(0): 231-249.
- Oasmaa, A. and C. Peacocke (2010) "Properties and fuel use of biomass-derived fast pyrolysis liquids :A guide."
- Ohtsuka, Y., N. Tsubouchi, T. Kikuchi and H. Hashimoto (2009). "Recent progress in Japan on hot gas cleanup of hydrogen chloride, hydrogen sulfide and ammonia in coal-derived fuel gas." Powder Technology **190**(3): 340-347.
- Oziemen., D. and F. Karaosmanoglu. (2004). "Production and Characterization of Bio-oil and Biochar from Rapeseed Cake." Renewable Energy **29**: 779- 787.

- Papadakis, K., S. Gu, A. V. Bridgwater and H. Gerhauser (2009). "Application of CFD to model fast pyrolysis of biomass." Fuel Processing Technology **90**(4): 504-512.
- Peters, M. S. (1991). Plant design and economics for chemical engineers. New York.
- Pharmainfo.net. (2007). "Fluidised Bed Systems: A review." Retrieved 05/12/2011, 2011, from <http://www.pharmainfo.net/free-books/fluidized-bed-systems-review>.
- Purchas., C., S. Tammik., T. Hewitt. and A. Hutchinson. (2009). Organic Waste Options Study. B. Clarke. and N. Milton.
- PYNE (2006). UPR 42 Biomasse – Energie CIRAD - FORET Material Safety Data Sheet. France.
- Rezaiyan, J. and N. P. Cheremisinoff (2005). Gasification Technologies.
- Richardson, Y., J. Blin and A. Julbe (2012). "A short overview on purification and conditioning of syngas produced by biomass gasification: Catalytic strategies, process intensification and new concepts." Progress in Energy and Combustion Science **38**(6): 765-781.
- Sauerbrunn, S. and P. Gill Decomposition kinetics using TGA.
- Sewry, J. D. and M. E. Brown (2002). "“Model-free” kinetic analysis?" Thermochimica Acta **390**(1–2): 217-225.
- Sharma, S. D., M. Dolan, D. Park, L. Morpeth, A. Ilyushechkin, K. McLennan, D. J. Harris and K. V. Thambimuthu (2008). "A critical review of syngas cleaning technologies — fundamental limitations and practical problems." Powder Technology **180**(1–2): 115-121.
- Sichone, K. (2012). Optimisation of an organic waste pyrolysis economic feasibility model by pre-drying feedstock, The University of Waikato.
- Simpson, W. and J. Tschernitz (1979). Importance of Thickness Variation in Kiln Drying Red Oak Lumber. Madison, Wisconsin, Forest Products Laboratory U.S. Forest Service.



- Sipilä, K., E. Kuoppala, L. Fagernäs and A. Oasmaa (1998). "Characterization of biomass-based flash pyrolysis oils." Biomass and Bioenergy **14**(2): 103-113.
- Slessor, M. and C. Lewis. (1979). Biological Energy Resources.
- Smith, J., M. Garcia-Perez. and K.C. Das. (2009). "Producing Fuel and Speciality Chemicals from the Slow Pyrolysis of Poultry DAF Skimmings." Journal of Analytical and Applied Pyrolysis **86**: 115-121.
- Sonobe, T. and N. Worasuwannarak (2008). "Kinetic analyses of biomass pyrolysis using the distributed activation energy model." Fuel **87**(3): 414-421.
- Strezov, V., T. J. Evans and C. Hayman (2008). "Thermal conversion of elephant grass (*Pennisetum Purpureum* Schum) to bio-gas, bio-oil and charcoal." Bioresource Technology **99**(17): 8394-8399.
- Sutton, D., B. Kelleher and J. R. H. Ross (2001). "Review of literature on catalysts for biomass gasification." Fuel Processing Technology **73**(3): 155-173.
- Taylor, P., Ed. (2010). The Biochar Revolution.
- The Engineering Toolbox Solids- Specific Heats, The Engineering Toolbox.
- Thompson, R., Ed. (1995). Industrial Inorganic Chemicals: Production and Uses
- Vamvuka, D. (2011). "Bio-oil, solid and gaseous biofuels from biomass pyrolysis processes-An overview." International Journal of Energy Research **35**(10): 835-862.
- Van de Velden, M., J. Baeyens, A. Brems, B. Janssens and R. Dewil (2010). "Fundamentals, kinetics and endothermicity of the biomass pyrolysis reaction." Renewable Energy **35**(1): 232-242.
- Várhegyi, G. b., B. z. Bobály, E. Jakab and H. Chen (2010). "Thermogravimetric Study of Biomass Pyrolysis Kinetics. A Distributed Activation Energy Model with Prediction Tests." Energy & Fuels **25**(1): 24-32.
- Verheijen, F., S. Jeffery, A. C. Bastos, M. v. d. V. and I. Diafas (2010). Biochar Application to Soils - A Critical Scientific Review of Effects on Soil Properties, Processes and Functions Luxembourg: Office for Official Publications of the European

Communities, European Commission, Joint Research Centre Institute for Environment and Sustainability.

White, J. E., W. J. Catallo and B. L. Legendre (2011). "Biomass pyrolysis kinetics: A comparative critical review with relevant agricultural residue case studies." Journal of Analytical and Applied Pyrolysis **91**(1): 1-33.

Xu, X. D., Y. Matsumura, J. Stenberg and M. J. Antal (1996). "Carbon-catalyzed gasification of organic feedstocks in supercritical water." Industrial & Engineering Chemistry Research **35**(8): 2522-2530.

Zhang, L. (2010 ). "Overview of recent activities in thermo-chemical conversion of biomass. ." Energy Conversion and Management **51**: 969-982.

---

<sup>i</sup> Hasler P, Nussbaumer T. Gas cleaning for IC engine applications from fixed bed biomass gasification. *Biomass Bioenergy* 1999;16:385–95.